

# **Monitoring of nano-scaled particles in polymerization processes using photon density wave spectroscopy**

Dissertation

With the aim of achieving the doctoral degree at the Faculty of Mathematics, Informatics and  
Natural Sciences

Submitted to the Department of Chemistry  
Institute of Technical and Macromolecular Chemistry  
University of Hamburg

Execution of experiments at  
University of Potsdam  
innoFSPEC Potsdam  
Institute for Fiber Optical Spectroscopy and Sensor Technology  
Am Mühlenberg 3, 14476 Potsdam

Stephanie Martha Schlappa

Hamburg 2025



## Reviewers

1. Dr. Marvin Münzberg, University of Potsdam
2. Prof. Dr. Gerrit A. Luinstra, University of Hamburg

## Examination commission:

1. Prof. Dr. Gerrit A. Luinstra, University of Hamburg
2. Prof. Dr. Volkmar Vill, University of Hamburg
3. Dr. Werner Pauer, University of Hamburg
4. Dr. Marvin Münzberg, University of Potsdam
5. PD Dr. Christoph Wutz, University of Hamburg

Date of Submission 03.03.2025

Disputation 23.05.2025

urn:nbn:de:gbv:18-ediss-128415

This work was carried out from October 2019 to May 2024 at the Institute of Chemistry of the University of Potsdam at innoFSPEC, Institute for Fiber Optical Spectroscopy and Sensor Technology under the supervision of first Dr. L. Bressel and then Dr. M. Münzberg. All syntheses and analyses described here were carried out, monitored and evaluated independently.

The submission was made in March 2025 at the Faculty of Mathematics, Informatics and Natural Sciences in the Department of Chemistry at the University of Hamburg, under the supervision of Dr. W. Pauer.



für Papa und Mama

und ein wenig für mich

## I. Publications

### Peer reviewed papers:

1. Schlappa S, Brenker LJ, Bressel L, Hass R, Münzberg M. Process Characterization of Polyvinyl Acetate Emulsions Applying Inline Photon Density Wave Spectroscopy at High Solid Contents. *Polymers*. 2021; 13(4):669.  
<https://doi.org/10.3390/polym13040669>  
impact factor: 4.6
2. Schlappa S, Bressel L, Reich O, Münzberg M. Advanced Particle Size Analysis in High-Solid-Content Polymer Dispersions Using Photon Density Wave Spectroscopy. *Polymers*. 2023; 15(15):3181.  
<https://doi.org/10.3390/polym15153181>  
impact factor: 5.0
3. Schlappa S, Pauer W, Reich, O, Münzberg, M. Harnessing Photon Density Wave Spectroscopy for the inline monitoring of up to 100 L vinyl acetate-Versa® 10 polymerization: Insights into dispersion dynamics and mixing. *Polymers*. 2025, 17(5):629  
<https://doi.org/10.3390/polym17050629>  
impact factor: 4.7

### Research Stay

I stayed at POLYMAT Institute, San Sebastián, Spain for a cooperative research stay from 15.10.2019 to 31.01.2020. Main focus area of the research stay was the temperature sensibility of inline monitoring of PMMA polymer dispersions at high solid contents. The results found are not published nor discussed here but have an influence on the research and findings presented in this work.

## Scientific talks

28.09.2018: Fallen Walls Lab 2018 at Bundesanstalt für Materialforschung und –prüfung, Berlin Adlershof, Germany. Topic: Breaking the wall of innovation collaboration

19.03.2019: 13<sup>th</sup> international PhD Seminar on Process Analytical Technologies of GDCh 2019 in Berlin-Adlershof, Germany. Topic: Inline monitoring of growth of nano-scaled particles in turbid emulsion polymerization using Photon Density Wave spectroscopy

13.06.2019: 13<sup>th</sup> international Conference on Polymer Reaction Engineering 2019 in Hamburg, Germany. Topic: see above

15.06.2019: 8<sup>th</sup> international PhD-Workshop of the Working Party on Polymer Reaction Engineering 2019 in Hamburg, Germany. Topic: see above

23.09.2019: 49. Kolloidtagung „Complex Fluids“ Tagung der Deutschen Kolloidgesellschaft in Stuttgart, Germany. Topic: Process Characterization of Polyvinyl Acetate Emulsions Applying Inline Photon Density Wave Spectroscopy at High Solid Contents

27.11.2019: 15. Herbstkolloquium Prozessanalytik in Marl, Germany. Topic: Inline characterization of highly turbid dispersions during emulsion polymerization using Photon Density Wave spectroscopy

13.01.2020 Seminar on Polymer Characterization, Polymat Institute in San Sebastian, Spain. Topic: see above

24.09.2020 Materials, Science, Engineering, Online Conference. Topic: Inline Process Analytics for high solid content polymer samples using Photon Density Wave spectroscopy

23.04.2021 APACT`21, Online conference. Topic: Process characterization of polyvinyl acetate emulsions applying inline photon density wave spectroscopy at high solid contents

24.06.2021 Nanotech France 2021, Online conference. Topic. Challenges on inline monitoring of nanosized polymer materials

23.11.2021: 9<sup>th</sup> PhD-Workshop on Polymer Reaction Engineering, Online conference. Topic: Inline monitoring of nanosized polymer materials using Photon Density Wave spectroscopy

20.04.2022: 10<sup>th</sup> PhD-Workshop on Polymer Reaction Engineering, in San Sebastian, Spain. Topic: Inline monitoring of nanosized polymer materials using Photon Density Wave spectroscopy

## Conference posters

31.08 – 02.09.2018: 7<sup>th</sup> international PhD-Workshop of the Working Party on Polymer Reaction Engineering 2018 in Prague, Czech Republic, Topic: see above

08. – 12.10.2018: 5<sup>th</sup> International Conference “Dynamics of Systems on the Nanoscale” in Potsdam, Germany, Topic: In-line Monitoring of growth of nano-scaled particles and droplets in concentrated liquid dispersions by photon density wave spectroscopy

14.06. – 16.06.2019: 8<sup>th</sup> international PhD-Workshop of the Working Party on Polymer Reaction Engineering 2019 in Hamburg, Topic: Inline monitoring of growth of nano-scaled particles in turbid emulsion polymerization using Photon Density Wave spectroscopy

12.06.2019: Tag der Chemie – University of Potsdam, Topic: Inline monitoring of growth of nano-scaled particles in turbid emulsion polymerization using Photon Density Wave spectroscopy

11.07.2019: Tag der Chemie – Technische Universität Berlin, Topic: Inline monitoring of growth of nano-scaled particles in turbid emulsion polymerization using Photon Density Wave spectroscopy

23.11. – 25.11.2020: 16. Kolloquium Prozessanalytik, Online conference. Topic: Influence of monomer content on the polymerization of vinyl acetate monitored by Photon Density Wave spectroscopy. **3<sup>rd</sup> place for best poster contribution**

20.04.2022: 10<sup>th</sup> PhD-Workshop on Polymer Reaction Engineering, in San Sebastian, Spain. Topic: Inline monitoring of nanosized polymer materials using Photon Density Wave spectroscopy

## II. Table of content

1.	Zusammenfassung.....	1
2.	Abstract.....	3
3.	Introduction .....	5
3.1	Emulsion polymerization .....	6
3.1.1	Polymerization Interval I: Redox Initiation.....	8
3.1.2	Particle nucleation .....	9
3.1.3	Particle growth and termination .....	12
3.1.4	Aggregation .....	13
3.1.5	Starved feed emulsion polymerization.....	14
3.2	Polyvinyl acetate synthesis .....	16
3.2.1	Copolymerization VAc:Versa® 10 .....	19
3.2.2	Polyvinyl alcohol as stabilizing agent.....	19
3.3	Process analytical technologies* <sup>gAl</sup> .....	21
3.3.1	PAT implementation into reactor .....	24
3.4	Photon Density Wave spectroscopy .....	26
3.4.1	Transformation of experimentally determined $\mu_s'$ to particle diameter $d$ .....	27
3.4.2	Inline PDW spectroscopy measurements.....	29
3.4.3	Offline PDW spectroscopy measurements .....	30
3.4.4	Data curation .....	30
3.5	Polymer Dispersion Analysis .....	32
3.5.1	Polymer dispersions .....	32
3.5.2	Density of polymer particles in dispersion .....	32
3.5.3	Refractive index of polymer particles.....	33
3.5.4	Offline particle size determination.....	34
3.6	Technology readiness level .....	35
4	Aim .....	37
5	Cumulative part of the dissertation.....	38

5.1	Process Characterization of Polyvinyl Acetate Emulsions Applying Inline Photon Density Wave Spectroscopy at High Solid Contents .....	38
5.1.1	Aim of this research .....	38
5.2	Advanced Particle Size Analysis in High-Solid-Content Polymer Dispersions Using Photon Density Wave Spectroscopy .....	55
5.2.1	Aim of this research .....	55
	Synopsis .....	74
	Polyvinyl acetate with SDS ( <i>not published</i> ) .....	74
5.3	Harnessing Photon Density Wave Spectroscopy for the inline monitoring of up to 100 L vinyl acetate-Versa® 10 polymerization: Insights into dispersion dynamics and mixing.....	75
5.3.1	Aim of this research .....	75
6	Discussion.....	92
7	Conclusion .....	96
8	Outlook.....	98
9	References.....	99
10	Appendix .....	106
10.1	Supplementary Materials .....	120
11.	Acknowledgements .....	121
12.	Declaration on oath .....	122

### III. List of abbreviations and symbols

[ ]	Molar concentration
[M]	Monomer concentration
$\mu_a$	Absorption coefficient
$\mu_s'$	Reduced scattering coefficient
a	Particle radius
AA	Ascorbic Acid
d	Particle diameter
$d_f$	Fiber distance between emission and detection fiber in a PDW spectroscopy measurement
DLS	Dynamic light scattering
$d_p$	Mean particle diameter
DSC	Differential scanning calorimetry
DV	Volume-average particle diameter
EM	Electron microscopy
f	Modulation frequency of PDW spectroscopy measurement
FAS	Ferric ammonium sulfate
g	Anisotropy factor
$j_{crit}$	Critical degree of polymerization
$k_{com}$	Rate of polymer radicals combination
$k_d$	Radical desorption rate
$k_l$	Intensity coefficient
$k_{ini}$	Rate of initiator decomposition
$k_m$	Rate of monomer addition
$k_t$	Rate of disproportionation
$k_p$	Propagation rate constant
$k_\phi$	Phase coefficient
$m_M$	Moles of Monomer
m	Refractive index ratio
n	Refractive index
$\bar{n}$	Average number of radicals per particle
NA	Avogadro's number
NaPS	Sodium persulfate
$n_m$	Refractive index of medium

$N_P$	Number of particles
$n_P$	Refractive index of particle
PAT	Process analytical technology
PDW	Photon density wave
PIDS	Polarization intensity differential scattering
PS	polystyrene
PSD	Particle size distribution
PVA	Poly vinyl alcohol
PVAc	Poly vinylacetate
$Q_s$	Scattering efficiency
$R_a$	Feedrate Monomer
Redox	Reduction and Oxidation
$R_P$	Rate of polymerization
SDS	Sodium dodecyl sulfate
SLS	Static light scattering
STEM	Scanning transmission electron microscopy
tbd	To be discussed
TBHP	tert-butylhydroperoxide
TEM	Transmission electron microscopy
$T_J$	Reactor jacket temperature
$t_R$	Reaction time
$T_R$	Reaction temperature
TRL	Technology readiness level
V	Volume
VAc	Vinyl acetate
Versa <sup>®</sup> 10	Vinyl neodecanoate
$w$	Solid content
$\lambda$	wavelength
$\rho$	Density
$\rho_M$	Density of medium
$\rho_P$	Density of polymer
$\varphi$	Volume fraction
$X$	Conversion





# 1. Zusammenfassung

In dieser Arbeit werden Polymerisationsprozesse untersucht und mittels Prozessanalytik inline, sowie offline verfolgt und begleitet. Zu Beginn wird verdeutlicht, dass eine zeitlich eng aufgelöste Beobachtung der durchgeführten Polymersynthesen zu Erkenntnissen über den Prozess führt. Durch die inline Prozessanalyse mittels Photonendichtewellen Spektroskopie und der inline Verfolgung von optischen Koeffizienten wird gezeigt, dass die verschiedenen Phasen der Polymersynthese sich auch in den optischen Eigenschaften der Dispersion widerspiegeln.

Diese Arbeit liefert Einblicke in Polymerisationsprozesse verschiedener Art, insbesondere in die Polyvinylacetat- (PVAc) und Polystyrolsynthese (PS). Es wird eine eingehende Analyse der Vinylacetat-Homopolymerisation durch Monomer verarmte, semikontinuierliche Synthese beschrieben. Zunächst wird gezeigt, dass die Partikelgröße und die Partikelgrößenverteilung des Systems durch Änderung einfacher Polymerisationsparameter, wie der Gesamtmenge des dem System zugesetzten Monomers, verändert werden können und eine klare Abhängigkeit besteht. Ein Unterschied in der mittleren Partikelgröße und der Partikelgrößenverteilung wurde erstmalig durch die Photonendichtewellen (PDW) Spektroskopie ermittelt und quantifiziert. Die PDW-Spektroskopie zeigt sich nicht nur für die Analyse des produzierten Dispersionsproduktes als geeignet, sondern auch für die Inline-Überwachung des gesamten Polymerisationsprozesses bis hin zu Massenanteilen des Polymers von weit über 40 %. Weiterhin wird gezeigt, dass der gemessene reduzierte Streukoeffizient der Dispersion eine Korrelation mit dem Partikelwachstum aufweist. Es wird ebenso gezeigt, dass die Implementierung von Inline-PDW Spektroskopie in Echtzeit, Hinweise auf mögliche thermische Durchbruchsreaktionen und unsichere Reaktionen geben kann. In Kombination mit anderen Inline-Prozessanalytik (PAT)-Trends, wie z.B. der Auswertung der Reaktionstemperatur, kann eine Durchbruchsreaktion durch gezielte PAT-Anwendung der PDW Spektroskopie verhindert werden.

In weiteren Experimenten wurde festgestellt, dass das untersuchte System aufgrund der Verwendung von Polyvinylalkohol (PVA) als Stabilisierungskolloid dazu neigt, Wasser auf der Partikeloberfläche zu absorbieren. Da dieses Phänomen in der Literatur bekannt ist, wird ein iterativer Ansatz zur Berechnung des volumenbasierten Quellungsfaktors verschiedener PVAc-Homopolymere vorgestellt. Eine Versuchsreihe mit sequentieller Erhöhung der Gesamtmenge von PVA als kolloidalem Stabilisator wurde hinsichtlich der Wasserquellung analysiert. Um die Fähigkeit der PDW-Spektroskopie zur Partikelgrößenbestimmung in diesem Ansatz zu beweisen, wurde Polystyrol, welches mit Natriumdodecylsulfat (SDS) stabilisiert wurde, zusätzlich als Best-Practice Beispielsystem untersucht. Es zeigt sich, dass die PS/SDS-Partikel aufgrund des hydrophilen Charakters der Partikel und des SDS-Stabilisators

erwartungsgemäß nicht zur Wasserquellung neigen. Es wird demonstriert, dass die theoretisch berechnete Streuung sehr gut zu den mittels PDW-Spektroskopie experimentell ermittelten Streukoeffizienten  $\mu_s'$  übereinstimmt, ohne Anpassungen der Partikel hinsichtlich Wasserquellung vorzunehmen. Mittels des vorgestellten iterativen Ansatzes zur systematischen Fehlerminimierung wurde die Wasserquellung der PVAc/PVA-Partikel in Lösungen von bis zu 50 % w/w Massenanteil Polymer berechnet. Demnach wurde hingegen festgestellt, dass die PVAc/PVA-Teilchen in Dispersion bis zu 40 Volumenprozent Wasser aufnehmen. Erst durch die Annahme der individuell iterativ ermittelten Wasserquellung konnte eine Ermittlung der Partikelgröße mit annehmbaren Fehlerwerten erzielt werden. Da die Wasserquellung eine große Herausforderung für die Inline-Überwachung der Partikel darstellt, und die Analyse der Partikelgröße während ihrer Nukleierung und ihres Wachstums sehr schwierig ist, wurde ein verwandtes System für weitere Untersuchungen gewählt.

Die Co-polymerisation von Vinylacetat und Versa® 10 ist ein industriell relevanter Prozess. Es ist bekannt, dass der Prozess sehr exotherm verläuft und bei der Produktion im Großmaßstab Sicherheitsprobleme auftreten können. In einer Kooperation mit der Universität Hamburg wurden Scale-up-Experimente durchgeführt und mittels inline PDW-Spektroskopie verfolgt. Es zeigte sich auch hier, dass die inline gemessenen optischen Parameter über den ganzen Reaktionsverlauf von bis zu 63 % Massenanteil Polymer darstellbar sind. Es konnte anfängliche Inhomogenität durch unzureichende Durchmischung mittels PDW-Spektroskopie ermittelt werden, die letztendlich zu geringen Umsätzen in den Polymerisationen führten.

Durch den Einsatz der PDW-Spektroskopie als PAT-Werkzeug kann die Polymerisation von Polyvinylacetaten durchgehend in Echtzeit verfolgt werden. Dadurch können sicherheitsrelevante Aspekte minimiert, Inhomogenität der Emulsion detektiert und die resultierenden Produkteigenschaften gezielt gesteuert werden. Der Einsatz der in dieser Arbeit angewandten PDW-Spektroskopie erzielt eine deutliche Erhöhung der Messdatenpunkte während einer Reaktion im Vergleich zu offline Messmethoden, wodurch deutliche Kosten- und Zeitersparnisse im Betrieb erzielt werden können.

## 2. Abstract

In this research polymerization reactions are examined and monitored using a process analytical technology (PAT) approach. It is shown that observations with a small time resolution (< 2 min per datapoint) lead to insights into the polymerization process. Through inline PAT by Photon Density Wave (PDW) spectroscopy and the sub-minute tracking of optical coefficients like absorption and scattering of the dispersion polymerization trends are mimicked.

This work delivers insights into polymerization processes of various types, especially on poly vinylacetate (PVAc) and polystyrene (PS). In-depth analysis of the vinyl acetate homopolymerization by semi-continuous starved-feed synthesis is developed. First it is shown that the particle size and particle size distribution (PSD) of the system can be altered by changing simple polymerization parameters like the total amount of monomer added to the system. A difference in the mean particle size and PSD has been obtained and quantified by PDW spectroscopy. PDW spectroscopy cannot only be used for the analysis of the final dispersion, it is on top of that employed as suitable technique for the inline monitoring of the polymerization process. The inline measured reduced scattering coefficient shows correlation to particle growth determined offline by light scattering techniques and electron microscopy. The implementation of inline PDW also gives real-time hints about possible thermal runaway and unsafe reactions. In combination with other inline PAT trends, like evaluation of the reaction temperature, runaway reactions could be impeded and hindered.

In further experiments on the PVAc stabilized by polyvinyl alcohol (PVA) it is found that the PVAc/PVA system is prone to absorb water onto its particle surface due to the use of PVA as stabilizing agent. As this phenomenon is known in literature, an iterative approach to calculate the volume based swelling factor of different PVAc/PVA homopolymers is presented. An experimental series with an increase of the total amount of PVA as colloidal stabilizer was analyzed regarding the water swelling. To prove the capability of PDW spectroscopy in this approach, PS stabilized with sodium dodecyl sulfate (SDS) polymer particles have been analyzed as best-practice. It is shown that, as expected, the PS/SDS particles are not prone to water swelling due to the hydrophilic character of the particle and SDS stabilizer. It is further shown that theoretically calculated PDW spectroscopy reduced scattering data fits very well to the experimentally determined  $\mu_s'$ . Via an iterative approach of systematic error minimization, the water swelling of the PVAc/PVA particles in solutions of up to 50 % w/w polymer is calculated. Accordingly, it is found that the PVAc/PVA particles in dispersion must incorporate water up to 40 % volume. By assuming the individually determined water-swelling a conclusive determination of the PSD with minimized error values are achieved. Since this presents a big challenge for the inline monitoring of particle size a further co-polymer system was used for further investigation.

Copolymerization of vinyl acetate and Versa®10 is an industrially relevant process. The process is known to be very exothermal and unfolds safety issues during large scale production. During a cooperation with the University of Hamburg, scale-up experiments are conducted and simultaneously monitored inline with PDW spectroscopy. In systems of 100 L reaction volume monitoring of the polymerization could be successfully monitored up to solid contents up to 63 % w/w polymer content. Initial inhomogeneity due to insufficient mixing was detected by PDW spectroscopy, which ultimately led to low conversions in the polymerizations.

By using PDW spectroscopy as a PAT tool, the polymerization of polyvinyl acetates can be continuously monitored in real time. This allows safety-relevant aspects to be minimized, inhomogeneity of the emulsion to be detected and the resulting product properties to be controlled and consistent in quality. PDW spectroscopy applied in this work achieves a significant increase in the number of measurement data points during a reaction compared to offline measurement methods, leading to significant cost and time savings.

### 3. Introduction

Our daily lives are determined by the things that affect us in our surroundings and from the inside. As a matter of fact, every smallest aspect causes changes to our behavior and feelings. It's the little things in life that make the biggest differences. In science, the smallest molecules and particles have been subject to research since its beginning. In this thesis one of the most present and investigated small players are in the spotlight of intensity modulated laser light: nanoparticles in emulsion polymerization processes.

This thesis applies and adapts an inline monitoring approach to detailed dispersion analysis in challenging materials. The work done proves that implementation of inline analysis techniques delivers a reliable and safe source to monitor polymerization processes and guarantee efficiency and high-quality products in emulsion polymerization.

Monitor the change to minimize the risk!

This thesis aims to deliver an approach of translation from knowledge to application. From laboratory to industrial scale.

In the spotlight: Photon Density Wave (PDW) spectroscopy. As it will be demonstrated PDW spectroscopy is applicable to many stages of a process and for many purposes. It can be used as an indicator for the reproducibility of syntheses of the same characteristics, but can also be applied to gain deep insights into the process. It can be used to independently determine product parameters such as the absorption and scattering of a sample. With this, specific product parameters can be evaluated in depth. The biggest achievement and advantage is the inline, calibration and dilution free particle size determination. This work has been carried out in order to further specify the limitations of PDW spectroscopy use in emulsion polymerization systems as well as to eliminate these limits and adapt the application range of PDW spectroscopy for the inline analysis of emulsion polymerization processes.

One of the model systems studied is the emulsion polymerization of vinyl acetate to polyvinyl acetate. Vinyl acetate monomer is used widely over the polymer and coatings industry. In the next ten years a global value of more than 16.2 billion US\$ of vinyl acetate systems and products are produced.<sup>1</sup> These products range from paints, coatings, textiles and adhesives to even further specialty applications in different industries.

In the presented work focus is on polyvinyl acetate dispersion productions as used in industry for adhesive purposes. Patent based syntheses have been analyzed by PDW spectroscopy. First a general approach to the inline monitoring of the patent based semi-continuous synthesis of polyvinyl acetate homopolymer stabilized by poly vinyl alcohol is established by using PDW spectroscopy. It is shown that the principle investigation of polymerization is possible during

the whole course of the synthesis up to high solid contents exceeding 40 % w/w polymer. Based on the inline monitoring of the optical trends of absorption and scattering, parallels can be drawn to offline measured particle sizes. A facilitated approach to PDW spectroscopy-based particle size was tackled by adding in-depth analysis of the water swelling potential of the polyvinyl alcohol protective colloid. It was shown that water-swelling of the protective colloid shell accounts for a significant change in the properties of the produced particles. Integration of the water-swelling into the translation from scattering properties to particle diameter lead to a good agreement of final particle sizes between PDW spectroscopy measurements, diluted light scattering measurements and electron microscopy image analysis. Lastly a scale-up approach up to 100 L reaction volume has been successfully monitored with PDW spectroscopy and reproducibility of the synthesis on all analyzed process scales was proven. Early limitations in homogeneity of the emulsion were detected based on inline intensity measurements and showed that homogeneity in the initial stages is crucial to reach high conversion rates.

### 3.1 Emulsion polymerization

Latexes, or dispersions, describe a mixture of a dispersed phase in another continuous phase. In this research dispersions are characterized as colloidal stabilized mixtures of solid polymer nanoparticles within an aqueous medium. Emulsion polymerization is widely used for the production of water-borne polymer latexes. Typical components of an emulsion polymerization synthesis are water-insoluble monomer(s), water-soluble initiator and stabilizing agents (cf. Emulsion polymerization is however challenging in terms of mechanistic understanding and continuous process monitoring. The multiphase system is hard to monitor already at very early reaction stages due to emulsification of the components. State of the art turbidity measurements quickly reach their limits.<sup>9</sup> Modelling is on a very good way however still many challenges arise in these multifactorial systems.<sup>10–13</sup>

Table 1). This method offers advantages compared to other types of polymer synthesis reactions. Sustainability and environmental concerns are minimized, as no or little use of solvents is involved. High solid contents can be achieved by remaining low dispersion viscosities. High monomer conversions can be achieved at short reaction times with high reaction rates. Even economic benefits are present as less waste is produced and therefore cost reductions are evident.<sup>2–7</sup> The radical compartmentalization is a special aspect of emulsion polymerization. Active radicals are statistically possible in all emulsion entities. The radicals are locally separated from each other leading to suppressed and slowed down

---

\* In this work stabilizing agent or colloidal stabilizer is used as a term in order to stay consistent in nomenclature with the published research. Synonyms that are widely used are surfactant, stabilizer or emulsifying agent or further.

termination reactions. Results of this compartmentalization is achieving high molecular weights of the polymer with a high rate of polymerization  $R_p$ .<sup>8</sup>

Emulsion polymerization is however challenging in terms of mechanistic understanding and continuous process monitoring. The multiphase system is hard to monitor already at very early reaction stages due to emulsification of the components. State of the art turbidity measurements quickly reach their limits.<sup>9</sup> Modelling is on a very good way however still many challenges arise in these multifactorial systems.<sup>10–13</sup>

*Table 1 Emulsion polymerization general components and examples used in this work for PVAc and PS syntheses.*

Compound	PVAc synthesis	PS synthesis	Further examples
Medium	Water	Water	Solvents, organics, ethanol, etc.
Colloidal stabilizer	PVA (Mowiol 4-88®)	SDS	PVA (further hydrolysis grades), polyethylene glycols, proteins
Monomer	VA	Styrene	Butyl acrylates, methyl methacrylates, methacrylic acid
Initiator	Redox System NaPS/AA	KPS	AIBN, persulfate salts
Catalyst	Ferric ammonium sulfate	-	Aluminum porphyrins

The emulsification process plays a particularly important role, as it influences properties such as the stability and droplet size of the resulting emulsion and subsequent respective polymer particle size. According to Smith-Ewart theory of emulsion polymerization, the reaction consists of three intervals, initiation, propagation and termination (Figure 1) characterized by the rate of polymerization  $R_p$ . In the first Interval I of nucleation and initial particle growth  $R_p$  increases up to a certain rate. As  $R_p$  levels off the second interval II sets in, where particle growth is the dominant process. Interval III, defined by a decrease of  $R_p$  is predominantly caused by termination reactions due to monomer deficiency.



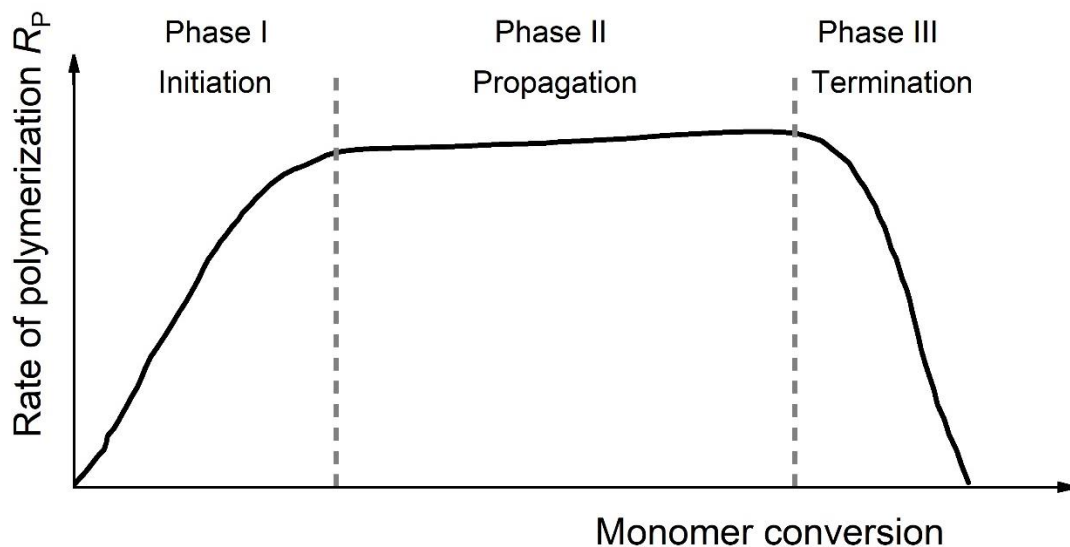


Figure 1 Intervals of emulsion polymerization, based on rate of polymerization and monomer conversion.

### 3.1.1 Polymerization Interval I: Redox Initiation

Initiation of particle nucleation and growth starts by the dissociation of water-soluble initiator molecule  $I_2$  into two active Initiator radicals  $I^*$  by the system specific rate of initiation  $k_{Ini}$ .



The small initiator molecules stay within the aqueous phase due to their solubility. Propagation into available entities by diffusion is very limited. The used redox initiator pair L-ascorbic acid (AA) and sodium persulfate (NaPS) and its dissolution and initiation mechanism has been investigated deeply by SCHROETER and NAGARAJA.<sup>14,15</sup> The rate of radical formation is found to show dependencies on all three components, [AA], [NaPS] and water, their individual concentration and even the ratio between these components. SCHROETER proposes a reaction mechanism where radicals are formed by reaction of the peroxide with  $Fe^{2+}$  ions by breaking the peroxidic O-O bond and simultaneous oxidation of  $Fe^{2+}$ . Regeneration of the  $Fe^{2+}$  happens via reaction with AA to form  $Fe^{3+}$ . The reaction has a low indication time and a wide range of possible reaction temperatures. Ongoing research has been conducted on the actual mechanism of the redox initiator system and possible formation of an Fe-AA-complex is anticipated.<sup>15</sup> Details on the reaction kinetics in the used redox initiator system NaPS, AA and Fe-catalyst are described in SCHROETER chapters 5.2.8 to 5.2.10. He found that at equimolar ratios the redox decomposition follows strict first order kinetics and only very small catalytic amounts of  $Fe^{3+}$  ions are needed. Further AGIRRE ET AL. found that the iron ammonium sulfate is used to accelerate the radical generation when using PVA as colloidal stabilizer, as done here.<sup>16</sup> Water borne redox initiator system including AA has proven to accomplish high

conversions of VAc at low reaction temperatures already and forms very strong reactive radicals which minimize the amount of residual monomer.<sup>17</sup>

A further redox initiator system used here was TBHP/AA for a few syntheses in the later part of the thesis. Whereas initiation with TBHP and AA promotes radical entry as hydrophobic tert-butoxy radicals are formed, which integrate into the polymer particles, research shows that initiator pair TBHP/AA leads to a smaller number of particles and therefore larger particle diameters in comparison to KPS, NaPS or further redox initiator pairs.<sup>16,18</sup> TBHP/AA was not used throughout the experiments presented here, as it leads to the microscopic formation of coagulum in the dispersions. After long term storage (approx. 48 months) at room temperature and ambient conditions in a dark storage cabinet all dispersions produced with TBHP/AA were completely coagulated, whereas the dispersions produced with NaPS/AA showed an increase in viscosity but were still stirrable and showed little to no coagulum.

### 5.1.2 Particle nucleation

The formation of a particle or particle-like structure is called nucleation. The nucleation process has different driving forces based on physical, chemical and mechanical conditions. Nucleation mechanisms have been proposed for a very long time and are still subject to a lot of discussions and research. In polymerization theory, especially emulsion polymerization, different nucleation mechanisms have been proposed. In general terms, the colloidal stabilizer added to the polymerization system forms agglomerates, clusters or micelles due to its amphiphilic character. Micelles are only formed if the critical micellar concentration (*CMC*) of the stabilizer is reached and exceeded. These micelles act as the reaction center of polymerization in micellar nucleation. Due to the low solubility of the monomer in the medium, dimers and small oligomers form and enter monomer swollen micelles, based on diffusion and solubility issues. Oligomer species formed in the aqueous phase diffuse into monomer swollen micelles and propagate to a polymer particle. In homogeneous nucleation, monomer is dissolved to a small extent in the aqueous phase. Radicals generated in the aqueous phase react to form oligomers, which reach a  $j_{cr}$  critical degree of polymerization and precipitate as primary particle. These might undergo limited aggregation and thereby reduction of the particle surface.<sup>19</sup> The polymerization rate within the polymer particle is described by:

$$R_p = k_p [M]_p \frac{\bar{n}}{N_A} N_p \quad (3.2)$$

where  $k_p$  is the propagation rate constant,  $[M]_p$  the monomer concentration in the polymer particles,  $\bar{n}$  the average number of radicals per particle,  $N_A$  Avogadro's number, and  $N_p$  the number of particles with

$$N_P = \left( \frac{6M}{\pi \rho_P D_V^3} \right) \quad (3.3)$$

where  $M$  is the total amount of monomer fed to the system,  $\rho_P$  is the density of the pure polymer and  $D_V$  is the volume-average particle diameter here determined by PDW spectroscopy\*. Typical values for particle numbers in emulsion polymerization are in the range of  $10^{18}$  to  $10^{20}$  particles per Liter. The resulting PSD of a particular system depends strongly, among others on the nucleation process. The shorter the nucleation step, the narrower the PSD.<sup>5</sup> Current research nowadays cannot completely define the end of the nucleation period as secondary nucleation is always a possibility due to remaining active radicals in the reaction system. By definition, nucleation can be terminated with stopping of monomer feed, however it can also be ongoing to a certain extend during the whole synthesis. Dispersions with ongoing nucleation phases will show a negatively skewed PSD as small particles are continuously formed. Experimentally, the end of nucleation is determined by analysis of  $d_P$  and PSD at the end of the monomer addition stage.

In polymerization reactions available initiator radicals from initiator decomposition (Eq. 3.1) are present in the medium. Monomer addition to the system causes a reaction between the active initiator radical  $I^*$  and a monomer unit  $M$ . Monomer molecules are added to the continuous medium, where it is attached to initiator radicals and produces oligomer chains:



Addition of monomer units to an active chain takes place until the oligomer reaches a critical length  $j_{crit}$  where it becomes insoluble in the aqueous medium. Due to the increase in hydrophobicity it either diffuses into a readily available colloidal structure (micell) or colloidal stabilizer diffuses to the oligomer to form a colloidal stabilizing cage around the now water-insoluble oligomer. Further polymerization of these active chains proceeds only inside the colloidal stabilized structures. The polymer radical stays active until another active radical enters the reaction loci and termination of both active chains occurs. Radical desorption might occur as a radical is, in principle, able to leave the colloidal structure. Influence on radical

---

\*If not stated otherwise particle diameters used for calculations were determined by PDW spectroscopy.

desorption rate  $k_d$  by the number of particles and further is described by ASUA.<sup>2</sup>

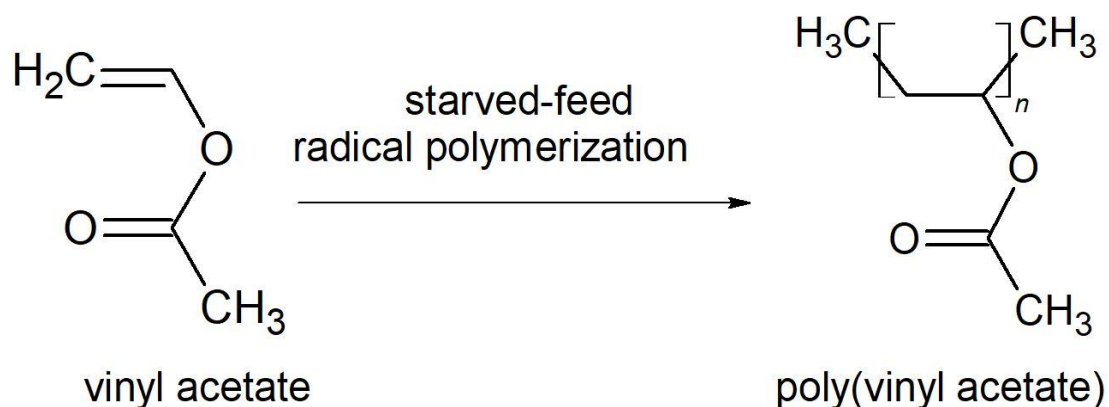


Figure 2 Free radical polymerization scheme of vinyl acetate monomer by radical cleavage of vinyl C=C double bond and subsequent polymerization.

In semi-continuous emulsion polymerization monomer is added subsequently to the system. In this special case aqueous initiator solution is also added causing a significant change in volume  $V$  to the system. This change is even more pronounced in the beginning of the reaction when the overall volume  $V$  is still small. According to WESSELING the expression of the rate of polymerization  $R_P$  then changes to:<sup>20</sup>

$$R_P = \frac{d[M]}{dt} = k_P[M][M^*] - \left(\frac{m_M}{V^2}\right)\left(\frac{dV}{dt}\right) \quad (3.6)$$

With  $m_M$  as moles of Monomer converted to polymer. As calculations with molar rates are difficult to standardize it is simplified to:

$$\frac{dm}{dt} = k_P \frac{[MM^*]}{V} \quad (3.7)$$

The kinetics of polymerization within the latex particle follow this equation (3.7) but the macroscopic rate (total rate of conversion) is a measured variable. In order to deduce the total rate, further calculations are necessary.<sup>21</sup> Even if the reaction volume changes, the number of particles  $N_P$  is the limiting factor for  $k_P$ . If  $N_P$  stays constant,  $k_P$  is controlled by  $R_a$ , the rate of monomer addition, also reaching a constant value. If secondary nucleation occurs  $N_P$  increases and determining  $k_P$  gets more complicated.

To avoid secondary nucleation in the experiments the total amount of protective colloid PVA was kept at a constant high level, monomer was feed at very low feed rates and stirring of the reaction mixture was high to create homogeneous systems. The concentration of colloidal

stabilizer influences the dispersion properties and also early particle nucleation activity. If the concentration stays below the critical micellar concentration (*cmc*) homogenous nucleation is dominant. The amount of stabilizer is not sufficient to create colloidal structures yet.

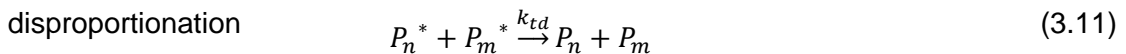
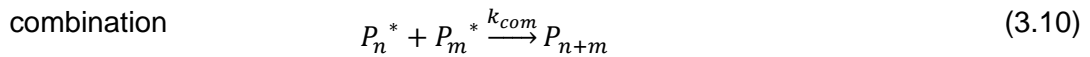
### 5.1.3 Particle growth and termination

Particle nucleation and growth are competing processes occurring at the same time. Monomer starved conditions generally lead to a higher number of particles.<sup>22</sup> Commonly it is defined that polymerization phase II starts, as  $N_p$  stays constant with the diminishing of particle nucleation. Monomer  $M$  is added continuously to active polymer chains  $P_n$ . The instant conversion of monomer to polymer is very high in the beginning. By adding only little amount of monomer to the system the ratio  $[P]_p / [M]_p$  of polymer in the active particle  $[P]_p$  to monomer inside the particle  $[M]_p$  is high. This ratio is defined by the diffusion of active monomer and oligomer chains from the medium into the active particles. As nucleation stops, particle growth dominates the reaction. Conversion stays low as no additional active radicals are formed.



$$\mu_g = \frac{R_a}{N_p} \quad (3.9)$$

As long as monomer is added to the system, growth  $\mu_g$  is the dominant process. A larger number of particles are created as the growth rate is reduced by the monomer rate of addition. As larger particles tend to grow and smaller particles are neglected by small  $R_a$  a positive skewness of the PSD might result from monomer-starved conditions. To avoid this and to create a symmetrical monomodal PSD,  $R_a$  is kept low and concentration of colloidal stabilizer and initiator are high. Termination reactions may not be neglected, however due to the addition of initiator solution the polymerization is kept alive. Only if monomer addition is stopped the depletion of monomer causes the chains to terminate each other. The most prominent ways of terminating an active polymer chain are stated below.



With  $k_{com}$  as rate constant for the combination of two active polymer chain radicals to form one inactive chain of combined length and  $k_{td}$  the rate of disproportionation to create two dormant polymer chains with varying length. Further, chain transfer reactions are involved in the

termination process, Chain transfer process cannot be neglected as it is likely to occur.<sup>23</sup> However, this is not focus of this work and will not be discussed further.

#### 5.1.4 Aggregation

Stabilized polymer particles in solution are clearly separated from each other and each particle is freely movable in its surrounding. The stabilization of the dispersion is caused by the systemic electrochemical double layer surrounding each particle. The diffuse electrochemical double layer consists of an inner and outer shell forming around the particle. If this sensible equilibrium between the forces in-between the particles gets interrupted, the particles in dispersion will start to aggregate. Different factors might cause particle aggregation. For example, electrochemical changes to the system may cause aggregation as the electrostatic equilibrium is shifted. At too high solid content or too less colloidal stabilizer, the particles get too close to each other and the electrochemical double layer is distorted or deformed and particles collapse together to aggregates.

This is described by DLVO THEORY and shown in Figure 3. Figure 3 shows the total interaction potential energy  $E_T$  in dependency of the particle distance of two particles to each other.  $E_T$  is a combination of the repulsive electrostatic and VAN DER WAALS attractive potential forces between particles in solution. The closer two particles get to each other they reach distinctive energy barriers. A decreasing particle distance causes the particles to fall within the secondary minimum, in which reversible aggregation occurs. The aggregation might be reversed by adding medium to the particles or increasing the ion strength of the medium. If particles are reaching even smaller inter particle distances the high energy barrier is overcome and irreversible agglomeration of particles happens in the primary minimum.

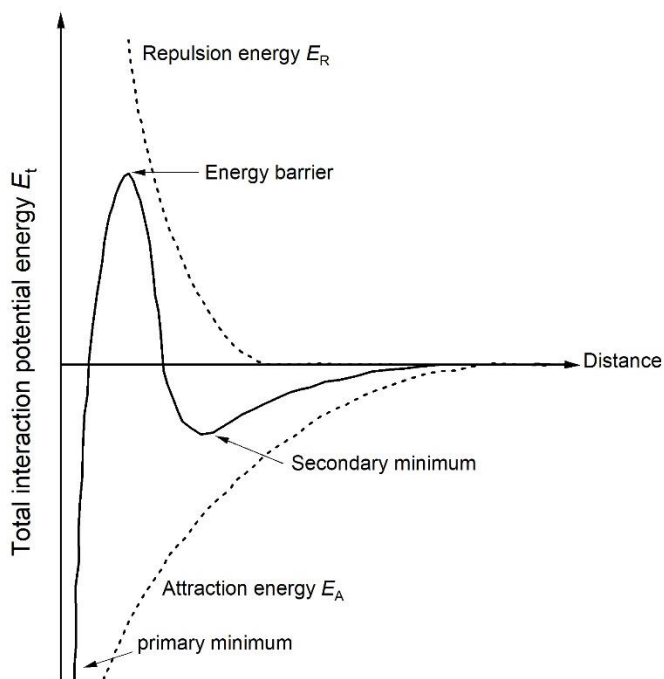


Figure 3 DLVO theory of colloidal particle stabilization based on the electrochemical double layer of the particle and the distance between the individual particles in dispersion.

### 5.1.5 Starved feed emulsion polymerization

In addition to batch process emulsion polymerizations, in this work reactions have been done in semi-continuous operation. Aqueous initiator solution and monomer are continuously fed into the reactor at low feed rates, deliberately slower than  $R_p$ . No product is drawn from the reactor during the synthesis. The monomer added to the system supposedly reacts immediately, no particle swelling of droplets with monomer occurs. The reaction system is purposely kept in the monomer depletion phase. Contrary to batch emulsion polymerization reactions where the rate of particle growth is controlled by diffusion of monomer from the monomer reservoirs to the active particles, in starved-feed synthesis no such monomer reservoirs exist and the rate of particle growth can be controlled via the rate of monomer addition.<sup>20,24</sup> The monomer concentration in already formed polymer particles, as well as in the medium is kept very low. Inhibition periods of a few minutes are common due to remaining inhibitor in the monomer. These can alter the starved feed process as accumulation of monomer might occur. These inhibition periods can be shortened by sufficient mixing of the reaction solution and an excess of radicals in the medium by continuous feeding of initiator solution.

If a polymerization is held at monomer-starved conditions, it is continuously ranging in polymerization interval  $|||$ . According to SAJJADI<sup>22,25–27</sup> monomer starved semi-continuous polymerizations lead to number of particles higher than in conventional emulsion polymerization in the range of  $10^{18}$  to  $10^{20}$  L<sup>-1</sup>. Figure 4 shows exemplarily five experiments

conducted during this research and the respective number of particles and average particle diameter  $d_p$  measured by PDW spectroscopy. All syntheses show  $10^{18} \text{ L}^{-1}$  number of particles.

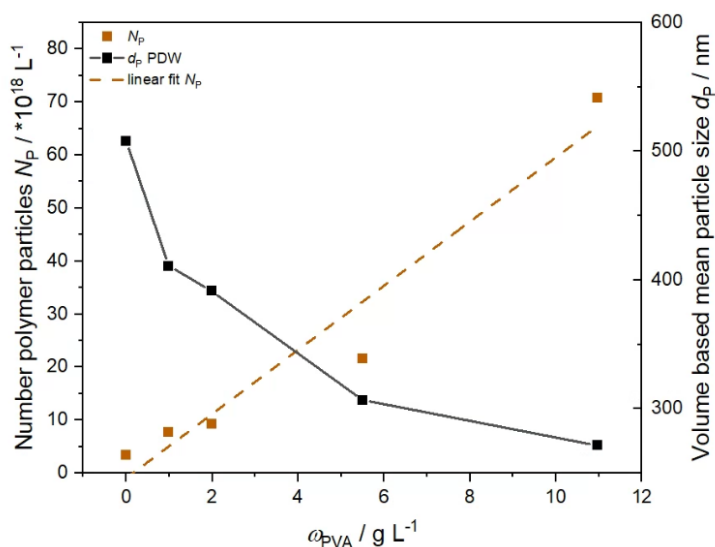


Figure 4 PVAc homopolymerization under presumed monomer starved conditions. Number of particles  $N_p$  calculated and mean diameter  $d_p$  produced, measured by PDW spectroscopy.

It is also possible to use an already polymerized dispersion containing seed particles and further polymerize additional layers onto the pre-existing particles (seed polystyrene syntheses in this work, cf. 5.2). From starved-feed synthesis particles with specifically controlled sizes and morphologies can be produced. Especially in copolymerization the starved-feed approach is used to design polymers with a specific copolymer composition. A crucial aspect of starved feed syntheses is to avoid secondary nucleation and a resulting skewness or polydispersity of the particle size distribution. Secondary nucleation can occur when an initiated radical or oligomer encounters an empty micelle, terminates in solution or the polymer chain precipitates before the radical reaches a growing particle. To avoid secondary nucleation, one can adjust several parameters of the system: the radical concentration, the total amount of protective colloid, the monomer concentration, and mixing of the reaction mixture. The radical concentration depends on the initiators decomposition rate  $k_{\text{ini}}$ . It influences the number of active chains in the system. It must not fall below a certain level, as instantaneous conversion of monomer would decrease and monomer might accumulate in the system, preventing starved-feed conditions. In practical implementation, it is essential to ensure that the feed is introduced at the point of optimal mixing within the reactor to prevent the formation of a monomer layer.

Due to addition of initiator solution and monomer during the semi-continuous syntheses, the overall reaction volume does not stay constant. The system experiences more complicated kinetics than in a constant-volume batch reaction. The reaction system needs to be kept stable



and the polymerization running by addition of initiator molecules while maintaining a small average radical number.

## 5.2 Polyvinyl acetate synthesis

Vinyl acetate (VAc) and its polymers have been widely used, developed and intensively analyzed since the early days of polymerization theory.<sup>28,29</sup> In 2022 approx. 6.6 million tons of VAc monomer were produced globally. This number is estimated to grow more than 4 % in an industry forecast,<sup>30</sup> especially in the paint, coatings and sealants chemical industry in various applications, forms and polymer variations.<sup>31</sup> The polymerization of VAc proceeds only via free-radical mechanism.<sup>32</sup> Reaction temperatures above 60 °C are necessary to guarantee high conversion of VAc monomer.<sup>18</sup> Below 50 °C high amounts of residual monomer were still present in the reaction mixture. The polymerization of VAc to polyvinyl acetate (PVAc) by emulsion polymerization investigated in this work, is based on the Patent No.US 9,650,507 B2 by H. ZECHA and H.-P. WEITZEL of WACKER CHEMIE AG (Munich, Germany).<sup>33</sup> The patent describes different methods for the protective-colloid stabilized production of polyvinyl esters in aqueous dispersions by free radically initiated emulsion polymerization. High solid content dispersions of PVAc are created by use of different protective colloids and their respective concentration as well as different types of Redox initiator systems and their concentration. As a result, stable, high solid content, aqueous dispersions with various mean particle diameter  $d_P$  and PSD are obtained. The methods of the patent have been analyzed and syntheses have been recreated accordingly. A full list of experiments can be found in the appendix from Table 4 ff.

To show examples of the PVAc particles produced, Figures 5 to 7 show Scanning Transmission Electron Microscopy (STEM) and Transmission Electron Microscopy (TEM) images, as indicated respectively, of the PVAc homopolymers. An electron beam is used on dry samples in a vacuum chamber to image the polymer particles on the sample grid. The electrons are emitted from an electron source, focused to a beam and onto the sample. After interaction with the sample, i.e. the particle electrons of various energy are scattered back to the detector where an image is created.<sup>34,35</sup> Specific EM settings are given where appropriate.

Spherical particles with various particle diameters have been produced throughout the experiments. It can be seen that the particles within one sample show a distinctive size distribution. Some particles are observed that have a smaller diameter than some others within the same sample. The particles are mostly separated from each other. Small clusters of few particles are visible, especially in Figure 6, which might have aggregated in the dispersion already or the aggregation might have occurred due to the sample preparation and drying of the sample for electron microscopy analysis.

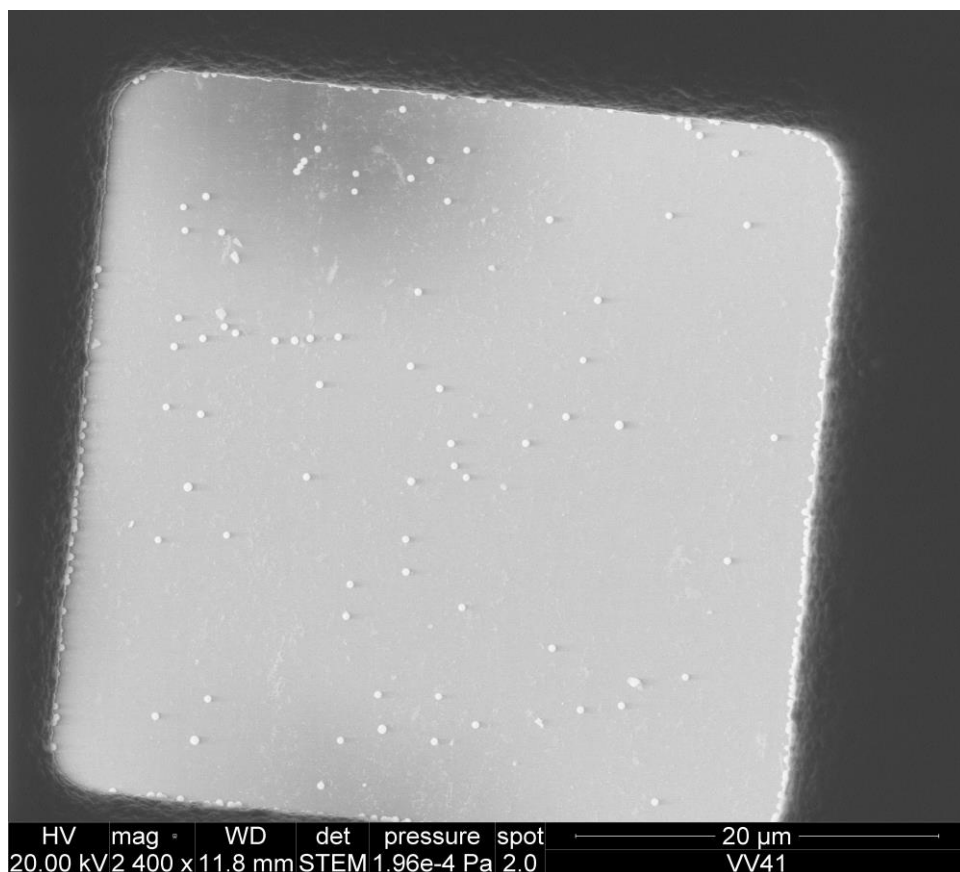


*Figure 5 STEM image of PVAc homopolymer produced with 5 g L<sup>-1</sup> PVA in the initial charge. Highly diluted sample. Particles show a mean diameter of approximately  $274 \pm 24$  nm determined by Hough Circle Transformation, circularity > 0.5 on 35 particles.*

Mean particle diameter indicated have been analyzed with an automated FIJI Image J statistical evaluation of circular shapes. A circularity threshold was set to > 0.5. Hough Circle Transformation was used as method of choice for detecting the circular shapes.<sup>36</sup>

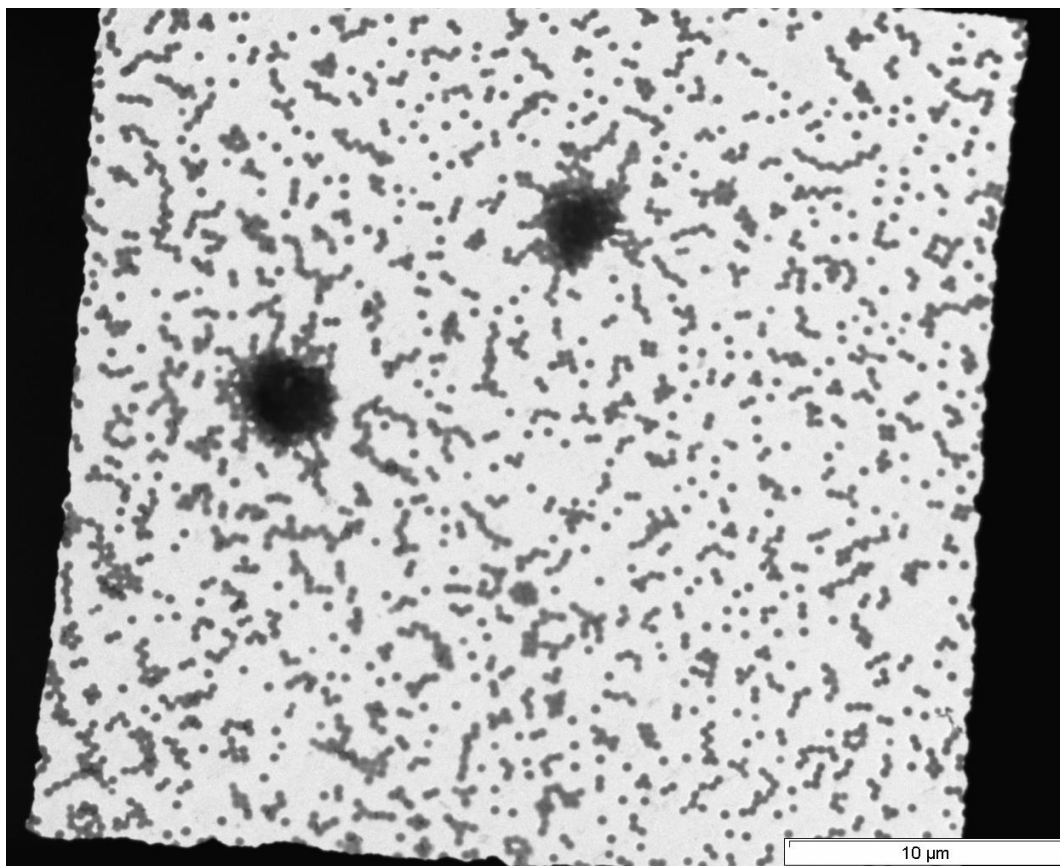


*Figure 6 TEM image of PVAc homopolymer particles produced during this research. Synthesis with 1 g L<sup>-1</sup> PVA in the initial charge. Mean  $d_p$  of approximately  $445 \pm 38$  nm determined by Hough Circle Transformation, circularity > 0.5 on 557 particles.*

Figure 6 shows two particle clusters in the size of up to 5  $\mu\text{m}$ , i.e. aggregates of particles in the sample. The aggregation is evident as many particles are close together and not clearly separated from each other anymore. Particles are possibly aggregated in a spherical shape on the copper grid. It can however not be deduced from the image whether the aggregation already happened in the dispersion or the sample preparation for TEM caused the particles to aggregate. Further it cannot be observed whether the aggregation is irreversible or merely a reversible flocculation occurred due to the convergence of particles by TEM sample preparation. Dispersions prepared during this research stayed colloidal dispersed and stable over a period of more than 4 years, stored in airtight containers at room temperature. At continuous sampling from the produced dispersions, a little amount of dried sample (PVAc glue) was removed from the screw caps and samples were used for further analysis without further purification or sample preparation, except indicated otherwise.

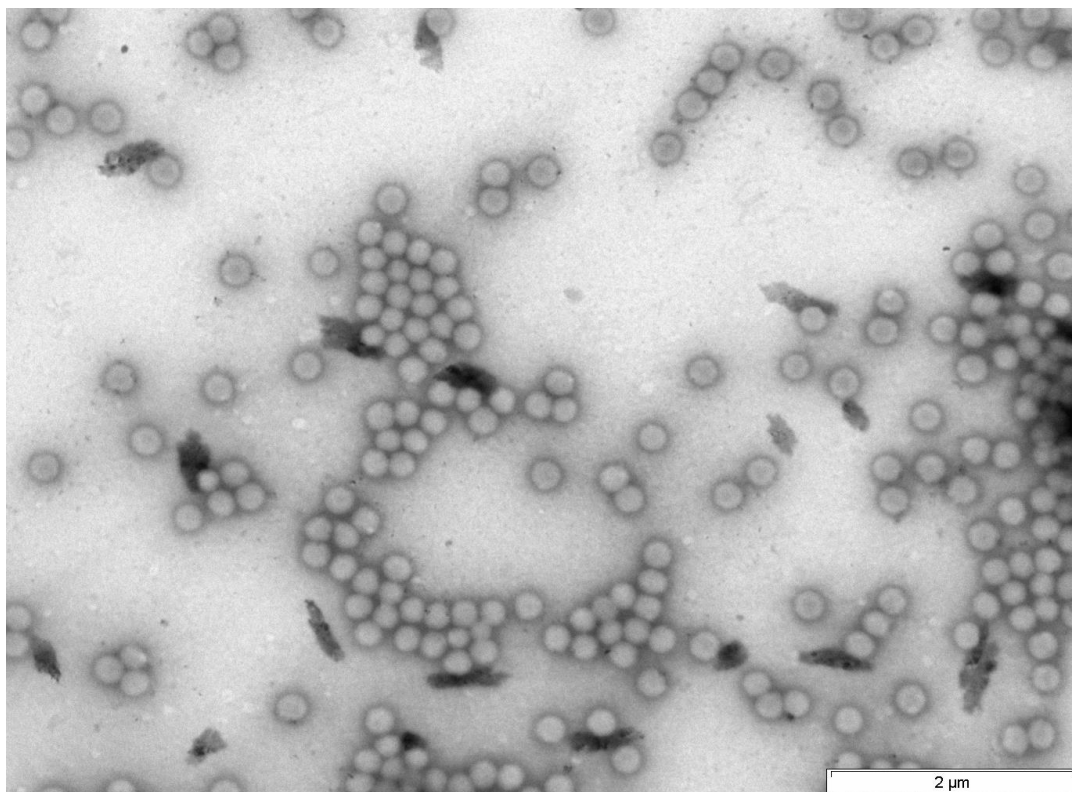


Figure 7 TEM image of PVAc homopolymer particles produced during this research. Synthesis with  $11 \text{ g L}^{-1}$  PVA in the initial charge. Mean  $d_p$  of approximately  $238 \pm 17 \text{ nm}$  determined by Hough Circle Transformation, circularity  $> 0.5$  on 42 particles.

### 3.2.1 Copolymerization VAc:Versa® 10

Another system studied in this research was the copolymerization of VAc and vinyl neodecanoate (trade name Versa® 10). Versa® 10 is a commonly used co-monomer for VAc. The resulting copolymer is used as well in the paints and coatings industry especially in sealants for inorganic substrates like brick or concrete.<sup>16</sup> Due to its bulky and hydrophilic structure it inhibits the hydrolyzation of the nearby acetate blocks in the co-polymer. Reaction strategies to optimize the co-polymerization have been already studied.<sup>37</sup> For this system the polymerization method of choice has to be semi-continuous starved feed emulsion polymerization as reported by BOHÓRQUEZ and ASUA. A batch reaction resulted in irreversible aggregation of the polymer particles and unfolds safety issues regarding the strong heat generation of the copolymerization.<sup>38</sup> As the copolymer is however used in industry nowadays it is important to find a proper method of inline safety control and PAT to maintain safe production cycles for the producing manufacturers. This aspect has been deeply analyzed by JACOB<sup>39</sup> and further as part of this thesis in chapter 5.3.

### 3.2.2 Polyvinyl alcohol as stabilizing agent

As synthetic homopolymer polyvinyl alcohol (PVA) has gained attention in the polymer synthesis field due to numerous reasons. Its low-risk character, cheap price and full

biodegradability are useful characteristics when producing polymers in a sustainable and green way. It is commonly produced by the partial hydrolysis of polyvinyl acetate. Nowadays products with 4 % - 12 % hydrolysis degree can be purchased. The hydrophobic acetate groups added by hydrolyzation adds an amphiphilic character to the homopolymer and increases attachment to hydrophobic surfaces.<sup>40</sup> It is used in many fields of daily life, like medical treatment for burns in hydrogels, in cement-composites as construction material, in paints and coatings as polymer adjuvant and many more. PVA high molecular weight-based polymers (as used here as Mowiol 4-88® ~ 31.000 g mol<sup>-1</sup>) define as polymeric surfactants, known and used as colloidal stabilizing and thickening agents. Due to the high stability and low toxicity they are used in the food and pharmaceutical industry.<sup>40,41</sup> Due to its chemical structure it is prone to water absorption, as many hydroxyl groups are available in its polymeric matrix.<sup>42</sup> It is used in countless composites with other materials to enhance defined characteristics as for example tensile strength, elastic modulus and elongation.<sup>43</sup>

In this research polyvinyl alcohol, a colloidal stabilizer, was used to stabilize the formed particles. It is commonly known that polyvinyl alcohol, forms colloidal structures, that stabilize high concentrated polymer dispersions. Polyvinyl alcohol can interact via hydrogen bonding to increase the dispersion viscosity and increase the dispersions overall colloidal stability.

Analyzing the specific mechanical characteristics of PVA is most commonly done on PVA and PVA-blend films.<sup>44–46</sup> A film of the PVA material is casted, let dry and put into water. The swelling is then calculated by comparing the dimensions of the dry film with the film after water immersion. This method is widely applied however does not represent how the PVA behaves regarding water absorption in a solvent, or in a polymer dispersion respectively. In this thesis PVA in dispersion will be analyzed regarding its water swelling abilities on PVAc homopolymers in chapter 5.2. PVA is used in this thesis as stabilizing agent for the polymerization of PVAc homo- and copolymers. Due to its chemical structure and available hydroxyl group it has been investigated to bound water in different states.<sup>42,44</sup> These states are defined as:

- **Freezable bound water:** Water molecules are weakly bound to the polymer chain. Melting occurs at elevated temperatures due to weak interactions between the freezable bound water molecules and PVA molecule.
- **Non-freezable water:** Water molecules are strongly bound to the hydroxyl groups. No thermal transition is observed during differential scanning calorimetry (DSC) measurements.
- **Free water:** Water molecules that exhibit the same properties as the surrounding bulk water.

### 3.3 Process analytical technologies<sup>\*gAI</sup>

Smart sensors and monitoring techniques of (polymerization) processes are gaining more and more attention and momentum in the community. The implementation of smart sensors which guarantee safe, cost effective and reproducible processes has its origin in the U.S. pharma industry only as late as the early 2000s.<sup>47</sup> Still up to date most processes are evaluated and optimized after trial-and-error principles wasting time, money and resources based on historical evolution of scientific methods.<sup>48–51</sup> By definition, process analytical technologies (PAT) offer measurements of critical time dependent process parameters. These measurements are implemented regularly into a process to gain process understanding and maintain quality assurance.<sup>52–54</sup> Implementation of PAT indicates an approach away from trial-and-error. A deep understanding of the process is derived with significant economic and scientific impacts. Understanding the process in its multi-functionalities delivers options for process control as deviations from safe and regular production process are measured and visualized. Visualization of a time dependent defined parameter of the reaction can be easily used to detect irregularities. Nowadays a wide variety of PAT is readily available at the market. This PAT toolbox is equipped with thermocouples, pressure sensors and multiple spectroscopic methods.<sup>55,56</sup> Figure 8 shows the applied golden batch concept exemplarily. Via PDW spectroscopy as PAT the measured optical coefficients are necessary to stay within predetermined limits to achieve optimal reaction conditions and respective dispersion and particle properties in the final product. Figure 8 shows two identical synthesis of PVAc homopolymers. Advantages of inline PAT are the real-time data acquisition analogous to the progress of the process. Time dependent data on the reaction components and reaction progress is studied. The green area corresponds to the limits in which the reduced scattering coefficient  $\mu_s'$  needs to be in order to produce consistent polymer products. Both experiments shown here agree to the golden batch conditions. Strong and unexpected deviations from the anticipated trajectory of the trend also indicate malfunctions in the process. This has been shown and evaluated in the published research in chapter 5.1. In such a multifunctional system nearly every parameter can be used for process control via PAT monitoring. Thermal properties, concentration of the components, pressure, mechanical properties and optical properties are just few examples.<sup>57</sup>

---

<sup>\*gAI</sup> This paragraph has been drafted and written by the author. Proofreading has been done using generative AI via perplexity.ai.



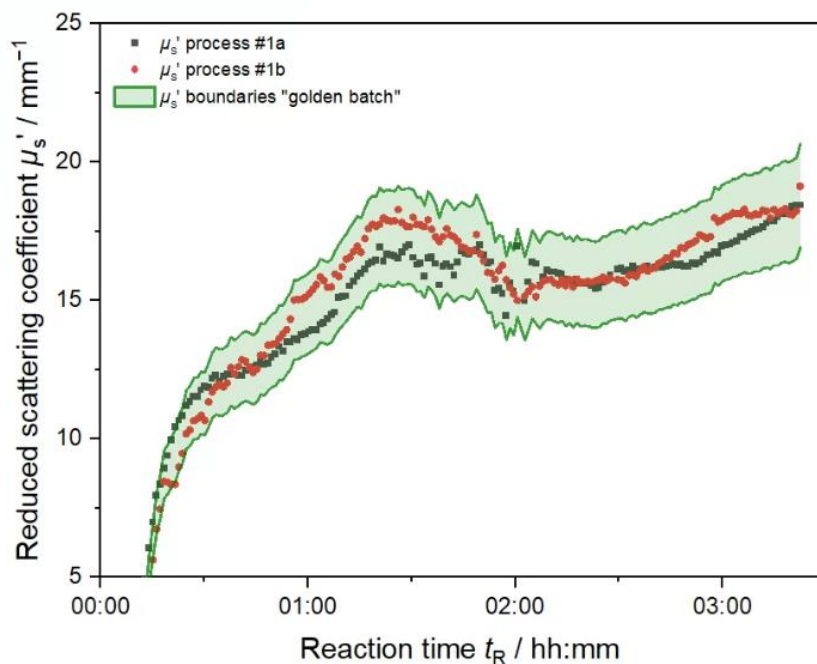


Figure 8 Concept golden batch measurements by PDW spectroscopy with limits to  $\mu_s'$  by percentile deviation from the process indicated by the green area.

A differentiation between inline, atline, online and offline PAT measurements is at hand where

- **Inline** parameters are measured during the process inside the process vessel in the process stream.
- **Online** parameters are measured during the process at the process site but outside the process vessel itself in a bypass or sample which is then redispersed into the process.
- **Atline** parameters are measured during the process at the process site but outside the process vessel in a sample.
- **Offline** parameters are not necessarily measured during the process. Samples are drawn and analyzed, possibly at a later point in time.

Whereas inline and online are often used interchangeably, a clear differentiation is not retained in literature. In this work process measurements by PDW spectroscopy are defined as inline measurements as the PDW spectroscopy probe is directly inserted into the reaction vessel and process stream. Advantages of inline PAT, especially in polymerization reactions comes with the omission of sampling and sample dilution. Dilution of a sample always induced changes to the system. Polymer particles in solution behave differently as dried samples or diluted samples.<sup>58</sup> Overall changes in absorption of the dispersion, changes in ionic strength, conductivity and interactions between particles can be induced by dilution. Therefore, dilution-based measurements might not reflect the same values as the inline PAT approach. The

determination of the real PSD in polymer dispersions remains a critical challenge in emulsion polymerization research and especially for industrial applications. Real-time, in situ measurement of PSD is essential for maintain a good product quality. Offline PSD analysis of polymer dispersions is used in most quality assurance laboratories today as state of the art but is still challenging. Several studies were conducted that show for monomodal, monodisperse latexes, light scattering measurements like Dynamic Light Scattering (DLS) and Static Light Scattering (SLS) are able to determine the average particle size. Offline PSD measurement technologies are still prone to be erroneous and do not reflect the actual conditions in the sample. Sampling, dilution of the sample, and analysis over several minutes renders them inadequate for capturing rapid changes in PSD during polymerizations. The development of accurate, rapid, and in situ PSD measurement techniques remains a crucial area for future research in emulsion polymerization, as it would significantly enhance the understanding of particle evolution dynamics and improve process control strategies.

Offline sampling changes the polymerization kinetics, as reduction in pressure and temperature affect the sample. Even quenching alters the process by addition of a dilute quenching agent. Effects on the polymer particles can be swelling of the polymer particles, aggregation or possible disintegration.<sup>59–61</sup> The representative sampling of such complicated multiphase systems is unhandy and hardly reproducible. Unreacted monomer and the viscosity of the dispersion can induce heterogeneity inside the reactor. As polymer reactions are often done at distinctive high temperatures and high pressures, as well as toxic chemicals might be involved sampling also induces a risk to the worker. PAT is potentially able to reduce offline sampling and time-consuming analysis in polymer industry and subsequent analysis.

Using PAT to monitor scale-up processes can help creating reproducible product qualities over a production scale range. It is used for risk management and minimization in possible runaway polymerization reactions. For scale up emulsion polymerization processes are beneficial as water as medium has very high heat capacities minimizing the risk of runaway reactions and gelation.<sup>62</sup> As polymerization reactions are exothermic reactions possibility of thermal runaway reactions is always a specific safety measure. Rapid changes in the temperature can have different reasons. The primary causes of accidents in general in the chemical production industry are technical failures. Additionally, human failures, and the chemical reaction itself. Lack of process knowledge and thermo- and the reaction kinetics thereof. PAT can be implemented into processes to avert accidents, save money and time and to guarantee the workers and process safety. Emulsion polymerization derisks some of the critical safety issues of suspension polymerization processes due to maintaining low viscosity throughout the process and supportive heat removal by the aqueous medium. However sudden conversion of accumulated monomer, wrong stoichiometric parameters in reaction components, too high



reaction temperature and/or failing of the cooling system can lead to runaway reactions with severe damages and accidents.<sup>63</sup>

### 3.3.1 PAT implementation into reactor

To maintain continuous data acquisition and inline monitoring the used reactors have been equipped with an inlet for the PDW spectroscopy probe. The PDW spectroscopy probe is inserted into the initial charge (*iC*) of the reaction mixture so that all eight fiber tips of the probe reach into the reaction mixture even if stirring of the mixture is applied. A schematic set-up can be seen in Figure 9. The creation of a vortex while stirring needs to be taken into account and the probe has to be adjusted accordingly if the fiber tips are not immersed in the *iC* while stirring.

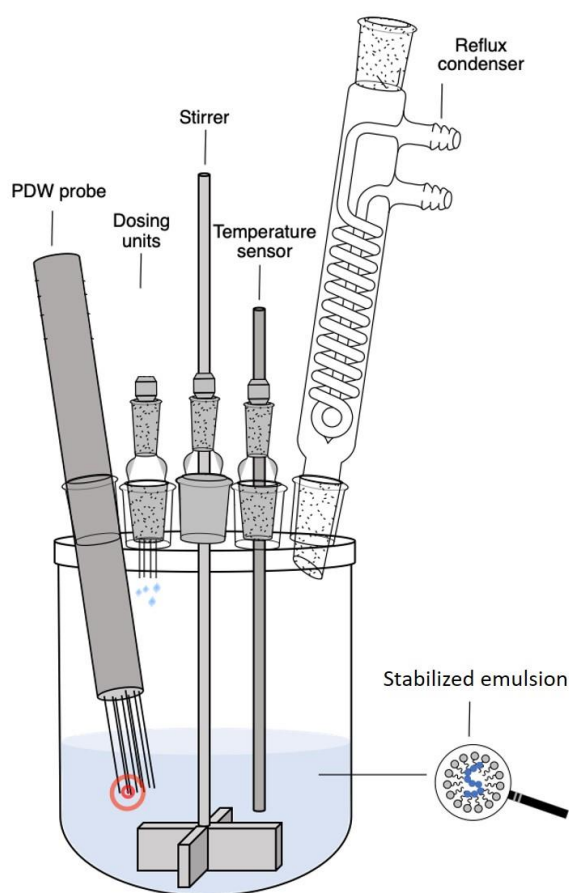


Figure 9 Schematic representation of inline PDW spectroscopy measurement inside the reaction vessel in the process stream. © L. J. Brenker, 2020, reprinted with permission from the author.<sup>64</sup>

Reactions at 1 L scale have been done in an automated reactor system OptiMax 1001 by Mettler Toledo (Gießen, Germany).<sup>65</sup> The system is equipped with automated temperature, pressure, dosing and stirrer control by an automated process control system. Therefore, data on temperature etc. is acquisitioned in real time and is readily available in addition to implemented PAT probes. The reaction vessel is equipped with a stirrer, a temperature sensor and the PDW spectroscopy probe. Further a reflux condenser is used and a dosing inlet for

dosing of individual components to the reactor. No pre-emulsion was formed in order to demote conditions for miniemulsion polymerization and the resulting skewness of the PSD to smaller particle sizes.

### 3.4 Photon Density Wave spectroscopy

Photon Density Wave spectroscopy as a spectroscopic technique has been developed at INNOFSPEC POTSDAM<sup>66</sup> for the last 20 years. Especially the works by REICH, HASS and BRESSEL at the group of PROF. LÖHMANNSRÖBEN at UNIVERSITY OF POTSDAM developed and enhanced the technique<sup>67–69</sup> to an industrially applicable level. The inline analysis of polymer and other high solid content dispersions gained interest in the recent years in the process analytics community. Photon Density Wave spectroscopy is a new but highly relevant technique. Its progress from basic principles and understanding to real-life application has been published in various research articles.<sup>39,70–74</sup>

In general, it is a method for the independent determination of the optical properties, the absorption coefficient  $\mu_a$  and the reduced scattering coefficient  $\mu_s'$  of a sample. Since it allows for the separation of absorption and scattering properties, chemical information can be derived from  $\mu_a$ , and structural information can be obtained from  $\mu_s'$ . Measurements of the absorption coefficient are indeed measurements of the uptake of energy of molecules (or atoms). On a microscopic level the absorption coefficient of a sample gives information about its physical and chemical composition, e.g. temperature. In low concentration ranges, the absorption of a sample can be described by the LAMBERT-BEER law, however in emulsion polymerization high solid contents are quickly achieved and LAMBERT-BEER is not valid anymore due to interactions in between the particles.<sup>67</sup> As the absorption coefficient does not play such a significant role in this dissertation it is not discussed in detail. The focus is on the reduced scattering coefficient  $\mu_s'$  and polymer particle size derived from  $\mu_s'$ .

The fundamentals of PDW spectroscopy are described in detail by REICH<sup>67</sup>, HASS<sup>68</sup> and BRESSEL.<sup>69</sup> As basic measurement principle counts the phase and intensity shift of a photon density wave introduced to a sample. The photon density is hereby described as temporal and spatial variation of photons within a defined volume. The temporal change in the photon density is only affected by interactions with the analyzed sample, i.e. absorption and scattering. The absorption causes a decrease in the photon density, whereas the scattering is direction dependent and might cause either a de- or increase in the photon density. Scattering in the direction of the light source causes an increase, scattering in any direction other than the initial light source will cause a decrease in the overall scattering intensity. Combining all these effects leads to the overall radiative transport theory equation based on BOLTZMANN-transport theory. To solve the radiative transport theory equation a so called P1 approximation is used, assuming that the PDW evolved spherically in the sample. Hence the assumption and prerequisite of a spherical, point like light source (isotropic optical fiber) as emission fiber. Further this approximation accounts for the assumptions that the scattering within the sample needs to be much higher than the absorption, see equation 3.14 in 3.4.1 below.

Experimentally two coefficients can be derived, the reduction of the introduced intensity  $I$  by an intensity coefficient  $k_i$  and the phase shift of the PDW  $k_\phi^*$ . To determine the optical coefficient  $\mu_a$  and  $\mu_s'$  the photon density needs to be analyzed as a function of the distance between the detection and emission fiber  $d_f$  and the used modulation frequency  $f$  of the measurement. If  $k_i$ ,  $k_\phi$ , and photon density are calculated as functions of distance and modulation frequency, with alterations in  $\mu_a$  and  $\mu_s'$  these can be determined by fitting the theoretical photon density and phase to the experimentally determined values. This is done by a global fit analysis. A deviation in theoretical and experimentally derived values will occur. This difference is minimized by minimizing the sum of the weighted quadratic errors  $\chi^2$  between theory and the experiment for all used distances and modulation frequencies.

### 3.4.1 Transformation of experimentally determined $\mu_s'$ to particle diameter $d$

For the investigation of dependent scattering and determination of particle size from  $\mu_s'$ , a separation of the scattering and absorbing properties is necessary. The relevant parameter in PDW spectroscopy for polymer particle analysis is the reduced scattering coefficient  $\mu_s'$ . To determine the particle diameter from the experimentally derived reduced scattering coefficient  $\mu_s'$ , the following assumptions about the dispersed particles have to be made:

- The dispersed particles are spherical particles with a diameter  $d$ .
- The dispersed particles have a distinctive volume fraction  $\phi$ , which can be measured by gravimetric analysis.
- The dried particles do not differ in volume nor density from the dispersed particles in liquid.
- For multiple scattering to occur,  $\phi$  must not be too low. At very low volume fractions ( $\phi < 0.05$ ) based on MIE theory of independent scattering and further assumptions of the particles geometry,  $\mu_s'$  is related to the particle diameter by the scattering efficiency  $Q_s$  and further dispersion properties:

$$\mu_s' = \frac{3\phi}{2d} Q_s [1 - g] \quad (3.12)$$

These dispersion properties are the volume fraction  $\phi$  and the anisotropy factor  $g$ , which is calculated by MIE theory, too. For volume fractions higher  $\phi > 0.05$ , dependent scattering between particles causes a nonlinear deviation in the dependency on  $\phi$  described by:

---

\* the abbreviation  $k_\phi$  for the phase of the photon density does coincide with the nomination  $\phi$  for the volume fraction of a polymer dispersion. It is noted that the phase coefficient  $k_\phi$  and the volume fraction  $\phi$  do not correlate to each other and are two independent variables. Due to overlapping nomination in literature the labelling of both variables is not changed for better understanding and comparison for the reader.

$$\mu_s' = \frac{3\varphi\pi Q_s}{2d} \int_{-1}^1 f(\cos(\theta)) S(\theta, \varphi) [1 - \cos(\theta)] d \cos(\theta) \quad (3.13)$$

- Only hard sphere interactions take place between the dispersed particles.

Further the following assumptions account for the analyzed dispersions:

- Infinite spatial expansion of light within the sample, i.e. the introduced light from the light source cannot be lost by spatial boundaries.
- Dependent multiple scattering of introduced radiation by the laser light source, i.e.

$$\mu_s' \gg \mu_a \quad (3.14)$$

- Statistical normal distribution of the dispersed particles with assumed Gauß distribution of the particles in dispersion.
- Colloidal stability of the dispersion: no or very little aggregation of particles is present in the dispersion.
- The measurement distance between the emission and detection fiber  $d_f$  must be significantly larger than the reciprocal  $\mu_s'$  as multiple scattering is a prerequisite. i.e. between the emission and the detection fiber multiple scattering events need to take place:

$$d_f \gg \frac{1}{\mu_s'} \quad (3.15)$$

If all the assumptions above do apply to the analyzed material, a determination of the particle size is in principle possible. However as will be evident from this research, the determination of the particle size is a complicated and multifactorial mathematical model which needs to comply to real-life particle properties. Even if all the model assumptions are met, determination of particle size is not trivial and additional factors need to be accounted for when applying the models to real-life samples.

Figure 10 shows the dependency of  $\mu_s'$  on the particle diameter  $d$  based on the aforementioned principles. For very small particles  $d < 50$  nm still a linear dependency of  $\mu_s'$  on  $d$  can be observed, based on Rayleigh scattering. With increasing  $d$  the trend oscillates before decreasing again in the higher nanometer and micrometer size regime of  $d$ . Due to the nonlinear trend course two (or more) particle diameters are theoretically possible for one measured value of  $\mu_s'$ . This ambiguity in particle size can be solved by multiple wavelength measurements. Figure 10 shows that for at least two measurement wavelengths only one correct solution of  $d$  is given.

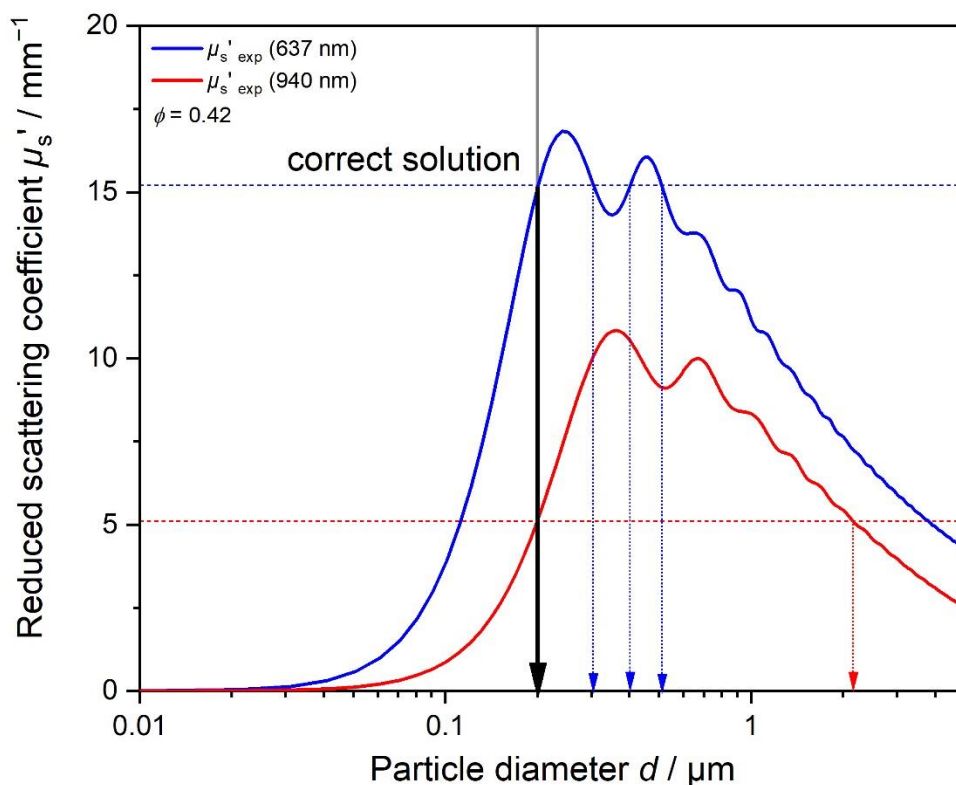


Figure 10 Reduced scattering coefficient  $\mu_s'$  in dependency of particle diameter  $d$ , based on Mie theory. Measurements of PVAc/PVA 5 g L<sup>-1</sup> sample. Ambiguity of two possible solutions for one  $\mu_s'$  value can be solved by multiple wavelength measurements and conformity of one correct solution for the particle diameter  $d$ .

With the current set-up at innoFSPEC up to eight measurement wavelengths can be used between 500 and 1000 nm. The measurement wavelengths used are indicated each time at the respective experiments.

### 3.4.2 Inline PDW spectroscopy measurements

During the synthesis the course of the polymerization reaction is monitored by continuous data acquisition of the temperature, dosing of components and inline PDW spectroscopy measurement of  $\mu_a$  and  $\mu_s'$ . For inline PDW spectroscopy data acquisition a specific PDW spectroscopy probe has been designed. The design and optimization of the probe has been done in-house at INNOFSPEC – UNIVERSITY OF POTSDAM.<sup>66,68</sup> The crucial aspect of the probe design is the smart positioning of the eight optical fibers at the probe head. These are positioned at distinctive distances from each other so that 28 individual fiber distances between 2 - 20 mm are created. This range of the path length between the emission and detection fiber offers a wide range of application without design-changes of the robust probe. Data acquisition time depends on the number of distances and wavelengths used. Usually the resolution

between two data points is in the range of 30 s. As polymer dispersions are highly turbid not all available distances can be used as too little intensity reached the detector at the larger distances. In the measurements shown here only the first 15  $d_i$  were used.

Probe fouling has not been an issue as the smart probe design and photon density based measurement principle offers a very large measurement window in spherical expansion, a local accumulation of particles will not influence the PDW <sup>75,76</sup>.

### 3.4.3 Offline PDW spectroscopy measurements

The produced polymer dispersions are analyzed with a different PDW spectroscopy set-up than the inline PDW spectroscopy probe. The final dispersion products of the emulsion polymerization processes are analyzed offline with a so called PDW spectroscopy table set-up. In comparison to using an inline PDW spectroscopy probe, table measurements are done offline, after completion of the polymer synthesis. Instead of a PDW spectroscopy probe with eight optical fibers with defined distances, two movable optical fibers are directly inserted into the polymer dispersion. One of these fibers acts as the emission fiber, the other respectively as the detection fiber.

THORLABS precision stages with movements possible as low as 0.1 mm are used to move the detection fiber away from the emission fiber. This precise accuracy enhances the quality of the measurements as MIE Theory is highly distance dependent. For very turbid, high solid content samples, small iterative steps in a smaller overall measurement range can be analyzed. Enhanced data quality is achieved. The measurement range can be individually adjusted for each sample by the user.<sup>74</sup> There's no need for sample dilution as the measurement range is adapted individually. As the process of particle formation is already completed in the final dispersions, quick data acquisition is not crucial in these samples. Therefore data quantity and quality are enhanced by using all eight available wavelengths and a large number of fiber distances  $d_i$  (approx. 21) and 41 modulation frequencies leading to a total analysis time of approx. 2 h for ten measurement cycles.

### 3.4.4 Data curation

As data is acquisitioned based on manually set boundaries for the measurement distances  $d_i$  (only for precision offline measurements) and used modulation frequencies data curation after the measurement might be necessary. This is done manually after the experiment has been completed. The initially set number of distances  $d_i$  and modulation frequencies  $f$  can be cut if the signal to noise ratio is too high. Too high noise might be interpreted as valuable data. This leads to errors in the analysis as the used noise does not describe the particulate system. For each experiment data is analyzed thereof and used  $d_i$  and modulation frequencies are cut manually so that a fit of  $k_i$  and  $k\phi$  can be applied by the algorithm. Figure 11 shows this

automated fit exemplarily. Figure 11 shows recorded data without curation. Figure 11 b) shows data curation as modulation frequencies have been reduced from 310 MHz to 220 MHz manually by the user.

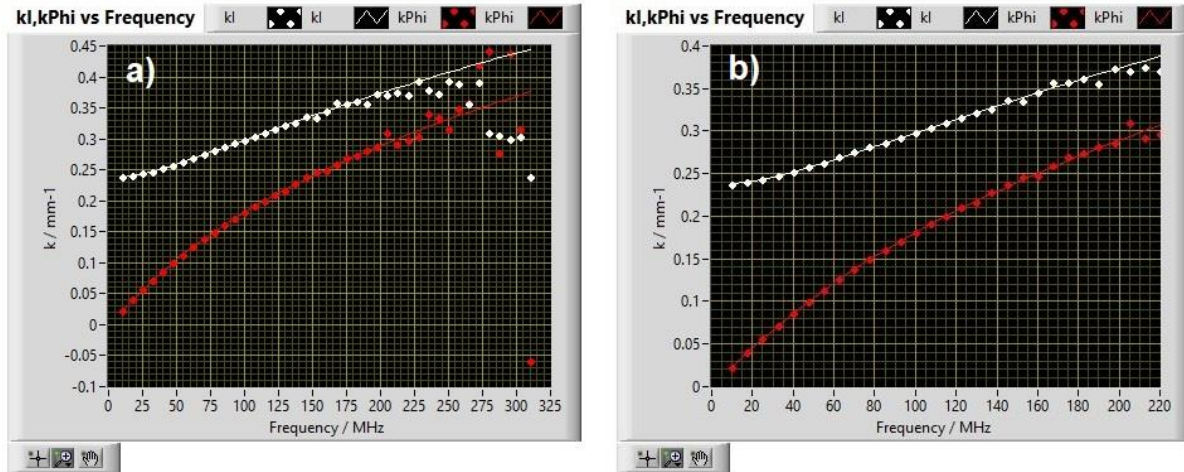


Figure 11. Snapshot from the PDW spectroscopy analysis software. Observation of both coefficients  $k_l$  and  $k_\phi$  in dependency of the modulation frequency  $f$  applied. a) Dataset as measured without data curation. b) Data curation as modulation frequencies involved are cut from 10 - 310 MHz to a shorter range of 10 - 220 MHz to improve fit data.



### 3.5 Polymer Dispersion Analysis

#### 3.5.1 Polymer dispersions

The refractive index of analyzed dispersions can be generally described as

$$n_{Disp} = \sqrt{\sum_i \phi_i n_i^2} \quad (3.16)$$

Using a summed squared weighted approach via the respective volume fraction of each component after Newton. Assuming only one dispersed phase this equation simplifies to:

$$n_{Disp} = \sqrt{\phi_P n_P^2 + (1 - \phi_P) * n_m^2} \quad (3.17)$$

Experimental determination of these parameters has been done accordingly in the laboratory as described below.

Gravimetric solid content analysis was done with approx. 500  $\mu\text{L}$  sample stored in weighted sampling tubes and dried at 72 °C for at least 24 h until mass consistency. Additionally, a small drop of sample was placed on a weighted piece of aluminum foil. The foil was folded together and opened again to create a very thin polymer film on the surface. The aluminum foils were dried in the same matter. After drying, the total weight of the solid residue was taken and handled as solid content of the dispersion at sampling time  $t$ . A solid content measurement consists of at least  $n = 2$  samples. Samples were weighted without purification. Solid content refers to all possible solid residues after drying.

#### 3.5.2 Density of polymer particles in dispersion

To determine the density of the particles in dispersion a concentration series of each polymer dispersion was measured with a densitometer (DM45 Delta Rage, Mettler Toledo, Gießen, Germany). The data was analyzed for the density of the particles (i.e., pure polymer, 100% (w/w)) using the following equation:

$$\rho_{Disp} = \frac{\rho_D \rho_P}{\omega[\rho_D - \rho_P] + \rho_P} \leftrightarrow \frac{1}{\rho_{Disp}} = \omega \left[ \frac{1}{\rho_P} - \frac{1}{\rho_D} \right] + \frac{1}{\rho_D} \quad (3.18)$$

with  $\rho_{Disp}$ ,  $\rho_D$ , and  $\rho_P$  as densities of the dispersion, the dispersant (medium), and the polymer and the solid content  $\omega$  of the dispersion respectively. The density of pure water was considered for zero polymer content (0% (w/w)). The density of the polymer was obtained from the slope of a linear fit; the error was obtained via error propagation.

The density of the polymer needs to be determined in the liquid state as stabilizing agents used are known to incorporate water in their macromolecular structure. For PVA the hydroxyl-groups are known to draw water molecules to the particles and bond water via VAN-DER-WAALS interactions. Therefore, dried polymer samples will not exhibit the same physical properties as liquid dispersed. Throughout the experimental part of this thesis the produced latexes stayed stable and dispersed, showing that the stabilizing ability of PVA is very high. During an experimental run it was tried to separate the particles from the medium by centrifugation and heating of the dispersion. Even after 10 minutes at 4000 g ( $\sim 5000 \text{ min}^{-1}$ ) centrifugation, the solutions stayed stable and dispersed. Only after heating the samples for 24 h in a 120 °C hot oil bath and subsequent centrifugation, separation of the dispersed and continuous phase was achieved. A few milliliters of supernatant were collected and showed a clear yellow color, which might indicate that PVA was present in the supernatant, dissolved from the particles in the dispersion. This supernatant was also analyzed regarding refractive index.

### 3.5.3 Refractive index of polymer particles

The refractive index in general can have real and imaginary parts. It is a measurement of how much the light entering a material is bent or refracted. It is an important optical parameter and often used in material sciences. Refractive indices of polymers have been determined for a very long time. There are literature values for the most common polymers. However, as polymers are such versatile materials it is difficult to set a distinctive refractive index value for a specific type of polymer. To determine the refractive index, commonly measurements with a simple refractometer at the sodium D line ( $\lambda \approx 589 \text{ nm}$ ) are performed. During this work and for further measurements the refractive index over a wavelength range between 400 nm and 1000 nm was determined. The true refractive index of polymer particles is hard to determine as the polymer particle may contain inconsistencies and the physical complex of the polymer particle may consist of different parts, like the hard particle core and soft stabilizing particle shell. The light hitting a polymer particle has to diffuse through multiple different phases and multiple level of refractions are possible. To determine the refractive index of the polymer particles in the dispersion a dilution series is necessary. The same dilution series as described in paragraph 3.5.2 was used. The highly concentrated samples exhibit a too high optical density to be undiluted. Typically, the refractive index of a polymer dispersion decreases with increasing wavelength, examples are shown in Figure 12. It can be seen that with increasing amount of stabilizing agent PVA in the iC (red to purple lines) the refractive index of the produced polymer decreases.

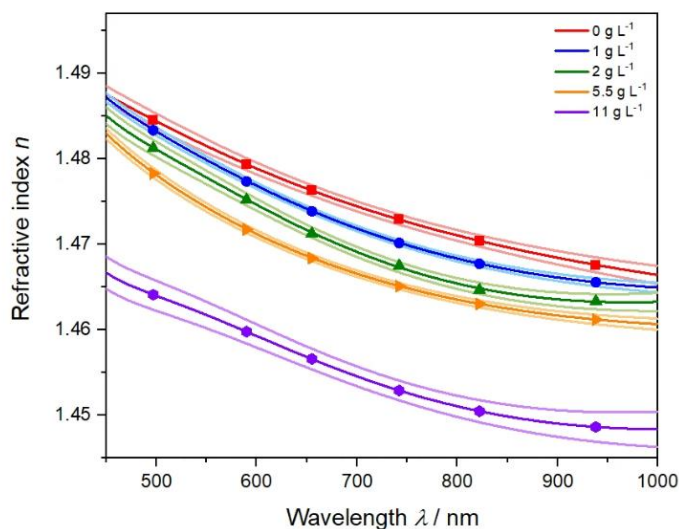


Figure 12 Refractive index measurements extrapolated to 100 % polymer content of an experimental series of five experiments with increasing amount of PVA in the iC from 0 to 11 g L<sup>-1</sup> cf. Table 4 in the appendix.

### 3.5.4 Offline particle size determination

Offline sample analysis was performed after the synthesis was completed. Dynamic light scattering is used as referencing method for offline (polymer-)particle sizing.<sup>77,78</sup> The measuring principle is based on time dependent measurement of the Brownian motion of particles in solution. A laser is guided through the sample and is scattered by the particles. The resulting intensity fluctuations are analyzed at the detector of the system and. From this a translational diffusion coefficient is determined and using Stokes-Einstein relationship the hydrodynamic radius of the particles is determined.<sup>79,80</sup>

Here, DLS analysis was done at a measurement angle of 173° using single-use cuvettes at 25 °C unless stated otherwise at the respective research published. Samples were diluted approx. 400-fold to visual transparency. Two devices were used throughout this research and are mentioned accordingly in the published articles.

Static Light Scattering (SLS) as opposed to DLS measures the photons scattered and averages the scattered signal intensity over time. It will give a mean average intensity over the measured particle population. The Zimm equation can be used to determine the average molecular weight of the measured sample, if the device is calibrated accordingly.<sup>77</sup> From this the radius of gyration of the particles is derived.<sup>78</sup>

Here, SLS measurements (LS13320, Beckman Coulter, Brea, CA, USA) samples were pre-diluted approx. 125-fold with Milli-Q® water and pipetted into the sample chamber. Using Polarization Intensity Differential Scattering (PIDS) as measuring method, the sample was pipetted into the reaction chamber until a PIDS signal of 40 % was achieved. For high quality analysis, low obscuration values beneath 2 % were retained.

### 3.6 Technology readiness level

The technology readiness level (TRL) defines the maturity of a technology to be used in industry nowadays. Historically TRLs were used at NASA to incorporate techniques addressing integrated technology planning, the first TRL scale with seven levels was devised by STAN SADIN in 1974.<sup>81</sup> The chemical industry and other have defined own scales of TRLs with nine levels overall today. TRL1, the lowest level indicates that information is treated and developed into an idea. At TRL9, the highest level, the technology is fully incorporated and running in a larger application environment. A good understanding of the different TRLs for the chemical industry is given by BUCHNER et al.<sup>82</sup>

*Table 2 Technology readiness levels in the chemical industry for technologies described in 1999 by the European Union for uniformity.*<sup>83</sup>

Level	Technology Readiness Explanation
TRL1	Basic principles observed
TRL2	Technology concept formulated
TRL3	Experimental proof-of concept
TRL4	Technology validated in laboratory
TRL5	Technology validated in relevant environment (industrially relevant environment in the case of key enabling technologies)
TRL6	Technology demonstrated in relevant environment (industrially relevant environment in the case of key enabling technologies)
TRL7	System prototype demonstration in operational environment
TRL8	System complete and qualified
TRL9	actual system proven in operational environment (competitive manufacturing in the case of key enabling technologies; or in space)

PDW spectroscopy was defined as TRL 5 - 6 by the definitions of the European Commission, Horizon 2020 Framework H2020 shown in Table 2, as it is used in industrially environments on different applications in projects which are funded by HORIZON2020. H2020 delivers only brief TRL definitions, as the TRLs are used to ensure that funded projects cover the full range of research and development activities. Table 2 is extracted from Part 19 – Commission Decision C(2014)4995.<sup>83</sup> Within a project a higher TRL can be achieved. Within the limits of this thesis and experimental procedure the aforementioned TRL 6 could be manifested as PDW spectroscopy was successfully applied in inline monitoring of up to 100 L reaction volume based on the industrially relevant polymerization of VAc:Versa® 10 as it is nowadays applied at manufacturers site.

PDW spectroscopy has been further developed to deliver reliable and consistent results in the analysis of PS and PVAc homopolymers as used in industry. Results agreed well to state of the art sizing techniques based on light scattering and electron microscopy. To reach TRL 7 and further, PDW spectroscopy is currently applied and tested in different measurement campaigns at polymer manufacturers in Europe within another EU H2020 research and innovation project NanoPAT grant agreement n° 862583. The results are not part of this thesis. However, model assumptions and further adjustments considered at these measurement campaigns, resulted from the work done here.

## 4 Aim

The aim of this thesis is to deliver monitoring tools for the emulsion polymerization of specific PVAc syntheses by means of photon density wave spectroscopy and show their advantages as well as disadvantages and limitations. State of the art techniques are compared to novel process analytical technologies which have been developed to high quality devices with technology readiness levels up to TRL 6. For this purpose, inline PDW spectroscopy has been applied and the polymerization process has been studied in detail. Information has been gained about early inhomogeneity of the reaction mixture over distinctive particle growth periods up to the properties of the final polymer product. This thesis aims to gain insight into the whole course of the polymerization process. It shows that with the use of PDW spectroscopy as PAT tool polymerization processes can be optimized. This optimization via inline process monitoring of the optical parameters, especially the reduced scattering coefficient  $\mu_s'$  will lead to new measures for reaction control and will help to gain understanding of the process in order to reduce waste batches and therefore save time, money and enhance workers safety.

## 5 Cumulative part of the dissertation

Three research articles have been published which describe the results found and manifested during the dissertation period. For all three publications I am the main and corresponding author as indicated on the publications themselves.

### 5.1 Process Characterization of Polyvinyl Acetate Emulsions Applying Inline Photon Density Wave Spectroscopy at High Solid Contents

This paper has been published in *Polymers*. **2021**; 13(14):669.

ISSN: 2073-4360

Digital object identifier (DOI): 10.3390/polym13040669

Online available at: <https://doi.org/10.3390/polym13040669>,

© 2021 The Authors. *Polymers* published by MDPI AG

Reproduced with permission of MDPI (Basel, Switzerland) under the terms and conditions of an Open Access license, creative commons licensing by mentioning who the research is by when its used (CC BY license).

Impact factor: 4.6

#### 5.1.1 Aim of this research

The aim of this research was to exploit PDW spectroscopy for the inline monitoring of high solid content PVAc dispersions stabilized by PVA. The implementation of the PDW spectroscopy inline monitoring aims at understanding the polymerization process and different phases of the polymerization. It has been established for the first time that the complete reaction course of a semi-continuous PVAc homopolymerization can be monitored in real time with PDW spectroscopy. An experimental series of five experiments has been conducted with an increasing amount of monomer added to the system during the reaction. The effect of the amount of monomer on the dispersion parameters has been analyzed thoroughly.

Further it was aimed to implement PDW spectroscopy as a PAT tool for the PVAc synthesis. In combination with the reaction temperature PAT analysis of a PVAc synthesis, it is evaluated if gelation of a sample occurs. The PAT implementation of PDW spectroscopy was successful by showing strong deviations in the inline measured trends of absorption and scattering as gelation of the sample occurs.

Article

# Process Characterization of Polyvinyl Acetate Emulsions Applying Inline Photon Density Wave Spectroscopy at High Solid Contents

Stephanie Schlappa <sup>1,\*</sup>, Lee Josephine Brenker <sup>1</sup>, Lena Bressel <sup>1</sup> , Roland Hass <sup>1,2</sup> and Marvin Münzberg <sup>1</sup>

<sup>1</sup> Department of Physical Chemistry, innoFSPEC, University of Potsdam, Am Muehlenberg 3, 14476 Potsdam, Germany; josie.brenker@googlemail.com (L.J.B.); bressel@uni-potsdam.de (L.B.); rh@pdw-analytics.de (R.H.); marvin.muenzberg@uni-potsdam.de (M.M.)

<sup>2</sup> PDW Analytics GmbH, Geiselbergstraße 4, 14476 Potsdam, Germany

\* Correspondence: stephanie.schlappa@uni-potsdam.de; Tel.: +49-331-977-206225



**Citation:** Schlappa, S.; Brenker, L.J.; Bressel, L.; Hass, R.; Münzberg, M. Process Characterization of Polyvinyl Acetate Emulsions Applying Inline Photon Density Wave Spectroscopy at High Solid Contents. *Polymers* **2021**, *13*, 669. <https://doi.org/10.3390/polym13040669>

Academic Editor: Maria Paulis

Received: 30 January 2021

Accepted: 19 February 2021

Published: 23 February 2021

**Publisher's Note:** MDPI stays neutral with regard to jurisdictional claims in published maps and institutional affiliations.



**Copyright:** © 2021 by the authors. Licensee MDPI, Basel, Switzerland. This article is an open access article distributed under the terms and conditions of the Creative Commons Attribution (CC BY) license (<https://creativecommons.org/licenses/by/4.0/>).

**Abstract:** The high solids semicontinuous emulsion polymerization of polyvinyl acetate using poly (vinyl alcohol-co-vinyl acetate) as protective colloid is investigated by optical spectroscopy. The suitability of Photon Density Wave (PDW) spectroscopy as inline Process Analytical Technology (PAT) for emulsion polymerization processes at high solid contents (>40% (*w/w*)) is studied and evaluated. Inline data on absorption and scattering in the dispersion is obtained in real-time. The radical polymerization of vinyl acetate to polyvinyl acetate using ascorbic acid and sodium persulfate as redox initiator system and poly (vinyl alcohol-co-vinyl acetate) as protective colloid is investigated. Starved-feed radical emulsion polymerization yielded particle sizes in the nanometer size regime. PDW spectroscopy is used to monitor the progress of polymerization by studying the absorption and scattering properties during the synthesis of dispersions with increasing monomer amount and correspondingly decreasing feed rate of protective colloid. Results are compared to particle sizes determined with offline dynamic light scattering (DLS) and static light scattering (SLS) during the synthesis.

**Keywords:** photon density wave spectroscopy; multiple light scattering; emulsion polymerization; process analytical technology; polyvinyl acetate

## 1. Introduction

Emulsion polymerization systems are of high importance to the chemical industry. Products like adhesives, sealants, and coatings are produced from emulsion polymerization processes at large scales. Polyvinyl acetate (PVAc) is one of the most common polymers. One possibility of producing PVAc at industrial scale is protective colloid stabilized emulsion polymerization. In such systems, the amphiphilic protective colloid forms a colloidal system that acts as reaction center in which the polymerization process takes place [1]. Oligomers formed in the water phase from monomer molecules and the water-soluble initiators diffuse into the protective colloid micelles and react there to polymer chains with further monomer molecules diffusing into the micelle. Emulsion polymerization provides numerous advantages like being a greener process [2], possessing low viscosity throughout the process, providing advanced heat transfer, and a narrower particle size distribution (PSD) than regular suspension polymerization processes [3–5]. For the industry the control of the PSD is of paramount interest to obtain specifically designed products as the PSD determines the characteristics and properties of such dispersions [6].

To control the particle size there are several options in emulsion polymerization. The amount of protective colloid influences the PSD and application properties of the produced dispersion. The more protective colloid in the system, the more reaction centers are formed, and a larger number of particles with a smaller size can be obtained [1,7,8]. The type of



protective colloid also plays an important role. Various types of protective colloids are currently under investigation. Polymeric or plant based emulsifying agents can be used to increase dispersion stability [7]. A common protective colloid used for the synthesis of PVAc is polyvinyl alcohol poly (vinyl alcohol-co-vinyl acetate) (PVA) due to its ability to form colloidal aggregates with different physico-chemical properties. Various studies on the blockiness, size, and interfacial tension behavior of formed PVA colloidal aggregates have been carried out [8–10]. These studies have shown, that the colloidal aggregates formed, strongly depend on the hydrophobic–hydrophobic interactions between the vinyl acetate sequences in the PVA and this strongly correlates with the degree of hydrolysis. As the above-mentioned properties of the PVA colloidal aggregates influence the particle size during synthesis of PVAc the hydrolysis degree therefore plays an important role for particle size control.

An additional possibility to control the PSD of the final product is via starved–feed synthesis. A starved–feed system guarantees nearly complete conversion of monomer to polymer [1,4,5], the possibility to obtain high solid contents in the final product and control of the particle size by addition of monomer to the reactor. Low feed rates of monomer in starved–feed conditions control the rate of particle growth. Using an initial charge without any monomer content forces particle growth to happen under starved-monomer conditions and particle growth to be fully controlled by the monomer feed rate. Stopping particle growth can instantaneously be achieved by stopping the addition of monomer to the emulsion system and desired particle sizes for specified applications can be targeted [11,12]. Further possibilities for size control include feed rates or types of initiators, the monomer, or the protective colloid [13–18]. As the relationship between particle size and all these parameters is complex, a simple approach to predict the exact evolution of the PSD from all these parameters is not possible. Here, monitoring the progress of the reaction inline would be desirable.

Due to the high turbidity already at low polymer solid contents, commonly used inline Process Analytical Technologies (PAT) to monitor reaction progress or even particle size (distributions), like turbidity probes or optical inline microscopy are limited in their application and are less suitable to investigate polymerization processes [19–21]. To monitor the reaction processes or particle growth in turbid emulsion polymerization processes, Photon Density Wave (PDW) spectroscopy has shown to be a reliable method under certain conditions [22,23] by measuring the optical scattering properties. PDW spectroscopy is a new inline PAT that determines the absorption coefficient  $\mu_a$  as well as the reduced scattering coefficient  $\mu_s'$  of the dispersion in real time without dilution or sampling. Here, physical and chemical characteristics of the analyzed sample can be calculated from the optical coefficients [24–29]. In a recent study [23] the evolution of the particle size during the synthesis of PVAc was monitored by PDW spectroscopy and increasing particle sizes were observed as expected. However, sudden steps in the obtained particle size during the synthesis revealed, that the particle size analysis for PVAc systems during synthesis might be more complex than anticipated.

In this study, the suitability of PDW spectroscopy as inline PAT to monitor the reaction progress from the optical coefficients in the highly turbid emulsion polymerization of PVAc is explored and PDW spectroscopy is introduced as an applicable method for real-time measurements in emulsion polymerization even without particle size analysis. The possibility to monitor the synthesis inline via the optical coefficients could already lead to enormous advantages like better reproducibility, consistent product properties and quality, as well as reduction of waste and cost.

## 2. Materials and Methods

Chemical reagents were used as follows: Monomer vinyl acetate (VAc,  $\geq 99\%$ , Sigma-Aldrich, Darmstadt, Germany) was purged with  $N_2$  (Nippon Gases, Duesseldorf, Germany) for 30 min prior synthesis. Redox initiator pair ascorbic acid (AA, 99%, Acros Organics, Geel, Belgium) and sodium persulfate (NaPS,  $\geq 99\%$ , Carl Roth, Karlsruhe, Germany) as

well as the catalyst ammonium iron (III) sulfate hexahydrate (FAS, 99+ %, Acros Organics, Geel, Belgium) were used as purchased. Mowiol® 4-88 (poly(vinyl alcohol-co-vinyl acetate), PVA, approx. 31.000 g mol<sup>-1</sup>, viscosity of a 4% solution at 23 °C is 4 mPAS, 86.7–88.7 mol% hydrolysis degree, Sigma-Aldrich, Darmstadt, Germany), was used as purchased. All solutions were prepared with analytical grade Milli-Q® water from an in-house Milli-Q® water dispenser (Milli-Q®, Integral 5, Merck Millipore, Darmstadt, Germany) and purged with N<sub>2</sub> for 30 min prior synthesis.

### 2.1. Synthesis of Polyvinyl Acetate Dispersions

The synthesis described here is based on the industrial process to produce vinyl ester polymers described in [30]. Various research has been done on the polymerization process, e.g., regarding the type or amount of initiators, the onset temperature or the types of copolymers [13–18]. All syntheses described here were performed in an automated lab reactor (OptiMax 1001, Mettler Toledo, Gießen, Germany) at 1 L reaction scale. Reactions were executed at 60 °C under nitrogen atmosphere applying reactor temperature control, stirring control, dosing control, overhead reflux condenser, and N<sub>2</sub> purging. Dosing of feeds was achieved using four computer controlled automated dosing units (SP-50, Mettler Toledo, Gießen, Germany) for vinyl acetate (two dosing units) and approx. 16.7% (*w/w*) PVA in water (two dosing units) as well as two automated syringe pumps (PHD ULTRA, Harvard Apparatus, Holliston, MA, USA) with one syringe for the redox initiator AA and one for NaPS. Redox initiator aqueous solutions of 3.5% (*w/w*) AA and 4.5% (*w/w*) NaPS were used for all syntheses. A scheme of the experimental set-up is shown in the Supplementary Information S1. Five experiments were performed with a varied amount of total monomer fed to the system at a constant feed rate and decreased feed rates of PVA. This results in the same duration of dosing PVA and monomer while keeping the total PVA amount ( $V_{PVA} = 190$  mL) fed to the system constant. The protective colloid PVA Mowiol® 4-88 was chosen to obtain particle sizes in the nanometer size regime. The chosen PVA has further advantages as it offers good solubility at the reaction temperature of 60 °C, is relatively dormant to hydrogen bonding and stays in solution upon cooling [31].

To start a synthesis 300 g Milli-Q® water were filled into the reactor and 0.33 g PVA ( $= 1$  g L<sup>-1</sup>) were dissolved under stirring and heating up to 60 °C. The reactor was closed, and the initial charge was purged with N<sub>2</sub> for 30 min. After complete dissolution of PVA in the initial charge, approx. 0.018 g FAS in 2 mL of water were added in order to catalyze the redox system. After adding the FAS catalyst, the syringe pump was started feeding AA and NaPS into the reactor at 0.33 mL min<sup>-1</sup> each. After approx. five minutes of initiator feeding, monomer and PVA feeding were started according to Table 1. PVA feeding was stopped simultaneously to the feeding of monomer. Redox initiators were dosed for 10–30 min after VAc and PVA feeding ended in order to achieve complete conversion.

**Table 1.** Total dosed volumes and feed rates of monomer, 16.7% (*w/w*) PVA-water solution and initiators listed for each synthesis.

Synthesis	Volume $V_{VAc}$ /mL	Feed Rate VAc /mL min <sup>-1</sup>	Feed Rate PVA /mL min <sup>-1</sup>	Volume $V_{AA}$ /mL	Volume $V_{NaPS}$ /mL
VAc_1	350	4.52	2.46	31.66	31.66
VAc_1.5	525	4.52	1.64	44.55	44.55
VAc_1.6	560	4.52	1.53	50.66	50.66
VAc_1.8	630	4.52	1.36	53.33	53.33
VAc_2	700	4.52	1.23	63.33	63.33

An additional synthesis PVAc\_1wr analogous to synthesis PVAc\_1 but with a reduced initial amount of 151.2 g of water, an increased amount of 5.52 g PVA ( $= 36.3$  g L<sup>-1</sup>), and an amount of 0.009 g of FAS in 2 mL of water, keeping the concentration of FAS in the initial charge constant, was carried out. Here, the same feeding rates as for synthesis VAc\_1 for monomer, PVA (15.7% (*w/w*)) were used. A total amount of 350 mL of monomer, 190 mL of



PVA solution, and 31.6 mL of each initiator was targeted. During this synthesis, the feeding of monomer and PVA had to be stopped before finishing the targeted amount. Table 2 displays targeted and actually dosed amounts. This synthesis was carried out to evaluate how a much higher amount of protective colloid and a total increase in solid content would affect inline measurements of PDW spectroscopy and whether process control via PDW spectroscopy would still be possible.

**Table 2.** Final composition of the dispersion P Polyvinyl acetate (PVAc)\_1wr with 36.3 g L<sup>-1</sup> PVA dissolved in 151.2 g of water in the initial charge after abortion of the dosing of monomer and PVA feeds.

Component	Dosed Volume V <sub>1</sub> /mL	Target Volume V <sub>2</sub> /mL	Fraction / %
Monomer VAc	339.16	350	96.90
PVA solution 15.7% (w/w)	184.125	190	96.90
Initiator solution 4.5% (w/w) NaPS	34.6	31.6	109.29
Initiator solution 3.5% (w/w) AA	34.6	31.6	109.29
Catalyst FAS	0.009	0.009	100
Total dispersion mass	743.96	745.67	

All syntheses were monitored in line with PDW spectroscopy regarding the trend of the optical coefficients. Offline-samples were taken for solid content and particle size analysis. Additionally, the density and refractive index of the particles in the final dispersion were analyzed. All syntheses described above were carried out a single time.

## 2.2. Analysis of Polymer Emulsions

For offline analysis, 1 mL samples were taken manually out of the reactor at approx. 40 mm depth using a single-use 1 mL syringe with a cannula length of 13.5 cm, diluted approx. 1:10 with Milli-Q<sup>®</sup> water to quench the reaction and stored in sample containers. For process analysis until  $t_R = 5$  min samples were taken every minute, until  $t_R = 30$  min samples were taken every 5 min, until  $t_R = 120$  min samples were taken every 10 min and for  $t_R > 120$  min samples were taken every 20 min.

Gravimetric solid content analysis was done with approx. 500 µL sample stored in weighted Eppendorf tubes and dried at 72 °C for at least 24 h until mass consistency. After drying, the total weight of the solid residue was taken and handled as solid content of the dispersion at sampling time  $t$ . Samples were weighted without purification, solid content refers to all possible solid residues after drying.

Offline sample analysis was performed after the synthesis was completed. Dynamic light scattering (DLS) analysis (Zetasizer Ultra, Malvern Panalytical, Worcestershire, United Kingdom) was done at a measurement angle of 173° using single-use 4 mL polystyrene cuvettes at 25 °C. Samples were diluted approx. 400-fold to visual transparency. For static light scattering (SLS) measurements (LS13320, Beckman Coulter, Brea, CA, USA) samples were pre-diluted approx. 125-fold with Milli-Q<sup>®</sup> water and pipetted into the sample chamber. Using Polarization Intensity Differential Scattering (PIDS) as measuring method, the sample was pipetted into the reaction chamber until a PIDS signal of 40% was achieved. For high quality analysis, low obscuration values beneath 2% were retained.

For data analysis of PDW spectroscopy measurements, the densities and the refractive indices of the particles and the dispersant are needed. To determine the density of the particles a concentration series of 30% (w/w), 20% (w/w), 10% (w/w), 1% (w/w), and 0.1% (w/w) of each polymer dispersion was measured at 25 °C with a densitometer (DM45 Delta Rage, Mettler Toledo, Gießen, Germany). The data were analyzed for the density of the particles (i.e., pure polymer, 100% (w/w)) using the following equation [22,32]:

$$\rho_{\text{Disp}} = \frac{\rho_D \rho_P}{w[\rho_D - \rho_P] + \rho_P} \leftrightarrow \frac{1}{\rho_{\text{Disp}}} = w \left[ \frac{1}{\rho_P} - \frac{1}{\rho_D} \right] + \frac{1}{\rho_D} \quad (1)$$

Here,  $\rho_{\text{Disp}}$ ,  $\rho_{\text{D}}$ , and  $\rho_{\text{P}}$  are the densities of the dispersion, the dispersant, and the polymer and  $w$  is the solid content of the dispersion. For the density of zero polymer content (0% ( $w/w$ )) the density of pure water was considered, determined with the same densitometer. The density of the polymer was obtained from the slope of a linear fit according to the right equation. The error was obtained via error propagation.

The same concentration series was used for refractive index measurements at 20 °C at seven different wavelengths between 403 and 938 nm with a multi-wavelength refractometer (DRS- $\lambda$ , Schmidt + Haensch, Berlin, Germany). The measured refractive indices are extrapolated to the refractive index of the particle using the Newton equation [28] and afterwards inter- or extrapolated to the wavelengths of PDW spectroscopy by a Cauchy formula [22,32].

Solid content, particle size, density, and refractive index analysis were carried out with three repeating experiments each. Values and errors shown in the results section reflect mean values and standard deviations from these repeating experiments.

### 2.3. Photon Density Wave Spectroscopy

Photon Density Wave (PDW) spectroscopy is a technique for the characterization of the optical properties of multiple light scattering materials, such as highly turbid polymer dispersions [27]. Using optical fibers, intensity modulated laser light is guided into the sample. Due to multiple scattering and absorption in the material, a PDW is created, which alters in amplitude and phase while passing the turbid material. The changes to amplitude and phase of the PDW are characterized as function of the modulation frequency and distance  $r$  between emission and detection fiber and can be related to the absorption coefficient  $\mu_a$  and the reduced scattering coefficient  $\mu_s'$  of the material.

Whereas the absorption coefficient  $\mu_a$  can be attributed to the concentration of absorbing species in the sample, the reduced scattering coefficient  $\mu_s'$  can in principle be attributed to the amount and size of the scattering material and is dependent on the physical properties like density and refractive index of the particles and dispersant. By using  $\mu_s'$  physical changes within the dispersion can be monitored. Previous research showed, that monitoring the scattering properties of various samples like milk, milk-fat, zeolites, or bioplastic producing bacteria leads to deeper insights into the processes and deeper understanding of underlying mechanisms like depletion flocculation, phase transitions or zeolite production [24–26]. For polymer syntheses monitoring  $\mu_s'$  is an important tool, as it mirrors polymerization phases and hence offers possibilities for process control. Additionally, applying Mie theory and theories for dependent light scattering [28] the size of the dispersed particles can in principle be derived from the reduced scattering coefficient in inline measurements [33,34]. For polydisperse systems a multi-wavelength approach is necessary [28]. However, due to the complexity of the PVAc system, containing high amounts of highly water soluble PVA as protective colloid, which forms a non-negligible protective layer on the particle surface rendering a simple PVAc-particle-in-a-medium-of-water model moot, particle size analysis based on PDW spectroscopy is beyond the scope of the present work.

Inline PDW spectroscopy was applied using a specially designed inline probe with eight optical fibers and a probe diameter of 25 mm. The probe was inserted into the reactor via an inlet in the reactor lid with the tip of the fibers' positions at approx. 40 mm beneath the initial charge–air-interface, to obtain stable PDW data from the beginning of the experiment. The PDW spectrometer used here is self-made. Commercial versions are available from PDW Analytics GmbH, Potsdam, Germany. Detailed technical description of the set-up can be found elsewhere [32,33]. Measurements for process characterization were executed at 637 nm, 690 nm, and 751 nm with modulation frequencies up to 1210 MHz and fiber distances between 2.4 and 19 mm. As syntheses were performed only once. PDW data shown here are therefore also obtained from a single measurement. Errors shown for  $\mu_a$  and  $\mu_s'$  are obtained from a non-linear fit process during the analysis of intensity and phase [35].



### 3. Results and Discussion

#### 3.1. Dispersion Analysis

Stable, highly turbid liquid dispersions were obtained in all cases. Drying a droplet of the dispersion at ambient air conditions leads to a transparent, hard, non-sticky film. Stored in airtight plastic containers, the dispersions are storable without any phase separation for at least six months. Dilution of the samples with Milli-Q® water was possible without phase separation or visible agglomeration of the particles. All produced dispersions exceeded 40% (*w/w*) solid content. Electron microscopy (cf. Supplement Figure S2) revealed that spherical, well separated particles were produced in all syntheses.

Figure 1 shows the gravimetrically derived solid content during the five syntheses PVAc\_1 to PVAc\_2. For all syntheses the solid content increases as long as monomer is added and then levels off. It reflects an evolution of the solid content typically achieved with free radical polymerization processes [36]. Following chain-growth mechanism, mostly monomer reacts with the active radical chain creating high instant conversion of monomer to polymer of 90 to 98% (data not shown). Propagation of polymer chains is the dominant process until no more monomer is added to the system and propagation stops. Calculated solid content assuming the direct conversion of monomer to polymer is shown in Figure 1. All experimental data match the theoretically calculated solid content fortifying the assumption of a starved-feed synthesis. Only for synthesis VAc\_2 the solid content shows some fluctuations at high solid contents, as sampling and drying of these samples is challenging. The synthesis VAc\_2 was the only one which led to a little amount of coagulate at the interface between air and dispersion in the final dispersion. Due to the high amount of total monomer dosed, visible agglomerates were formed. It is assumed, that the synthesis VAc\_2 with 700 mL monomer forms visible agglomerates, because the amount of protective colloid fed during the synthesis is not sufficient to stabilize the formed particles. The highest feedable amount of monomer to create a completely stable dispersion is therefore somewhere between synthesis VAc\_1.8 with 630 mL and synthesis VAc\_2 with 700 mL of dosed monomer under the reaction conditions presented here.

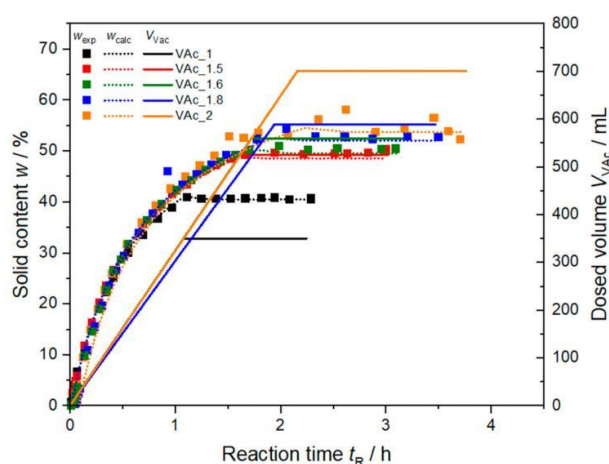


**Figure 1.** Gravimetrically determined and calculated solid content  $w_{\text{calc}}$  from PVAc and PVA combined and dosed volume of monomer  $V_{\text{VAc}}$  during polymerization for syntheses VAc\_1, VAc\_1.5, VAc\_1.6, VAc\_1.8, and VAc\_2.

Figure 2 shows the mean of the gravimetrically determined final solid content of all five dispersions from three repeating measurements. The final solid content increases with increasing monomer dosing as expected. Calculations for 100% conversion of monomer to polymer lead to an expected maximal solid content in the final dispersion  $w_{\text{calc, PVAc}}$  of 36.7% (*w/w*) to 51.1% for VAc\_1 to VAc\_2. As the high molecular protective colloid

anchors to the particle surface, it does not evaporate during the drying process. The gravimetrically determined solid content therefore consists of both polymer and protective colloid. The solid content calculated from 100% conversion of monomer to polymer including additionally the total amount of PVA in the dispersion  $w_{\text{calc, PVAc+PVA}}$  leads to values between 40.75% and 54.08% for syntheses VAc\_1 to VAc\_2. These calculated values match the experimental solid contents well. In case of VAc\_2 the experimental solid content is slightly smaller than the calculated value. This can be anticipated due to particle agglomeration as discussed above.

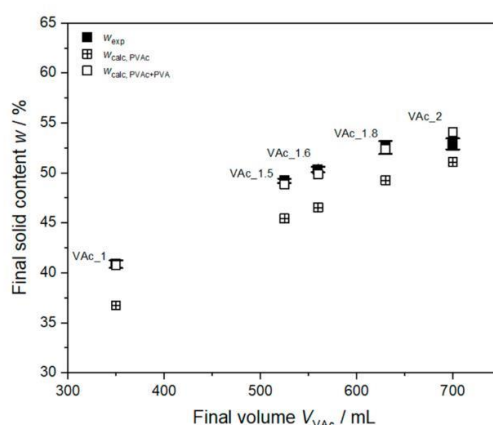


**Figure 2.** Final experimental solid content of all syntheses (full squares) in dependency of the total dosed volume of monomer  $V_{VAc}$  compared to the calculated solid content for 100% monomer to polymer conversion  $w_{\text{calc, PVAc}}$  (crossed squares) and calculated solid content for 100% conversion of monomer to polymer and attachment of the total amount of PVA to the particle  $w_{\text{calc, PVAc+PVA}}$  (open squares).

The extrapolated polymer density of the particles of  $(1.20 \pm 0.01) \text{ g cm}^{-3}$  (Table 3) as mean of all synthesized dispersions shows very good agreement between all batches and is in agreement with data from literature, where a density of 1.17 to 1.2  $\text{g cm}^{-3}$  for PVAc homopolymers, depending on the degree of polymerization, is found [37]. Extrapolated refractive index values of the particles for a wavelength range from 400 nm to 1000 nm are shown in Supplement Figure S3. Values between 1.48 and 1.49 at  $\lambda = 637 \text{ nm}$  were extrapolated from dilution measurements for the pure polymer particle. For the synthesis VAc\_2 with aggregated particles no determination of the density nor the refractive index was possible. Therefore, density and refractive index values obtained for VAc\_1.8 were used for PDW spectroscopy analysis of VAc\_2.

**Table 3.** Total volumes of dosed monomer  $V_{VAc}$ , extrapolated density  $\rho_p$  and refractive index  $n$  (at  $\lambda = 637 \text{ nm}$ ) of the particles for each synthesis.

Synthesis	$V_{VAc}/\text{mL}$	$\rho_p/\text{g cm}^{-3}$	$n (\lambda = 637 \text{ nm})$
VAc_1	300	$1.2015 \pm 0.0004$	$1.4797 \pm 0.0007$
VAc_1.5	525	$1.2026 \pm 0.0001$	$1.4827 \pm 0.0010$
VAc_1.6	560	$1.2055 \pm 0.0001$	$1.4851 \pm 0.0011$
VAc_1.8	630	$1.2023 \pm 0.0003$	$1.4906 \pm 0.0007$
VAc_2	700	—*1	—*1

\*1 No determination of extrapolated particle density and refractive index possible, due to the high solid content and viscosity of the dispersion.

### 3.2. Polymerization Monitoring Using PDW Spectroscopy

Figure 3 exemplarily shows the inline monitoring of synthesis VAc\_1.5. The system is first heated to a reaction temperature of 60 °C. The overshoot of a few degrees over 60 °C is due to insufficient PID correction of the automated reactor. To overcome long inhibition periods, the redox initiators were fed to the system five minutes before starting monomer dosing (not displayed here), to provide radicals for the instant nucleation and propagation of polymer chains. The polymerization is started by adding monomer VAc and protective colloid PVA to the reaction system ( $t_R = 0$  h). The start of the polymerization process can be observed in the temperature profile in Figure 3 by a characteristic release of reaction heat at  $t_R = 0$  h. A sudden increase in temperature of approx. 4 K is observed. During synthesis the reaction temperature stays nearly constant at 60 °C until approx.  $t_R = 2$  h where the addition of VAc and PVA is finished and a slight drop in the reaction temperature (less pronounced than the increase at  $t_R = 0$  h) occurs due to the final conversion of monomer to polymer and the termination of release of reaction heat. The temperature drop happens slightly after the finish of monomer and PVA feed indicating that small amounts of monomer are still converted to polymer. This small time lag however still is in accordance with the assumption of a starved-feed synthesis. After 2.7 h, the system is cooled down to 20 °C over 30 min.

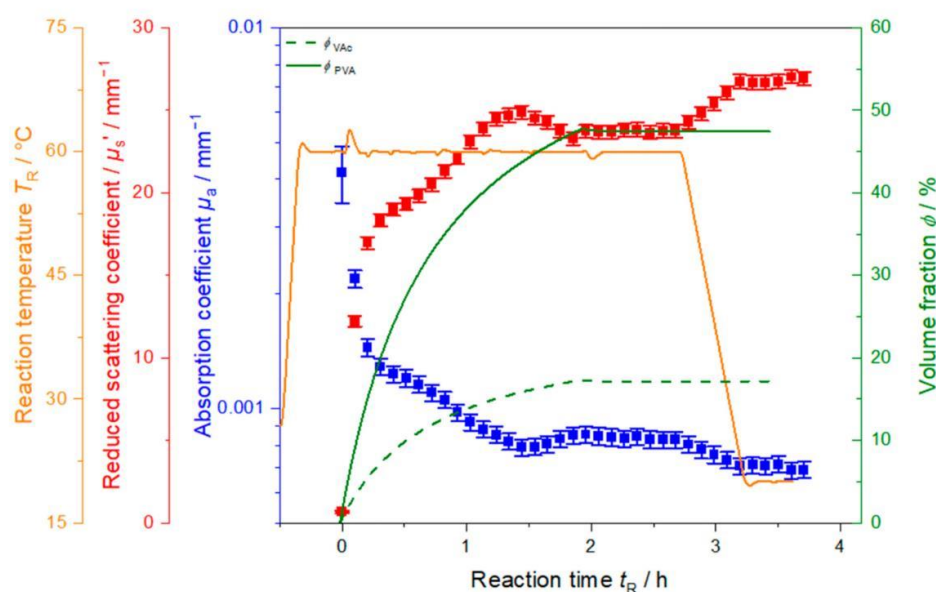


**Figure 3.** Reduced scattering coefficient  $\mu_s'$  (red) and absorption coefficient  $\mu_a$  (blue) at 637 nm, volume fraction of monomer  $\phi_{VAc}$  and protective colloid  $\phi_{PVA}$  (green solid and dashed lines, respectively), and reaction temperature  $T_R$  (orange) as function of time during polymerization of VAc\_1.5.

Monitoring the synthesis in line with PDW spectroscopy allows to observe changes in the optical properties of the sample, like the absorption coefficient  $\mu_a$  and the reduced scattering coefficient  $\mu_s'$ . With dosing monomer to the system,  $\mu_a$  at  $\lambda = 637$  nm drops from 0.004 mm<sup>-1</sup> to a local minimum of around 0.0008 mm<sup>-1</sup> at 1.5 h.  $\mu_a$  then increases slightly again and levels off, as soon as monomer dosing is stopped. With start of cooling at 2.7 h, again a slight decrease in  $\mu_a$  is observed with a subsequent levelling off as soon as 20 °C is reached.

The reduced scattering coefficient  $\mu_s'$  in Figure 3, obtained at  $\lambda = 637$  nm, increases rapidly as soon as monomer and protective colloid are added. After about 20 min,  $\mu_s'$  increases less pronounced and a maximum value of approx. 25 mm<sup>-1</sup> is reached at



$t_R = 1.5$  h, simultaneously to the absorption minimum in  $\mu_a$ . After the maximum, a decrease to approx.  $24 \text{ mm}^{-1}$  is observed and  $\mu_s'$  levels off in correspondence to stopping monomer and protective colloid dosing. Until start of cooling at  $t_R = 2.7$  h,  $\mu_s'$  stays constant. Cooling down the system to  $20^\circ\text{C}$  causes an increase in  $\mu_s'$  to significantly higher values of around  $27 \text{ mm}^{-1}$ .

Three different phases are represented in the trend of the reduced scattering coefficient  $\mu_s'$ . First,  $\mu_s'$  rises rapidly until  $t_R = 0.2$  h with a very steep slope, which might be due to fast particle formation and growth. After the initial steep increase  $\mu_s'$  continues to increase, with a less steep slope. During this second stage, until start of cooling, particles should still be growing as monomer is continuously added. During the cooling process,  $\mu_s'$  increases again and finally  $\mu_s'$  levels off, as the sample reaches room temperature and the cooling process is completed. The increase of  $\mu_s'$  during cooling might be due to temperature dependent changes of physical properties of the particles like density and refractive index. In this case, e.g., an increase in particle density, leading also to an increase in refractive index, would result in a decrease of particle size. Depending on the amplitude of each effect, the result can either be a decrease or increase of  $\mu_s'$ .

These stages can be observed for all syntheses carried out here. The inline measured reduced scattering coefficient for all five syntheses is shown in Figure 4 (cooling stages are omitted for better visibility). Each polymerization starts at  $t_R = 0$  h with the start of dosing monomer and protective colloid into the reactor. The initial steep increase of  $\mu_s'$  appears to be identical for all syntheses, and hence, seems not to be affected by the decreased feeding rate of PVA to the system.

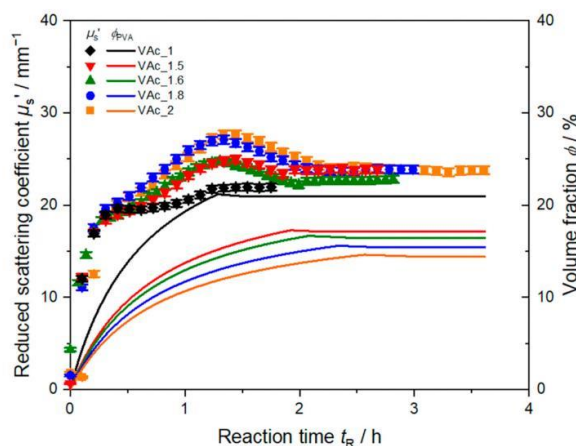


**Figure 4.** Comparison of inline determined reduced scattering coefficient  $\mu_s'$  at 637 nm for synthesis PVAc\_1 to PVAc\_2 with different feeding rates of PVA and hence volume fraction  $\phi_{\text{PVA}}$  during synthesis. Data shown without cooling phase for better visualization.

Except for VAc\_1, all syntheses exhibit a maximum in  $\mu_s'$  during the feeding of monomer and protective colloid. The maximum occurs at nearly the same time, a slight shift to the left with increasing monomer amount is visible. In emulsions with a lower amount of protective colloid, less reaction centers for particle formation and growth are formed. Therefore, fewer, but bigger particles are growing in the dispersion which should lead to an increase of light scattering at these still relatively small particle sizes in this early stage of synthesis. Although feeding of monomer and PVA is not yet finished,  $\mu_s'$  then decreases again. This might be due to the distinctive dependency of  $\mu_s'$  on particle size, refractive index, and volume fraction. Described by Mie theory,  $\mu_s'$  exhibits oscillations as function of particle size for given chemical and optical properties. These oscillations change their form and position in dependency of the measurement wavelength. Accordingly, as shown in Figure 5 for VAc\_1.5 and VAc\_1.8, shifts of the maximum in  $\mu_s'$  are observed



when applying measurements at different wavelengths. Hence, the presence, position, and height of these maxima contains the key to particle sizing in these systems during synthesis.

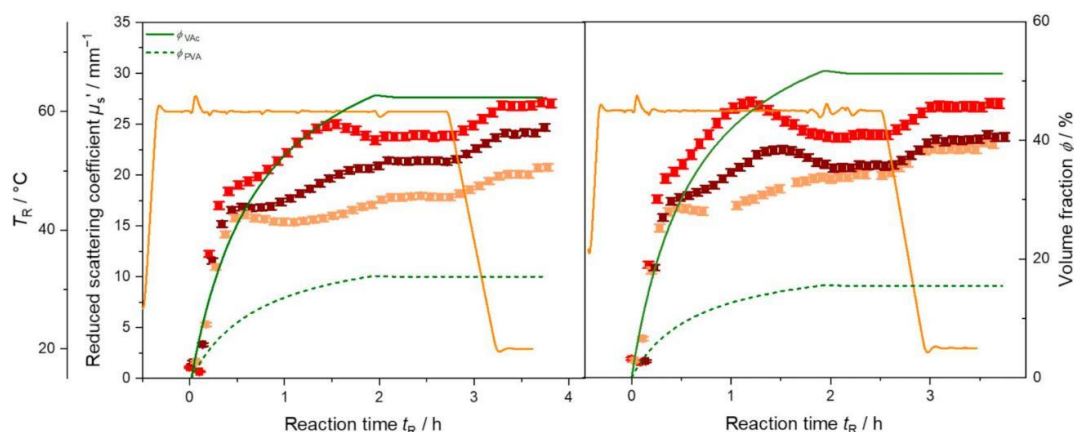


**Figure 5.** Reduced scattering coefficient  $\mu_s'$  (symbols) at  $\lambda = 637$  nm (red),  $\lambda = 690$  nm (brown) and  $\lambda = 751$  nm (orange), volume fraction of dosed monomer  $\phi_{VAc}$  and protective colloid  $\phi_{PVA}$  (solid green and dashed lines, respectively), and reaction temperature  $T_R$  (orange line) as function of time during polymerization of VAc for synthesis VAc\_1.5 (left) and synthesis VAc\_1.8 (right).

Due to the complex dependency of  $\mu_s'$  on particle size or particle size distribution and due a non-linear dependency on solid content, known as dependent scattering, particle sizing during the reaction at high solid contents and elevated temperatures is challenging. Here, changes in density and refractive index of the particles and medium might occur. Apart from the complexity of the PVAc-PVA-water system as mentioned before, determining all physical properties in the addressed temperature range, and including models for dependent light scattering might be therefore necessary to obtain correct particle sizes.

Stopping the feed of PVA and monomer corresponds well to reaching a plateau phase in  $\mu_s'$  in both syntheses (Figure 5). At the end of the syntheses  $\mu_s'$  exhibits different values, depending on wavelength and total amount of monomer. For synthesis VAc\_1.5 the final  $\mu_s'$  increases with decreasing wavelength. For synthesis VAc\_1.8 measurements at 690 nm and 751 nm end at nearly the same  $\mu_s'$  value of approx.  $23 \text{ mm}^{-1}$ , a higher value is obtained at 637 nm. Despite the different solid content in the final dispersions  $\mu_s'$  exhibits nearly the same value of  $26 \text{ mm}^{-1}$  for synthesis VAc\_1.5, VAc\_1.8, and VAc\_2 (cf. Figure 4) at 637 nm. The difference in the end values arises due to the underlying particle size distribution. To understand the exact form of  $\mu_s'$  in dependency of wavelength during the polymerization a light scattering model for the reaction needs to be set up. The evaluation of particle size, assuming pure polymer or additionally PVA as particle and water as surrounding medium seems currently not to be sufficient as data analysis model. Here, a more sophisticated model is required to describe the experimentally observed reduced scattering coefficients.

### 3.3. Comparison to Offline Size Analysis

Even though particle sizing still is challenging due to an insufficient optical model of the PVAc system, both the reduced scattering coefficient and the absorption coefficient contain process-related information. As soon as monomer and PVA addition is stopped, both coefficients level off, indicating the end of the reaction. In case of  $\mu_a$  this might be obvious as no more absorbing chemicals are consumed or absorbing products formed. However, in case of  $\mu_s'$  a levelling off does not only reflect the end of dosing but also the constancy of the size (distribution) of scattering material. In addition to monitoring changes of the reaction temperature to obtain information about the synthesis, e.g., a short increase at the beginning and a short decrease at the end of the feeding, the optical

coefficients are therefore a powerful tool to monitor the reaction progress inline. This is especially helpful when temperature changes are not visible or significant, as is the case for synthesis VAc\_1.8 (cf. Figure 5 right). In another case, where at the end of feeding the monomer is completely converted to polymer, a drop in temperature would suggest the end of the reaction. However, if aggregation between particles occurred,  $\mu_s'$  would still show changing values (cf. Section 3.4 and Figure 7).

To undermine the assumption of comparing particle growth to the reduced scattering coefficient, offline analysis of the particle size has been carried out with DLS and SLS. Results are shown exemplarily for VAc\_1.5 in Figure 6. In the beginning the inline trend in  $\mu_s'$  and both offline determined particle diameters start to increase rapidly. The sharp slope in the first PDW measurements corresponds directly to the particle growth up to  $t_R = 0.2$  h. First measurements in the early minutes of the reaction showed particle sizes of approx. 50 nm, agreeing to the theory, that colloidal aggregates of PVA formed to stabilize the particles are smaller than 50 nm in size [8,9]. The second, less rapid growth period of particles is also reflected in a more modest growth phase of  $\mu_s'$  until the maximum value is reached. A slight decrease in  $\mu_s'$  is evident, although still growth of the particles is apparent in DLS and SLS measurements. Hence, the maximum might derive from the assumed dependency of  $\mu_s'$  on particle size as described above. After  $t_R = 2$  h the monomer and protective colloid dosing is stopped and particle growth is inhibited. During cooling of the dispersion starting at  $t_R = 2.7$  h  $\mu_s'$  increases even though DLS and SLS values stay constant. It has to be pointed out that DLS and SLS data are always obtained after cooling to room temperature, whereas PDW spectroscopy measurements are performed at reaction temperature. The final particle diameter after  $t_R = 3.7$  h differs by approx. 140 nm between both offline measurements. While DLS provides a final  $d_p$  of  $(619 \pm 12)$  nm, SLS results in a value of  $(480 \pm 1)$  nm (error indicates the standard deviation of three repeating measurements). The results obtained by DLS represent the hydrodynamic radius, whereas SLS determines the geometrical diameter of the particles.

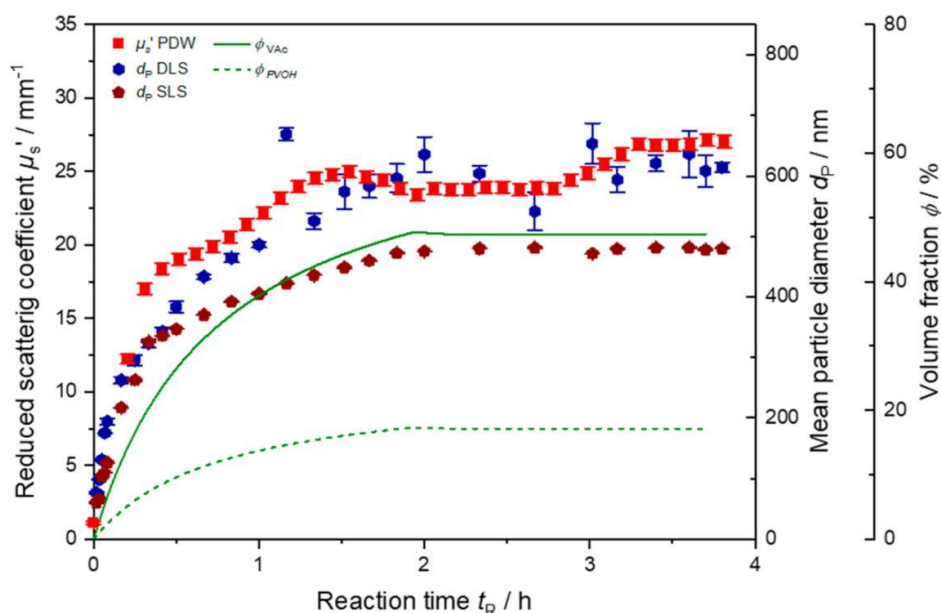


**Figure 6.** Inline  $\mu_s'$  at  $\lambda = 637$  nm and offline determined particle diameter from dynamic light scattering (DLS) (blue symbols) and static light scattering (SLS) (brown symbols). Volume fraction  $\phi_{VAc}$  and  $\phi_{PVA}$  (solid and dashed green line) in synthesis VAc\_1.5.

In principle, determining mean particle sizes directly in line with PDW spectroscopy is feasible [24,33,36]. However, due to the complexity of the system and the temperature dependent physical properties particle sizes might not yet be accessible. Further research needs to be executed for the correct description of wavelength dependent light scattering in this complex, size distributed, and concentrated particle system.

### 3.4. Inline Process Control Using PDW Spectroscopy

To show that PDW spectroscopy can in principle also be applied as technique for process control, a synthesis with a decreased volume of the initial charge but high PVA content is shown in Figure 7. Total amounts fed to the system are shown in Table 2. Here, only 150 mL of water were used as initial charge to increase the amount of PVA in the initial charge drastically. With continuously adding more monomer to the system the polymerization proceeds and particles continue to grow in the dispersion. Apart from the initial peak at  $t_R = 0$  h, during synthesis the reaction temperature stays nearly constant at 60 °C until approx.  $t_R = 1.1$  h where two sudden peaks of approx. 8 K to higher temperatures are observed shortly after each other. This rise in temperature is caused by gelation of the sample as gelation hinders the heat transfer in the sample.

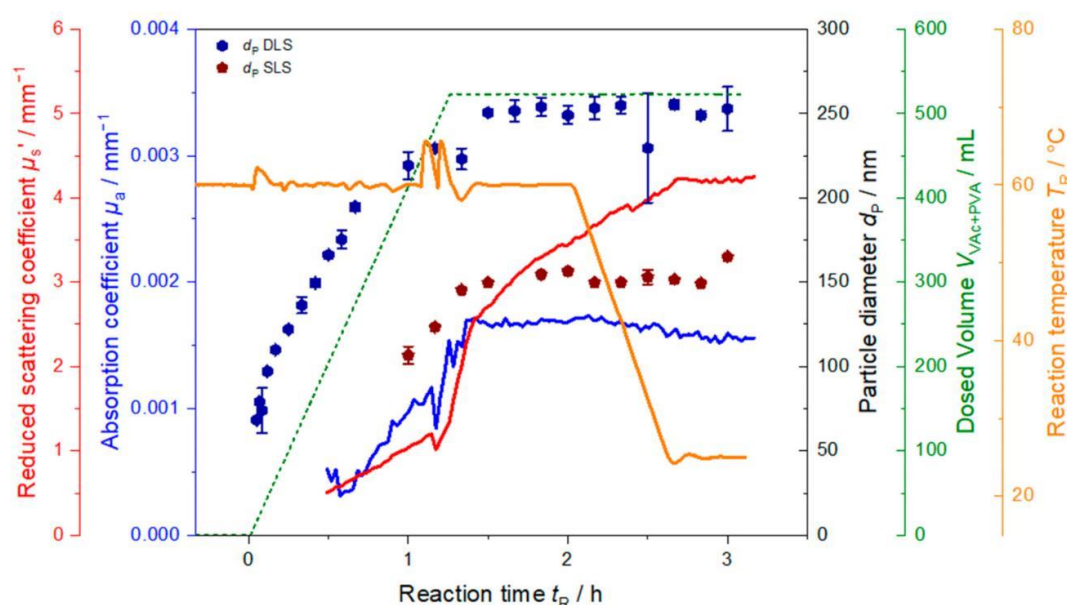


**Figure 7.** Reduced scattering coefficient  $\mu_s'$  (red), absorption coefficient  $\mu_a$  (blue) at  $\lambda = 637$  nm, combined dosed mass of monomer and protective colloid (dashed green line) and reaction temperature (orange) as function of time during synthesis PVAc\_1wr. The dosing of monomer and PVA had to be aborted due to gelation of the sample at  $t_R = 1.1$  h.

Monitoring the synthesis in line with PDW spectroscopy reveals a sudden drop at the same time in  $\mu_a$  as well as  $\mu_s'$ .  $\mu_s'$  then increases even steeper than before parallel to the two temperature peaks. Due to the observed temperature peaks and drops in the optical coefficients, the addition of monomer and PVA was stopped while continuing the initiator feeds to prevent further gelation in the sample. This resulted in the reaction temperature to decrease to 60 °C again. Initiator dosing was continued to decrease both viscosity and to achieve complete conversion of residual monomer. Shortly after returning to 60 °C and discontinuing the monomer and PVA feeds, the absorption coefficient levels off. At the same time the reduced scattering coefficient does not level off, but increases further, however, with a less steep slope. After  $t_R = 2.1$  h the reaction was cooled down to 25 °C within 30 min after dosing of the initiators was finished.  $\mu_s'$  only levels off shortly after



room temperature is reached. This indicates that the process is not yet finished when then monomer and then initiator feedings are stopped even though particle sizes measured offline did not change anymore after monomer feed is stopped. Further conversion of monomer to polymer in the monomer swollen particles might be the reason. The indirect dependency of  $\mu_s'$  on temperature due to its dependency on refractive index, density, and particle size might be an explanation for the sudden drop in  $\mu_s'$  during the peak in temperature in Figure 7, in contrast to the syntheses shown before (cf. Figures 3–5) where no such sudden drop in either optical coefficient is observed. The steeper slope after the drop might arise due to multiple reasons, such as changes in the sample properties, faster particle growth or particle agglomeration. Due to the gelation of the sample the synthesis was aborted and PVA and VAc feed were stopped earlier than planned. Because of the higher amount of water, no gelation occurred in the other syntheses shown above.

This synthesis shows that the optical coefficients can directly be used to control the process, i.e., in this case, stop the monomer feed. Additionally, a second possibility for process control could have been the continuing increase of  $\mu_s'$  during the cooling process. Here, the reaction was cooled down according to the reaction plan 20 min after the dosing of initiator feeds was finished. As  $\mu_s'$  was still rising at that time this change could have been used as an indicator to continue the reaction at 60 °C until  $\mu_s'$  levels off. This could prevent incomplete conversion of monomer to polymer in the final product. The inverse is also possible in batch processes. Here, typically the reaction temperature is held constant for a certain time which is obtained from experience to obtain complete conversion, these tempering periods are often longer than required. The monitoring of  $\mu_s'$  could help to decrease these unnecessary long reaction times by cooling down directly after  $\mu_s'$  reaches a plateau.

#### 4. Conclusions and Further Research

A series of starved-feed emulsion polymerizations of vinyl acetate dispersions with high solid contents of up to 54% (*w/w*) and high turbidity with increasing amount of monomer and decreasing feeding rate of PVA was successfully carried out. The reaction progress as well as particle size monitored with different inline and offline techniques is presented. Shown trends in solid content were in good agreement with expected reaction progress known from emulsion polymerization. To verify the high conversion rates in future experiments, gas chromatography (GC) could be applied to monitor the conversion of monomer to polymer.

PDW spectroscopy was applied to monitor the reaction progress inline throughout the whole polymerization, via the absorption and scattering properties. Absorption and scattering properties were successfully monitored and compared to polymerization stages evolving during emulsion polymerization. Three stages could be identified, agreeing well to emulsion polymerization theory. A first stage of initial particle formation and fast particle growth is reflected by a steep increase in the reduced scattering coefficient for all syntheses. In the second phase of synthesis, during particle growth,  $\mu_s'$  rises slower, depending on the feeding rate of protective colloid. In some syntheses, maxima are expressed, which might reflect the formation of different particle size distributions of polymer particles in the dispersions. Levelling off of  $\mu_s'$  during the third phase occurred as soon as feeding of chemicals was stopped and polymerization terminated. The subsequent cooling of the synthesis caused an increase in  $\mu_s'$ , probably due to temperature dependent physical properties, like refractive index and density of polymer particles and dispersant.

Comparison of inline  $\mu_s'$  with particle sizes obtained offline from DLS and SLS confirmed these three phases of the reaction, i.e., initial steep increase of particle size, further slower particle growth and finally levelling-off of the particle size. To obtain particle sizes or even distributions from PDW spectroscopy during the synthesis, as has been shown in previous studies [27,34], further studying of the system is necessary to set up an improved scattering model for the complex PVAc–PVA–water system. This includes temperature dependent physico-chemical properties like density and refractive index of all components,

determination of monomer to polymer conversion, e.g., with GC as well as a revision of the particle-water model.

In an additional synthesis with increased protective colloid amount, it was shown, that from combination of temperature data as well as inline PDW spectroscopy measurements of the optical coefficients process control is possible. Here, gelation of the sample was observed and the reaction stopped by stopping the monomer addition. Further gelation was hindered by adding dispersant, in this case low concentrated initiator solutions.

Both examples clearly show the capability of monitoring polymerization progress during synthesis of vinyl acetate via PDW spectroscopy. This allows for a better understanding of the synthesis as well as control of the reaction which will improve the quality of the obtained product and the prevention of waste batches.

**Supplementary Materials:** The following are available online at <https://www.mdpi.com/2073-4360/13/4/669/s1>, Figure S1: Schematic description of the reactor Set-Up. 1 L automated Lab reactor equipped with automated temperature control, stirring control, dosing control, overhead reflux condenser, and N<sub>2</sub> purging. The PDW inline probe is directly inserted into the reactor via an inlet port., Figure S2: Electron microscopy picture of produced particles from emulsion polymerization synthesis VAc\_1.5 with 525 mL VAc., Figure S3: Refractive index of the particles from syntheses VAc\_1, VAc\_1.5, VAc\_1.6, and VAc\_1.8 extrapolated from values of a concentration series of the dispersions measured with a refractometer at seven discrete wavelengths and inter- and extrapolated to wavelengths between 500 nm and 1000 nm, shown with +95% and −95% confidence interval as dashed lines., Figure S4: Density measurements of dilutions of dispersions VAc\_1 to VAc\_1.8 in dilutions up to 30% and extrapolated density values (i.e., 100% Polymer) measured with a densitometer.

**Author Contributions:** Conceptualization, S.S., L.B. and R.H.; Data curation, S.S., L.B. and R.H.; Formal analysis: S.S., L.J.B. and L.B.; Funding acquisition, R.H. and L.B.; Investigation, S.S. and L.J.B.; Methodology, S.S. and L.B.; Project administration, M.M.; Resources, S.S. and L.B.; Supervision, L.B. and M.M.; Validation, S.S., L.J.B., and L.B.; Visualization, S.S.; L.J.B.; Writing – original draft, S.S. and L.B.; Writing—review and editing, S.S., L.B., R.H., and M.M. All authors have read and agreed to the published version of the manuscript.

**Funding:** This research was funded by financial support of the German Federal Ministry of Education and Research (grants 03Z22AN12, 03IHS048A and 03Z22AB1B) and the University of Potsdam.

**Informed Consent Statement:** Not applicable.

**Data Availability Statement:** Not applicable.

**Conflicts of Interest:** The authors declare no conflict of interest.

## References

1. Yilmaz, F.; Yamak, H.B. *Emulsion Polymerization: Effects of Polymerization Variables on the Properties of Vinyl Acetate Based Emulsion Polymers*; InTech: Rijeka, Croatia, 2013; ISBN 978-953-51-0941-9.
2. Anastas, P.T.; Warner, J.C. *Green Chemistry: Theory and Practice*; Oxford University Press: New York, NY, USA, 2000; p. 30, ISBN 978-0-198-50698-0.
3. Behr, A.; Agar, D.W.; Jörisen, J.; Vorholt, A.J. *Einführung in die technische Chemie*, 2nd ed.; Springer Spektrum: Wiesbaden, Germany, 2016; ISBN 13.
4. Tieke, B. *Makromolekulare Chemie*, 3rd ed.; Wiley-VCH: Weinheim, Germany, 2014; ISBN 978-3-527-68351-2.
5. Lerche, D.; Miller, R.; Schaeffler, M. *Dispersionseigenschaften 2D-Rheologie, 3D-Rheologie, Stabilität, 1. Auflage*; Eigenverlag: Berlin-Potsdam, Germany, 2015; ISBN 978-3-00-045864-4.
6. Zhang, Y.; Pang, B.; Yang, S.; Fang, W.; Yang, S.; Yuan, T.-Q.; Sun, R.-C. Improvement in Wood Bonding Strength of Poly (Vinyl Acetate-Butyl Acrylate) Emulsion by Controlling the Amount of Redox Initiator. *Materials* **2018**, *11*, 89. [[CrossRef](#)]
7. Sekeri, S.H.; Ibrahim, M.N.M.; Umar, K.; Yaqoob, A.A.; Azmi, M.N.; Hussin, M.H.; Othman, M.B.H.; Malik, M.F.I.A. Preparation and Characterization of Nanosized Lignin from Oil Palm (*Elaeis Guineensis*) Biomass as a Novel Emulsifying Agent. *Int. J. Biol. Macromol.* **2020**, *164*, 3114–3124. [[CrossRef](#)]
8. Atanase, L.I.; Bistac, S.; Riess, G. Effect of Poly(Vinyl Alcohol-Co-Vinyl Acetate) Copolymer Blockiness on the Dynamic Interfacial Tension and Dilational Viscoelasticity of Polymer–Anionic Surfactant Complex at the Water-1-Chlorobutane Interface. *Soft Matter* **2015**, *11*, 2665–2672. [[CrossRef](#)] [[PubMed](#)]



9. Atanase, L.; Riess, G. Thermal Cloud Point Fractionation of Poly(Vinyl Alcohol-Co-Vinyl Acetate): Partition of Nanogels in the Fractions. *Polymers* **2011**, *3*, 1065–1075. [\[CrossRef\]](#)
10. Atanase, L.-I.; Boscher, V.; Lasuye, T.; Stasik, B.; Riess, G. Colloidal Characteristics of Vinyl Alcohol-Vinyl Acetate Copolymers by Complex Formation with Sodium Dodecyl Sulphate. *Rev. Roum. Chim.* **2009**, *54*, 557–581.
11. Chern, C.S. Emulsion Polymerization Mechanisms and Kinetics. *Prog. Polym. Sci.* **2006**, *31*, 443–486. [\[CrossRef\]](#)
12. Sajjadi, S. Particle Formation under Monomer-Starved Conditions in the Semibatch Emulsion Polymerization of Styrene. *J. Polym. Sci.* **2001**, *39*, 3940–3952. [\[CrossRef\]](#)
13. Suzuki, A.; Yano, M.; Saiga, T.; Kikuchi, K.; Okaya, T. Study on the Initial Stage of Emulsion Polymerization of Vinyl Acetate Using Poly(Vinyl Alcohol) as a Protective Colloid. *Colloid Polym. Sci.* **2003**, *281*, 337–342. [\[CrossRef\]](#)
14. Agirre, A.; Calvo, I.; Weitzel, H.-P.; Hergeth, W.-D.; Asua, J.M. Semicontinuous Emulsion Co-Polymerization of Vinyl Acetate and VeoVa10. *Ind. Eng. Chem. Res.* **2014**, *53*, 9282–9295. [\[CrossRef\]](#)
15. Agirre, A.; Weitzel, H.-P.; Hergeth, W.-D.; Asua, J.M. Process Intensification of VAc-VeoVa10 Latex Production. *Chem. Eng. J.* **2015**, *266*, 34–47. [\[CrossRef\]](#)
16. Lepizzera, S.M.; Hamielec, A.E. Nucleation of Particles in Seeded Emulsion Polymerization of Vinyl Acetate with Poly(Vinyl Alcohol) as Emulsifier. *Macromol. Chem. Phys.* **1994**, *195*, 3103–3115. [\[CrossRef\]](#)
17. Finetti, F.; Lugli, M.; Saija, L.M. Industrial Production of Poly Vinyl Acetate Dispersions: Relationship Between Latex Properties and Polymerization Start-Up Temperature. *Polym. Plast. Technol. Eng.* **2013**, *52*, 1133–1139. [\[CrossRef\]](#)
18. Kongr, X.Z.; Pichot, C.; Guillot, J. Characterization of Particle Surface and Morphology in Vinyl Acetate-Butyl Acrylate Emulsion Copolymers—Influence of the Copolymerization Pathway. *Colloid Polym. Sci.* **1987**, *265*, 791–802. [\[CrossRef\]](#)
19. Harner, R.S.; Ressler, R.J.; Briggs, R.L.; Hitt, J.E.; Larsen, P.A.; Frank, T.C. Use of a Fiber-Optic Turbidity Probe to Monitor and Control Commercial-Scale Unseeded Batch Crystallizations. *Org. Process Res. Dev.* **2009**, *13*, 114–124. [\[CrossRef\]](#)
20. Muenzberg, M.; Hass, R.; Dinh Duc Khanh, N.; Reich, O. Limitations of Turbidity Process Probes and Formazine as Their Calibration Standard. *Anal. Bioanal. Chem.* **2017**, *409*, 719–728. [\[CrossRef\]](#) [\[PubMed\]](#)
21. Muenzberg, M.; Hass, R.; Reich, O. In-Line Characterization of Phase Inversion Temperature Emulsification by Photon Density Wave Spectroscopy. *SOFW J.* **2013**, *139*, 38–46.
22. Hass, R.; Muenzberg, M.; Bressel, L.; Reich, O. Industrial Applications of Photon Density Wave Spectroscopy for In-Line Particle Sizing. *Appl. Opt.* **2013**, *52*, 1423. [\[CrossRef\]](#)
23. Jacob, L.I.; Pauer, W. In-Line Monitoring of Latex-Particle Size during Emulsion Polymerizations with a High Polymer Content of More than 60%. *RSC Adv.* **2020**, *10*, 26528–26534. [\[CrossRef\]](#)
24. Bressel, K.; Müller, W.; Leser, M.E.; Reich, O.; Hass, R.; Wooster, T.J. Depletion-Induced Flocculation of Concentrated Emulsions Probed by Photon Density Wave Spectroscopy. *Langmuir* **2020**, *36*, 3504–3513. [\[CrossRef\]](#) [\[PubMed\]](#)
25. Gutschmann, B.; Schiewe, T.; Weiske, M.T.H.; Neubauer, P.; Hass, R.; Riedel, S.L. In-Line Monitoring of Polyhydroxyalkanoate (PHA) Production during High-Cell-Density Plant Oil Cultivations Using Photon Density Wave Spectroscopy. *Bioengineering* **2019**, *6*, 85. [\[CrossRef\]](#)
26. Häne, J.; Brühwiler, D.; Ecker, A.; Hass, R. Real-Time Inline Monitoring of Zeolite Synthesis by Photon Density Wave Spectroscopy. *Microporous Mesoporous Mater.* **2019**, *288*, 109580. [\[CrossRef\]](#)
27. Bressel, L.; Hass, R.; Reich, O. Particle Sizing in Highly Turbid Dispersions by Photon Density Wave Spectroscopy. *J. Quant. Spectrosc. Radiat. Transf.* **2013**, *126*, 122–129. [\[CrossRef\]](#)
28. Bressel, L. Bedeutung Der Abhängigen Streuung Für Die Optischen Eigenschaften Hochkonzentrierter Dispersionen. Doctoral's Dissertation, University of Potsdam, Potsdam, Germany, 2016.
29. Bressel, L.; Wolter, J.; Reich, O. Particle Sizing in Highly Turbid Dispersions by Photon Density Wave Spectroscopy: Bidisperse Systems. *J. Quant. Spectrosc. Radiat. Transf.* **2015**, *162*, 213–220. [\[CrossRef\]](#)
30. Zecha, H.; Weitz, H.-P. Method for Producing Vinyl Ester Polymers Having Specifically Settable Dispersity and Low Polydispersity. U.S. Patent 9,650,507 B2, 16 May 2017.
31. Damas, C.; Leprince, T.; Ngo, T.H.V.; Coudert, R. Behavior Study of Polyvinyl Alcohol Aqueous Solution in Presence of Short Chain Micelle-Forming Polyols. *Colloid Polym. Sci.* **2008**, *286*, 999–1007. [\[CrossRef\]](#)
32. Hass, R. Angewandte Photonendichtewellen Spektroskopie. Doctoral Dissertation, University of Potsdam, Potsdam, Germany, 2011.
33. Hass, R.; Reich, O. Photon Density Wave Spectroscopy for Dilution-Free Sizing of Highly Concentrated Nanoparticles During Starved-feed Polymerization. *ChemPhysChem* **2011**, *12*, 2572–2575. [\[CrossRef\]](#)
34. Hass, R.; Munzke, D.; Reich, O. Inline-Partikelgrößenmesstechniken für Suspensionen und Emulsionen. *Chem. Ing. Tech.* **2010**, *82*, 477–490. [\[CrossRef\]](#)
35. Reich, O. Photonendichtewellenspektroskopie mit Intensitätsmodulierten Diodenlasern. Doctoral's Dissertation, University of Potsdam, Potsdam, Germany, 2005.
36. Flory, P.J. The Mechanism of Vinyl Polymerizations. *J. Am. Chem. Soc.* **1937**, *59*, 241–253. [\[CrossRef\]](#)
37. Jelinska, N.; Tupureina, V. Poly (Vinyl Alcohol)/Poly (Vinyl Acetate) Blend Films. *Sci. J. Riga Tech. Univ.* **2010**, *21*, 7.



## 5.2 Advanced Particle Size Analysis in High-Solid-Content Polymer Dispersions Using Photon Density Wave Spectroscopy

This paper has been published in *Polymers*. **2023**; 15(15):3181.

ISSN: 2073-4360

Digital object identifier (DOI): 10.3390/polym15153181

Online available at: <https://doi.org/10.3390/polym15153181>

© 2021 The Authors. *Polymers* published by MDPI AG

Reproduced with permission of MDPI (Basel, Switzerland) under the terms and conditions of an Open Access license, creative commons licensing by mentioning who the research is by when its used (CC BY license).

Impact factor: 5.0

### 5.2.1 Aim of this research

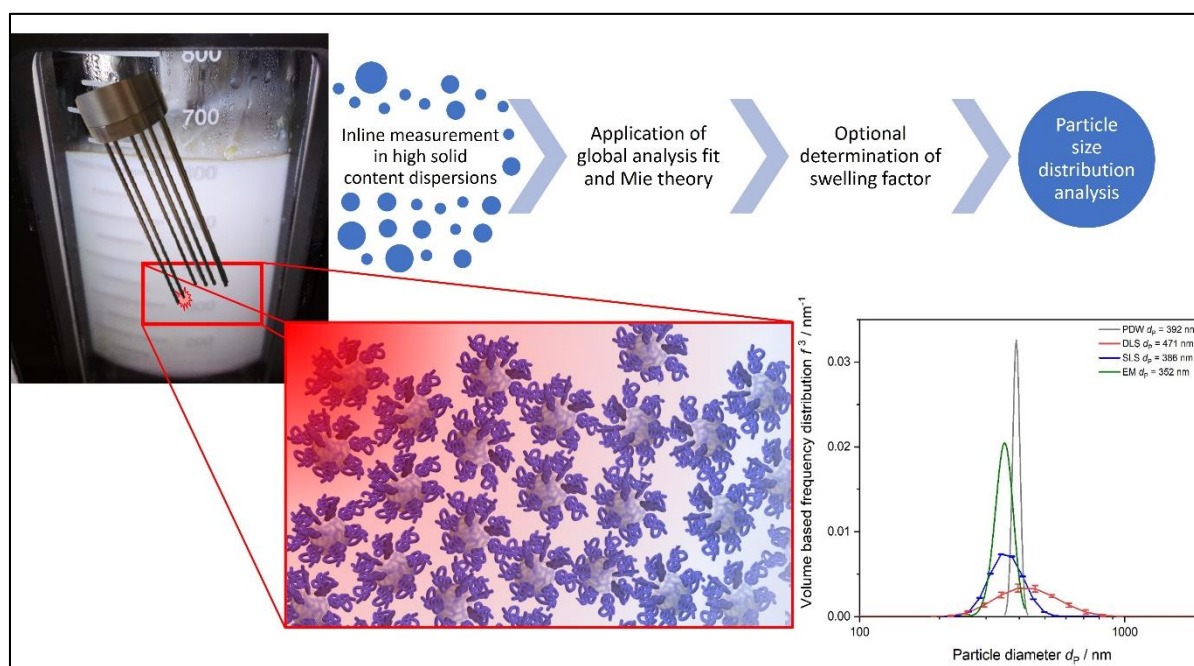


Figure 13 Schematic overview of inline monitoring process of high concentrated polymer dispersions by photon density wave spectroscopy to determine particle size and distribution via global fit analysis.

This research aims at establishing PDW spectroscopy as a tool for the determination of water binding abilities of PVAc-PVA particles by an error minimization approach. It is shown that by error minimization, which correlates with water-swelling of the PVAc particle, the experimentally determined  $\mu_s'$  true values can be fitted with the theoretically calculated PDW spectroscopy algorithm for monodisperse particles. The paper aims at manifesting PDW



spectroscopy as a standardized PAT tool by showing PS-SDS dispersions as a best practice and aims at adaptation of the methods for PVAc-PVA dispersions of very high solid contents > 40 % (w/w). It further aims at showing that after the adaptation of the iterative swelling-factor the PSD determined by PDW spectroscopy does agree very well to common light scattering sizing techniques SLS, DLS and EM.

## Article

# Advanced Particle Size Analysis in High-Solid-Content Polymer Dispersions Using Photon Density Wave Spectroscopy

Stephanie Schlappa <sup>1,\*</sup>, Lena Bressel <sup>1</sup>, Oliver Reich <sup>2</sup> and Marvin Münzberg <sup>1,2</sup>
<sup>1</sup> Department of Physical Chemistry, innoFSPEC, University of Potsdam, Am Mühlenberg 3, 14476 Potsdam, Germany; marvin.muenzberg@uni-potsdam.de (M.M.)

<sup>2</sup> Knowledge and Technology Transfer, Faculty of Science, University of Potsdam, Am Mühlenberg 3, 14476 Potsdam, Germany; oliver.reich@uni-potsdam.de

\* Correspondence: stephanie.schlappa@uni-potsdam.de

**Abstract:** High-solid-content polystyrene and polyvinyl acetate dispersions of polymer particles with a 50 nm to 500 nm mean particle diameter and 12–55% (*w/w*) solid content have been produced via emulsion polymerization and characterized regarding their optical and physical properties. Both systems have been analyzed with common particle-size-measuring techniques like dynamic light scattering (DLS) and static light scattering (SLS) and compared to inline particle size distribution (PSD) measurements via photon density wave (PDW) spectroscopy in undiluted samples. It is shown that particle size measurements of undiluted polystyrene dispersions are in good agreement between analysis methods. However, for polyvinyl acetate particles, size determination is challenging due to bound water in the produced polymer. For the first time, water-swelling factors were determined via an iterative approach of PDW spectroscopy error ( $X^2$ ) minimization. It is shown that water-swollen particles can be analyzed in high-solid-content solutions and their physical properties can be assumed to determine the refractive index, density, and volume fraction in dispersion. It was found that assumed water swelling improved the reduced scattering coefficient fit by PDW spectroscopy by up to ten times and particle size determination was refined and enabled. Particle size analysis of the water-swollen particles agreed well with offline-based state-of-the-art techniques.

**Keywords:** emulsion polymerization; multiple light scattering; photon density wave spectroscopy; particle sizing; swelling of polymers



**Citation:** Schlappa, S.; Bressel, L.; Reich, O.; Münzberg, M. Advanced Particle Size Analysis in High-Solid-Content Polymer Dispersions Using Photon Density Wave Spectroscopy. *Polymers* **2023**, *15*, 3181. <https://doi.org/10.3390/polym15153181>

Academic Editor: Sixun Zheng

Received: 27 June 2023

Revised: 21 July 2023

Accepted: 24 July 2023

Published: 26 July 2023



**Copyright:** © 2023 by the authors. Licensee MDPI, Basel, Switzerland. This article is an open access article distributed under the terms and conditions of the Creative Commons Attribution (CC BY) license (<https://creativecommons.org/licenses/by/4.0/>).

## 1. Introduction

Emulsion polymerization processes are one of the most common polymerization processes to produce high-solid-content polymer dispersions. In contrast to suspension polymerization, emulsion polymerization promotes higher solid contents, better heat transfer, faster polymerization rates, and better colloidal stability. A vast variety of polymers and stabilizers are already well-characterized. Accessible products range from low to high density polymers, branched and stretched, and homo- as well as co-polymers. Given the great variety of polymers, many different types of products and different product applications can be achieved [1,2].

The precise analysis of particle size and particle size distribution (PSD) is of the utmost importance for liquid polymer dispersions. These properties play an important role as they define the usage and applications of polymer dispersions, e.g., the fluidity and stability of high-solid-content polymer dispersions [3]. The mean particle size of polymers depends on many thermodynamic and kinetic factors during their synthesis, like the solubility of the monomer–polymer, composition of the reactants, temperature, solvent-to-medium ratio, or even reactor geometry [2,4]. The final mean particle size and PSD during emulsion polymerization are further influenced by the monomer amount introduced and the capability of the stabilizer in the dispersion to sustain the colloidal

stability of the particles growing. The amount of stabilizer added accounts for the amount of particles formed and, therefore, also the final mean particle size [5].

To access the mean particle size in high-solid-content polymer dispersions and to determine the PSD, different techniques are known and promoted like turbidimetry, fiber-optic quasi-elastic light scattering or focused beam reflectance measurement, and particle vision and measurement technology. Online measurements in undiluted processes are particularly challenging due to the high turbidity, high number of particles, and multiple scattering [6–11]. Most commonly, offline PSD analysis is used. However, offline techniques require extensive sample preparation like dilution, are time consuming, and are not easy to handle. Additionally, dilution always induces a change in the particle system, whose effects on the measurement are not well-known. Analysis of nanoparticle size distribution is possible by multiple techniques. Laser light-scattering techniques are shown to deliver reliable results; however, adding to the extensive sample preparation and dilution, the results are influenced strongly and shifted by the fractions of bigger particles in the sample. For multimodal or very polydisperse samples, light-scattering techniques lack resolution [12–15].

Input parameters for measurements like the solvent viscosity, the refractive index, the sample concentration, and the sample temperature play a significant role and are compulsory. Necessary sample dilution evidently affects these factors and provokes falsified results. For dynamic light scattering (DLS) measurements, the dilution of the sample affects the autocorrelation function and the resulting particle size. For samples with high particle concentration, i.e., high solid contents, the Stokes–Einstein equation is no longer valid and diffusion coefficients yield wrong hydrodynamic radii [16–19]. Photon density wave (PDW) spectroscopy offers dispersion analysis of highly turbid particle systems or emulsions without dilution by the independent experimental determination of the optical coefficients, reduced scattering coefficient and absorption coefficient, respectively [20–23]. This technique is used in this study to determine the PSD in undiluted concentrated polymer dispersions and compared to the DLS, Static Light Scattering (SLS), and Electron Microscopy (EM) analysis of diluted samples.

In this work, two polymer systems are produced and thoroughly analyzed—polystyrene (PS) particles, stabilized by sodium dodecyl sulfate (SDS), and polyvinyl acetate (PVAc), stabilized by poly (vinyl alcohol, PVA). The respective chemical structures of the polymers and stabilizers used in this study are shown in Figure 1. Stabilizers are shown in their deprotonated form. It is reported in literature that PS and SDS are not prone to incorporating water, due to their hydrophobic character, whereas PVAc and PVA, due to their significantly more hydrophilic character, especially PVA with plenty of accessible hydroxyl groups also shown in Figure 1, are not only known to bind water loosely by van der Waals interactions, but are also able to build hydrogen bonds, which bind the water strongly to the hydrophilic sites [24–27]. Due to the polarizability of SDS, it is possible that water molecules attach to the surfactants surrounding the polymer, but the amount and effect on the particle will be significantly lower than for the PVA stabilized particles. The hydrophobic alkyl chains will attach to the polymer and few loose interactions happen with the surrounding media and water.

Three states of bound water were found to be present in PVA: free water, bound-freezable, and bound-non-freezable water, which has nearly the same characteristics as bulk water [28–30]. The amount of freezable water accounts only for a very small percentage and is, therefore, complicated to detect. Only a combination of different thermal analyses may be able to determine the amount of water in the PVAc-PVA particle [31–33]. It is assumed that the PVAc-PVA particles are swollen with water and also have a swollen emulsifier shell around the PVAc particle core. The degree of swelling is hard to determine due to the different kinds of water-binding mechanisms. The swelling of the polymer particle has a significant influence on the density and refractive index of the particle as well as the solid content and the volume ratio between the PVAc polymer core, polymer shell, and medium in the dispersion. These are the main factors that have a great influence on



the PSD measurements. A lot of data on polymer swelling in literature concentrates on the swelling of dry polymer films in water or the swelling of hydrogels [34–36]. In this study, undiluted measurements of PVAc-PVA particles are analyzed regarding the swelling of the particle with the medium in high-solid-content dispersions.

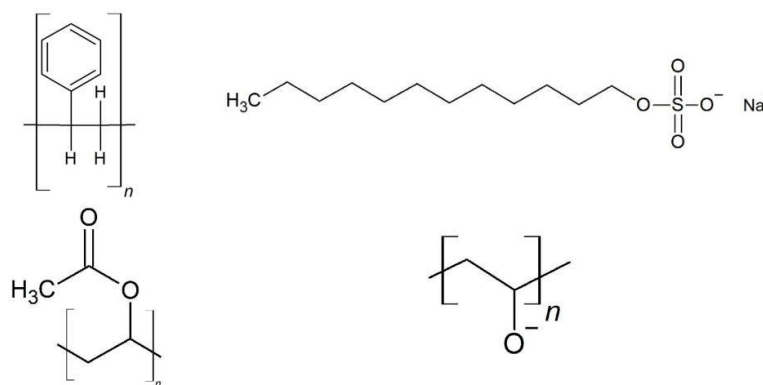


**Figure 1.** Representative chemical structures of polymers PS and PVAc, and stabilizers SDS and PVA used in this study. From top left to bottom right: structure of polymer PS, stabilizer SDS, polymer PVAc, and stabilizer PVA.

For both systems, PS-SDS and PVAc-PVA, particles with various mean particle sizes and PSD can be obtained by emulsion polymerization [5,37,38]. The polymers can be produced in numerous shapes, co-monomer compositions, and sizes from a few nanometers to the upper micrometer size regime [5,39,40]. To produce mean particle sizes between 50 and 500 nm, seeded emulsion polymerization was performed. Seeded emulsion polymerization is a well-known method to produce monodisperse PS dispersions.

Starved-feed emulsion polymerization was used to produce PVAc-PVA particles between 100 and 500 nm mean particle size [20,41,42].

## 2. Materials and Methods

All chemicals were used and handled as described. Styrene was purchased from different suppliers throughout the experiments ( $104.15 \text{ g mol}^{-1}$ ,  $\geq 99.5\%$ , Carl Roth, Karlsruhe, Germany and Merck, Darmstadt, Germany). Sodium dodecyl sulfate (SDS,  $288.38 \text{ g mol}^{-1}$ , Carl Roth, Karlsruhe, Germany), di-sodiumtetraborate decahydrate (Na-Tetra Borate,  $381.37 \text{ g mol}^{-1}$ ,  $\geq 99.5\%$ , Carl Roth, Karlsruhe, Germany), sodium hydroxide (NaOH,  $40.0 \text{ g mol}^{-1}$ ,  $\geq 99\%$ , Carl Roth, Karlsruhe, Germany), aluminum hydroxide ( $\text{Al}(\text{OH})_3$ , dried gel,  $78.01 \text{ g mol}^{-1}$ ,  $99\%$ , abcr GmbH, Karlsruhe, Germany), and potassium peroxodisulfate (KPS,  $270.32 \text{ g mol}^{-1}$ ,  $\geq 99\%$ , Carl Roth, Karlsruhe, Germany) were used as purchased.

Prior to use, the styrene was destabilized by filtering over granulated  $\text{Al}(\text{OH})_3$  in a flash column and, afterwards, washed repeatedly in 1 M NaOH using a separating funnel. The styrene showed a light transparent-yellowish color and was further handled at room temperature. Monomer vinyl acetate (VAc,  $86.09 \text{ g mol}^{-1}$ ,  $\geq 99\%$ , Sigma-Aldrich, Darmstadt, Germany) was purged with  $\text{N}_2$  (Nippon Gases, Duesseldorf, Germany) for 30 min prior to synthesis. Redox initiator pair ascorbic acid (AA,  $176.12 \text{ g mol}^{-1}$ ,  $99\%$ , Acros Organics, Geel, Belgium) and sodium persulfate (NaPS,  $238.10 \text{ g mol}^{-1}$ ,  $\geq 99\%$ , Carl Roth, Karlsruhe, Germany) and catalyst ammonium iron (III) sulfate hexahydrate (FAS,  $392.14 \text{ g mol}^{-1}$ ,  $99\%$ , Acros Organics, Geel, Belgium) were used as purchased. Mowiol® 4-88 (polyvinyl alcohol, approx.  $31,000 \text{ g mol}^{-1}$ , Sigma-Aldrich, Darmstadt, Germany) was used as purchased.

### 2.1. Synthesis

Preparation of solutions was performed with analytical grade Milli-Q<sup>®</sup> water from an in-house Milli-Q<sup>®</sup> water dispenser (Milli-Q<sup>®</sup>, Integral 5, Merck Millipore, Darmstadt, Germany). An automated lab reactor (OptiMax 1001, Mettler Toledo, Gießen, Germany) at approx. 1 L reaction scale was used for synthesis. Produced polymer dispersions were stored in airtight containers and showed no sign of destabilization for over twelve months.

#### 2.1.1. PS Seed Synthesis

Batch emulsion polymerization was used to produce PS particles with a narrow size distribution to be used further as seed particles. The recipe for the seed synthesis is given in Table 1.

**Table 1.** Recipe for batch emulsion polymerization of PS seed particles.

	Chemical	Amount [g]
Medium	Milli-Q <sup>®</sup> water	530
Monomer	Styrene	135
Stabilizer	SDS	6.2 <sup>a</sup>
Buffer	Na-Tetra Borate	0.125
Initiator	Potassium peroxodisulfate	5.0 <sup>b</sup>

<sup>a</sup> dissolved in 30 g Milli Q<sup>®</sup> water. <sup>b</sup> dissolved in 95 g Milli Q<sup>®</sup> water.

Emulsion polymerization was started by charging 500 g of Milli-Q<sup>®</sup> water in the 1 L batch reactor. Under stirring at 100 rpm and N<sub>2</sub> purging, the initial charge (iC) was heated to 100 °C for 60 min to degas. Temperature was reduced to 55 °C over 45 min. At 55 °C reaction temperature, 135 g styrene, 6.2 g SDS in water, and 0.125 g of Na-Tetra Borate were added. After a short waiting period for the emulsion to form, 30 mL of a 5% KPS solution were added automatically via a computer-controlled dosing unit at 6 mL min<sup>−1</sup>. Simultaneously, the stirrer was ramped to 200 rpm. The emulsion was left to polymerize at 55 °C reaction temperature for 24 h. After 24 h, a post-polymerization step at 83 °C for 3 h was initiated. The system was cooled to 20 °C over 30 min.

#### 2.1.2. PS-Seeded Emulsion Polymerization

To produce PS nanoparticles of different mean particle sizes, seeded emulsion polymerization was performed. A small amount of the PS seed produced after Table 1 was taken and the particles were grown to various mean particle sizes, as shown in Table 2.

**Table 2.** Recipe for seeded emulsion polymerization of PS particles.

	Chemical	Amount [g]	Feedrate [mL min <sup>−1</sup> ]
Medium	Milli-Q <sup>®</sup> water	308.6 <sup>a</sup>	
Seed	PS Seed	31.5 <sup>b</sup>	
Monomer	Styrene	337 <sup>c</sup>	2.1
Stabilizer	10% SDS solution <sup>d</sup>	164	
Buffer	Na-Tetra Borate	0.25	
Initiator	5% potassium peroxodisulfate solution	100	

<sup>a</sup> except for syntheses PS003, PS004, and PS005 where 301 g water, PS009\_1, and 009\_2 where 130 g water, and PS020 where 500 g water were charged. <sup>b</sup> except for syntheses PS009\_1 and PS009\_2 where 100 g of PS seed were used. <sup>c</sup> except for syntheses PS009\_1 and PS009\_2 where 240 g styrene were fed at 1.5 mL min<sup>−1</sup>. <sup>d</sup> except for syntheses PS014 and PS016 where 3%, and PS018 and PS019 where 5% SDS solution were used.

#### 2.1.3. Emulsion Polymerization of Polyvinyl Acetate Dispersions

Recipe for the produced PVAc-PVA dispersions is shown in Table 3 with determined density of the pure polymer and gravimetrically derived solid content after at least 48 h

drying at 74 °C in an oven. Details on the emulsion polymerization process can be found in Schlappa et al. [20].

**Table 3.** Recipe for PVAc-PVA dispersions. Experimental series of five syntheses with increasing amount of stabilizer in the iC.

Sample ID	PVA <sub>iC</sub> [g]	Milli-Q <sup>®</sup> <sub>iC</sub> [g]	<i>c</i> (PVA <sub>iC</sub> ) [g L <sup>−1</sup> ]	Solid Content $\omega$ [%]	Density $\rho_P$ [g cm <sup>−3</sup> ]
PVAc-PVA 0 g L <sup>−1</sup>	0	302	0	41.07	1.216
PVAc-PVA 1 g L <sup>−1</sup>	0.299	302	0.99	41.61	1.214
PVAc-PVA 2 g L <sup>−1</sup>	0.599	302	1.98	40.92	1.216
PVAc-PVA 5.5 g L <sup>−1</sup>	1.66	302	5.50	41.57	1.212
PVAc-PVA 11 g L <sup>−1</sup>	3.31	302	10.96	40.77	1.214

## 2.2. Dispersion Analysis

After completion of a synthesis, offline sample analysis was performed. After approx. 400-fold dilution with Milli-Q<sup>®</sup> water to visual transparency, three repetition measurements of each sample were performed by DLS analysis (Zetasizer Ultra, Malvern Panalytical, Worcestershire, UK), at measurement angle of 173°, in disposable 4 mL PS cuvettes, at 25 °C measurement temperature. Samples for SLS measurements (LS13320, Beckman Coulter, Brea, CA, USA) were manually diluted approx. 1:125 with Milli-Q<sup>®</sup> water and charged to the SLS sample chamber until a polarization intensity differential scattering (PIDS) signal of approx. 40% was achieved. Obscuration values lower than 2% were retained. Results shown for PSDs obtained by light-scattering techniques are mean values of three measurements. Out of the three individual measurements, the mean value is plotted with one standard deviation as error bars. For electron microscopy (EM) analysis, samples were diluted approx. 1000-fold with Milli-Q<sup>®</sup> water and a drop of sample was placed onto a copper-coal mesh (Plano GmbH, Wetzlar, Germany). The sample was left to dry for an hour at ambient conditions. Quanta FEI 250 electron microscope was used for analysis in STEM mode.

## 2.3. PDW Spectroscopy Dispersion Analysis

Photon density wave (PDW) spectroscopy is among few techniques which offers dispersion analysis by the determination of the optical coefficients of a highly turbid particle system without dilution even at high solid contents of the dispersed species. The PDW spectroscopy device used here is self-built (University of Potsdam—innofSPEC, Potsdam, Germany). No sample preparation is needed as the optical fibers can directly be inserted into the dispersion for measuring. Two optical fibers are immersed into the undiluted dispersion. These fibers act as light emission and detection source for intensity-modulated laser light. The detection fiber is mounted to a precision translations stage which moves in scalable distances to and from the emission fiber. Fibers used in this set-up have a 600  $\mu$ m core diameter. Intensity-modulated laser light (10–1210 MHz) is guided into the sample via the emission fiber and interacts with the sample regarding the samples' absorption and scattering properties. Due to the multiple scattered light, a PDW is expressed. A small portion of the PDW light is guided to an avalanche photo diode by the detection fiber. The electronic signal is amplified and then analyzed by a network analyzer with respect to phase shift and amplitude. The change in amplitude and phase in dependency of the distance between the emission and detection fiber and the modulation frequency can be related to the absorption coefficient  $\mu_a$  and reduced scattering coefficient  $\mu_s'$  of the sample. These optical coefficients can be obtained for different wavelengths one after another.

The reduced scattering coefficients are used to determine the mean particle size and particle size distribution, with the help of the Mie theory and the theory of dependent scattering [22,43]. Highly turbid polymer samples have already been successfully analyzed and characterized by PDW spectroscopy regarding their mean particle diameter



and PSD [44–47]. Inline monitoring of emulsion polymerization processes has also been successfully reported [20,21,48–50].

In this study, two polymer systems were evaluated, one which is not prone to incorporating water and one where water swelling of the particles is common, to show the differences in analyzing the particle size by PDW spectroscopy if water swelling of particles occurs. To determine the mean particle size and PSD, theoretical  $\mu_s'$  values are calculated that match the experimentally determined  $\mu_s'$  values by the applied PDW spectroscopy algorithm. If experimental and theoretical values agree well with each other, it can be assumed that the swelling, and particle characteristics represent the actual situation in the dispersion. To theoretically reproduce the experimentally determined  $\mu_s'$ , the refractive index, and density of the polymer and medium as it is present in the dispersion, as well as the solid content, an assumption of the mean particle diameter and width of a normal logarithmic Gauss distribution are necessary for a data fit. In a first step, the solid content will be determined gravimetrically. A small weighted sample is placed in a drying cabinet at low temperature (74 °C) in order to keep the polymer intact. Drying was achieved over a period of time >72 h to evaporate the medium and bound water inside the polymer. The dry weight is measured at mass consistency, and the solid content calculated.

A concentration series of 30% (w/w), 20% (w/w), 10% (w/w), 1% (w/w), and 0.1% (w/w) of each polymer dispersion was used to determine the density of the polymer particles. Each sample was measured at 20 °C with a densitometer (DM45 Delta Range, Mettler Toledo, Gießen, Germany). Density analysis of the particles for the pure polymer (100% (w/w)) was performed by [49]:

$$\rho_{Disp} = \frac{\rho_D \rho_P}{\omega[\rho_D - \rho_P] + \rho_P} \leftrightarrow \frac{1}{\rho_{Disp}} = \omega \left[ \frac{1}{\rho_P} - \frac{1}{\rho_D} \right] + \frac{1}{\rho_D} \quad (1)$$

with  $\rho_{Disp}$ ,  $\rho_D$ , and  $\rho_P$  as densities of the dispersion, the dispersant, and the polymer and the solid content  $w$  of the dispersion. The density of pure water was considered for zero polymer content (0% (w/w)). The density of the polymer was obtained from the slope of a linear fit; the error was obtained via error propagation.

The same samples were also used for refractive index measurements with a multi-wavelength refractometer (DRS-λ, Schmidt + Haensch, Berlin, Germany) at 20 °C at seven different wavelengths between 403 and 938 nm. The measured refractive indices are extrapolated to the refractive index of the particles using the Newton equation and, afterwards, inter- or extrapolated to the wavelengths of PDW spectroscopy by a Cauchy formula [49,51].

To speed up the PDW calculations, estimates of the mean particle size and PSD can be introduced based on offline reference methods or theoretical particle size considerations. With these parameters, a first PDW spectroscopy fit is obtained within a few minutes.

In the case that this first fit of theoretical  $\mu_s'$  does not match the experimental results, high error values  $X^2$  for the  $\mu_s'$  fit are given by the software. The value of  $X^2$  expresses how well the theoretically calculated values agree with the experimentally determined values and is a measurement of the fit quality. If  $X^2$  values are high, modifications of the input parameters are necessary, as the particle in solution expresses different properties as determined by this first rough estimation of its physical properties. Literature data already suggest that the bound water inside the PVAc-PVA polymer cannot be dried off completely by only drying in an oven. A combination of different thermogravimetric techniques is necessary to determine the exact water content, which is very time consuming, costly, and complicated. The water-swollen polymer in solution does not express the same properties like in a dried state. To validate the mean particle diameter and PSD measurement by PDW spectroscopy, iterative steps of water swelling  $\theta_{swollen}$  are assumed, affecting the density  $\rho_{P, swollen}$ , refractive index  $n_{P, swollen}$ , and volume fraction  $\phi_{P, swollen}$  of the polymer to a great extent. Various percentages of water swelling  $\theta_{swollen}$  in 0.05 steps (from 0% to

50%) are assumed and added to the experimentally derived solid content. A new volume fraction for the particle affected by water swelling is calculated:

$$\varphi_{P,swollen} = (1 + \theta_{swollen}) \frac{\left( \frac{\omega_{gravimetric}}{\rho_{Polymer}} \right)}{\left( \frac{\omega_{gravimetric}}{\rho_{experimental}} + \frac{(1 - \omega_{gravimetric})}{\rho_D} \right)} \quad (2)$$

with this new volume fraction of the swollen polymer  $\varphi_{P,swollen}$ , adjusted values for the density (Formula (1)) and refractive index (Formula (3)) are recalculated.

$$n_{P,swollen} = \sqrt{\varphi_{P,swollen} * n_P^2 + [1 - \varphi_{P,swollen}] * n_D^2} \quad (3)$$

with the recalculated refractive index of water-swollen polymer as  $n_{P,swollen}$ , the increased volume fraction  $\varphi_{P,swollen}$ , and the refractive index of the non-swollen particle  $n_P$  and dispersant  $n_D$ . These recalculated values are used with the assumed mean particle size and PSD to recalculate  $\mu_s'$  by the automated PDW spectroscopy algorithm. The resulting  $\mu_s'$  values are compared to the experimental values again and the  $X^2$  error parameter for the fit of theoretical-to-experimental  $\mu_s'$  is analyzed. The smaller the  $X^2$ , the better the agreement between experimental and theoretical values, meaning the better the fit quality, and the water-swelling factor  $\theta_{swollen}$  is assumed to represent the real properties of the particles in the analyzed dispersion.

This iterative approach is carried out for several percentages of water swelling until the lowest possible  $X^2$  value is found, starting with 10% water-swelling steps, finding the lowest  $X^2$  and minimizing the steps up to 1%. A parabola fit is used to find the minimum of  $X^2$  of the theoretically determined PDW spectroscopy fits. This percentage of water swelling represents the experimental data best and it can be assumed that the polymer is swollen with water by the derived percentage.

For comparison between size distribution data from DLS, SLS, and PDW spectroscopy, the mean particle diameter calculated from the volume frequency distributions are normalized regarding the bin width. PSDs are usually shown in different types of distributions. Most common types include intensity, number, and volume-based PSDs. PDW spectroscopy provides a volume-based PSD with a mean particle diameter comparable to the so-called De Brouckère mean ( $d_{43}$ ). The DLS measurement used for comparison gives a PSD in volume from measuring the hydrodynamic radius, calculated from an intensity weighted measurement [52–54]. To compare particle size distributions derived from PDW spectroscopy to distributions derived from offline, dilution-based techniques, an area normalization of the distribution is done. Normalization results in volume frequency distributions per nanometer ( $f_3$ ) for every measurement method.

### 3. Results and Discussion

All high-solid-content samples were synthesized as explained in the experimental section. For all dispersions, a white, turbid liquid without visible coagulation was obtained and stored in airtight containers until further use. Two polymer systems have been examined: the first, PS-SDS, is not known to incorporate water and no swelling of the particles is expected. Results are first shown for PS-SDS dispersions regarding reproducibility, PDW spectroscopy analysis of optical coefficients  $\mu_a$  and  $\mu_s'$ , and PSD analysis by PDW spectroscopy compared to offline standard PSD measurement methods as a best practice. The second particle system, PVAc-PVA, is analyzed in the same way regarding reproducibility and PDW spectroscopy with a focus on the determination of the particle swelling and size determination of the polymer particles.



### 3.1. Polystyrene—SDS Dispersions

#### 3.1.1. Reproducibility of Polystyrene Dispersions

To investigate the reproducibility during this work, up to four polymerizations have been performed at equal conditions. Figure 2 shows the absorption coefficient  $\mu_a$  and reduced scattering coefficient  $\mu_s'$  obtained by PDW spectroscopy measurements of four undiluted PS dispersions obtained by identical syntheses. Results show that the dispersions are alike in their physical and chemical properties. The solid content of the four experiments was determined gravimetrically and statistically analyzed to be  $w = 36.3 \pm 0.3\%$  ( $w/w$ ) ( $n = 4$ ). For  $\mu_a$ , very good agreement between the four experiments is obtained over the whole measurement range, whereas, for  $\mu_s'$ , measurements at the lower wavelengths show small deviations in between the experiments. At wavelengths  $> 700$  nm the obtained data points agree very well with each other. The small deviations occurring at the lower wavelength range might occur due to possible fluorescent interferences of the laser and the sample. Another factor which might cause these small deviations in  $\mu_s'$  are the polymer content and small deviations in size of the samples. The difference in PS content in between the measurements, however, is very small; the highest  $w$  was gravimetrically determined to be  $w = 36.8\%$  ( $w/w$ ) for PS\_015 and the lowest  $w$  of  $36.5\%$  ( $w/w$ ) for PS\_007. Even such small differences in the solid content, and possibly size of a few nanometers, can be detected by PDW spectroscopy via  $\mu_s'$ . Due to the higher polymer content of the dispersions, an increase in particle scattering can be observed with PDW spectroscopy, where other methods like gravimetric solid content determination fail to detect this minimal difference in solid content. PS-SDS syntheses are highly reproducible with very small differences in mean particle size.

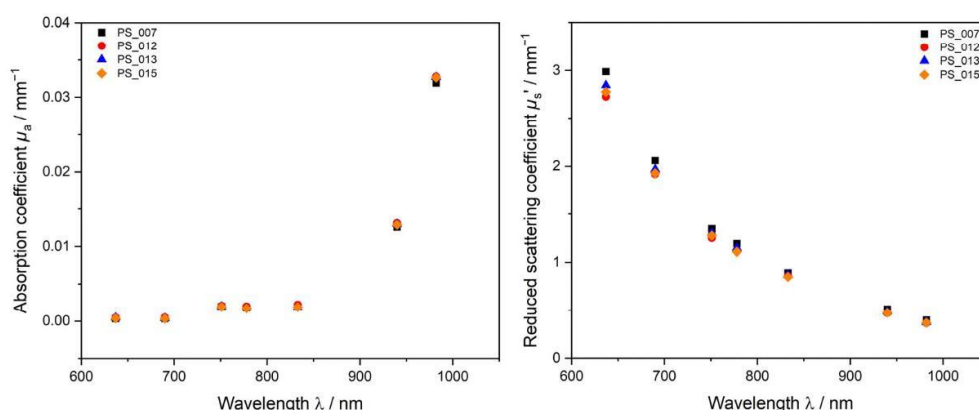


**Figure 2.** Four repeated emulsion polymerization PS-SDS experiments. Dispersions produced after the same recipe and procedure. Optical parameters  $\mu_a$  (left) and  $\mu_s'$  (right), determined in the undiluted sample at approx. 36.3% ( $w/w$ ) PS-SDS with PDW spectroscopy.

#### 3.1.2. PDW Spectroscopy Analysis of Undiluted PS-SDS Dispersions

The scattering behavior of a sample contains a lot of information about the particles in the dispersion. PDW spectroscopy measures the reduced scattering coefficient  $\mu_s'$  dependent on the laser wavelength  $\lambda$  in undiluted polymer samples. Figure 3 shows experimentally measured  $\mu_s'$  values of three different PS-SDS dispersions and theoretical values obtained by PDW spectroscopy size analysis from a fit to the experimental data points after assuming the respective input parameters density, refractive index, size, and width of the distribution. For PS-SDS dispersions in the lower nanometer size regime, i.e.,  $< 100$  nm mean particle diameter (PS 001 and PS 009\_1),  $\mu_s'$  values  $< 4$  mm<sup>-1</sup> were obtained with  $\mu_s'$  decreasing steadily with increasing wavelength. For a dispersion with a mean particle diameter of approximately 270 nm (PS 003), values for  $\mu_s'$  were up to twenty times higher and a significant change of the trend form and an elevation in the curve can

be observed at lower wavelengths around 700 nm. Even with the elevation and changed curve form, the measured  $\mu_s'$  values can be reproduced very well with assumptions of the physical parameters without necessary adjustment.

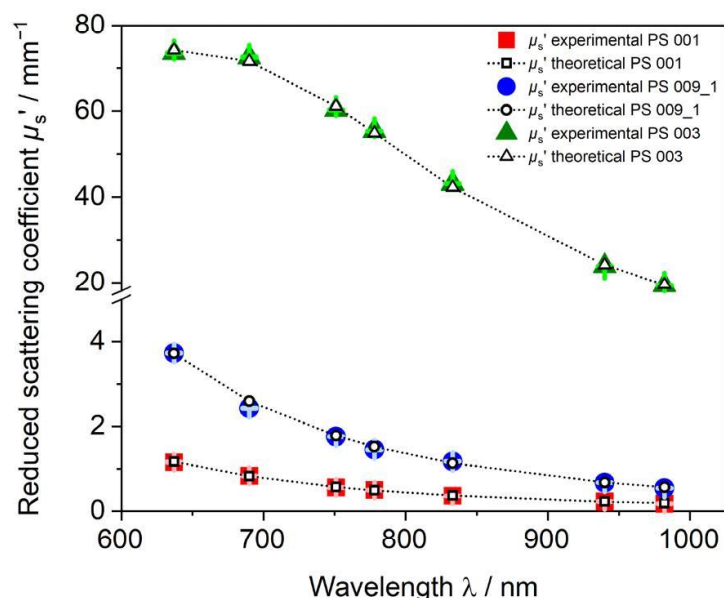


**Figure 3.** Calculated theoretical  $\mu_s'$  values obtained with Mie-theory- and global-analysis-based PDW spectroscopy fit (open symbols) fitted to experimental  $\mu_s'$  (closed symbols) with calculated error bars highlighted in light green, light blue and light red. PS-SDS dispersion with mean particle diameter of PS 001 = 49.0 nm (red squares), PS 009\_01 = 99.1 nm (blue circles), and PS 003 = 271.7 nm (green triangles).

PDW spectroscopy for polystyrene dispersions is applicable for a wide range of dispersions, mean particle sizes, PSDs, and values of  $\mu_s'$  between 0.1 and 80  $\text{mm}^{-1}$  at least. The theoretical  $\mu_s'$  values by PDW spectroscopy shown in Figure 3 as open symbols are calculated with gravimetrically derived solid content of PS 001 = 12.47% ( $w/w$ ), PS 009\_01 = 37.80% ( $w/w$ ), and PS 003 = 29.89% ( $w/w$ ). Density  $\rho$  and refractive index  $n$  of the pure PS-SDS sample without any further assumption of water swelling were calculated to  $\rho_{\text{PS-SDS}} = 1.055 \text{ g cm}^{-3}$  and  $n$  ranging from 1.59 at 637 nm to 1.57 at 982 nm. The very good agreement of the fitted  $\mu_s'$  values to the experimental values verifies that SDS as a stabilizer does not incorporate water and PS-SDS particles are not swollen in water-based dispersions. The calculated values for  $w_{\text{gravimetric}}$ ,  $n_{\text{Polymer}}$ , and  $\rho_{\text{Polymer}}$  represent the actual particle properties as no water swelling occurs, causing these parameters to change. Therefore, the theoretical  $\mu_s'$  values fit well to the experimental values and low  $X^2$  values are obtained.  $X^2$  values are PS 001 = 336, PS 003 = 271, and PS-009\_01 = 941.

### 3.1.3. Method Comparison DLS, SLS, and PDW Spectroscopy

The dependency of  $\mu_s'$  on the particle diameter can be described by the Mie theory and dependent scattering and is used to derive a PSD from PDW spectroscopy measurements. To compare the distributions of the three different particle-sizing techniques, normalization regarding the size bin width has been applied and volume-based frequency distributions  $f^3$  are calculated. Mean particle diameters determined by each technique are compared in Table A1 in the Appendix A.

DLS always gives mean particle diameter values of approx. 15 to 20% bigger than PDW (Table A1 in the Appendix A). This is caused by the fact that DLS measurements determine

the hydrodynamic radius of the particle, whereas PDW spectroscopy determines the size of a hard-sphere particle. The SLS determination of mean particle size shows deviations to DLS and PDW spectroscopy and determined values might be bigger or smaller than for the other techniques. The biggest deviations of up to 40% are found between PDW spectroscopy and SLS for mean particle sizes around 100 nm and smaller. SLS sizing is not suitable for such small particle diameters, as the measurement particle size range starts only at 40 nm on the device used and deviations are unavoidable which falsify the results. For the PSD determination by all three techniques, monomodality is assumed and verified in Figure 4. Comparison between dilution-based light-scattering techniques DLS and SLS and undiluted measurements via PDW spectroscopy are shown in Figure 4. The dilution-based methods result in far wider PSDs than data obtained from PDW spectroscopy, which gives the narrowest PSDs for all three dispersions shown. DLS measurements show tendencies to bigger particle sizes leading to bigger mean  $d_p$  than PDW spectroscopy measurements. Results found in earlier studies revealed similar results regarding DLS [20,21,48]. SLS measurements show no clear trend. For the smallest particles, SLS shows a big deviation from the other methods with a mean  $d_p$  of 81 nm rather than 50 nm like DLS and PDW spectroscopy. The SLS device used in this study starts measuring at 40 nm, leading to the assumption that particles of 50 nm mean  $d_p$  lie within the lowest possible measurement range. For the dispersions with bigger mean particle sizes, SLS shows better agreement to the other methods.

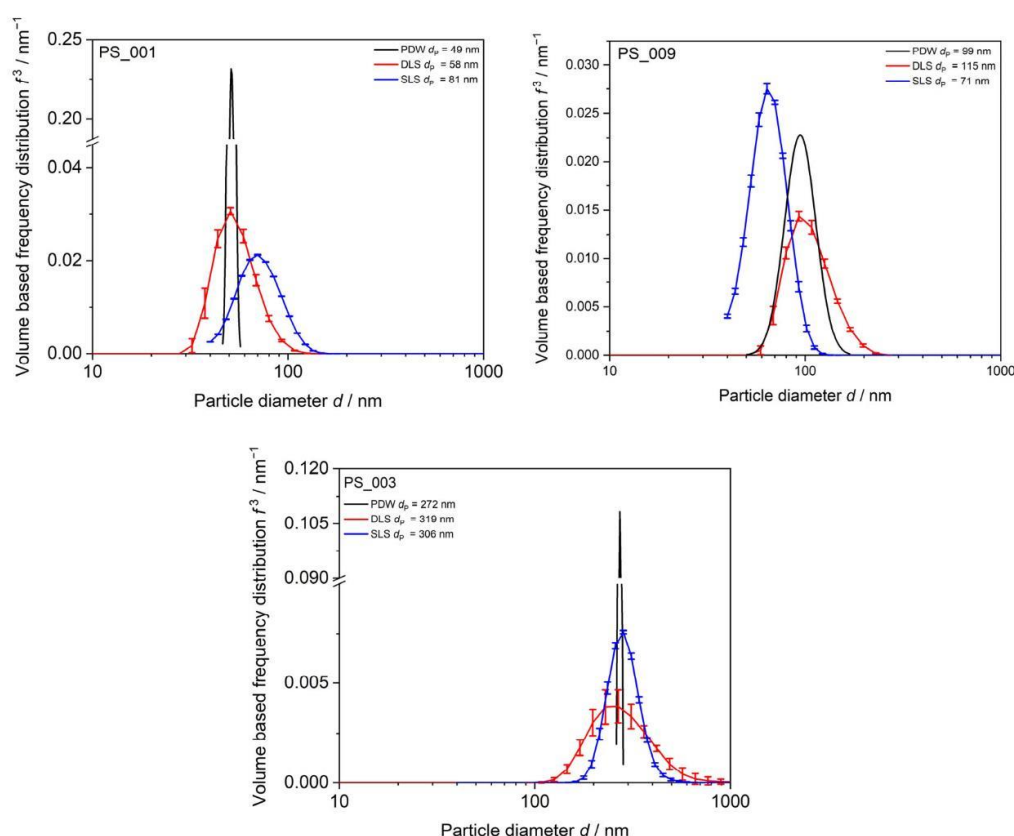


**Figure 4.** PSD of PS-SDS emulsions with mean particle diameters from approx. 49 nm to 272 nm. Comparison between dilution-based DLS, SLS, and undiluted PDW spectroscopy. DLS and SLS values are shown as mean out of three measurements with calculated mean value and standard deviation as error bars.



### 3.2. Polyvinyl Acetate—Polyvinyl Alcohol Dispersions

#### 3.2.1. Reproducibility PVAc-PVA

Figure 5 shows two emulsion polymerization products of PVAc-PVA with  $1 \text{ g L}^{-1}$  PVA in the initial charge produced under equal conditions. The left graph shows that, regarding the absorption properties, no differentiation between the two samples is possible. The trend of  $\mu_a$  is following the form of pure water absorption, due to the high amount of water as the dispersion medium and little expected absorption from the polymer indicated by literature values from Kou and Pope [55,56]. Lower values are obtained as the polymer is present by approx. 40% ( $w/w$ ) solid content. In Figure 5 (right), the  $\mu_s'$  trend versus wavelength shows small deviations in between the measurements. In the lower wavelength range, the first experiment  $1 \text{ g L}^{-1}$  PVA\_1 gives a slightly higher value for  $\mu_s'$ . For wavelengths  $>950 \text{ nm}$ , this order is inverted, and the second experiment gives higher values for  $\mu_s'$ . The solid content for both syntheses is nearly identical with  $1 \text{ g L}^{-1}$  PVA\_1 = 41.61% ( $w/w$ ) and  $1 \text{ g L}^{-1}$  PVA\_2 = 40.87% ( $w/w$ ), respectively. The slightly higher solid content might be responsible for the higher  $\mu_s'$  values for  $1 \text{ g L}^{-1}$  PVA\_1.

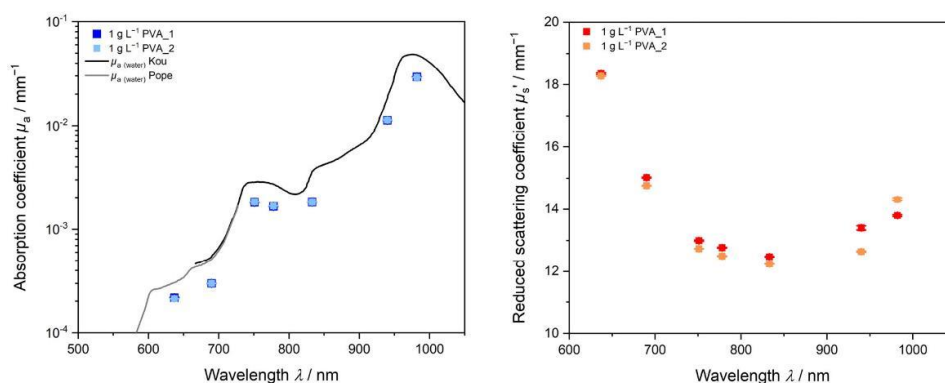


**Figure 5.** Reproducibility of PVAc-PVA dispersion with  $1 \text{ g L}^{-1}$  PVA in the initial charge. Repetition experiments were performed at equal reaction conditions.

#### 3.2.2. PDW Spectroscopy Size Analysis of Undiluted PVAc-PVA Dispersions

For PVAc-PVA syntheses, particles with mean diameters between approximately 270 nm and 510 nm were obtained by starved-feed emulsion polymerization. Regarding the analysis of the undiluted dispersions using PDW spectroscopy, it was found that, for the PVAc-PVA dispersions, the trend form of  $\mu_s'$  vs. wavelength deviates from the decreasing trends shown for the PS-SDS systems in Figure 3. Figure 6 shows experimental and theoretical data for  $\mu_s'$  without any assumption of water swelling. Density and refractive index were calculated from gravimetrically derived solid contents  $w$  of PVAc-PVA\_1  $\text{g L}^{-1}$  = 41.61% ( $w/w$ ), PVAc-PVA\_2  $\text{g L}^{-1}$  = 40.92% ( $w/w$ ), and PVAc-PVA 5.5  $\text{g L}^{-1}$  = 41.57% ( $w/w$ ). Theoretical  $\mu_s'$  as a function of wavelength is shown as open symbols with dotted lines as a guide for the eye.

The experimental values (closed symbols in Figure 6) cannot be fitted exactly, if only the pure polymer properties and no swelling are considered and used for analysis (open symbols). Contrary to the SDS-stabilized PS samples, the PDW spectroscopy fit for the PVA-stabilized PVAc samples is not easily applied, and the calculated data points do not agree well with the experimental  $\mu_s'$  values over the wavelength range. This relates to the physical properties and scattering behavior of the PVAc-PVA particles. The deviation is caused by bound water in the PVAc-PVA particle. Due to the difference in their macromolecular chemical structure of the polymers and stabilizers, the particles express different properties and different water-binding abilities. For the hydrophilic PVAc-PVA particles, water is penetrating inside the particle and causes swelling. For PDW spectroscopy analysis, the volume fraction, refractive index, and density of the particle influence the resulting

theoretical  $\mu_s'$  calculation, which is used for the exact size determination to a great extent. Water swelling of the PVAc-PVA particle causes changes to these factors and the calculated  $\mu_s'$  values are erroneous.

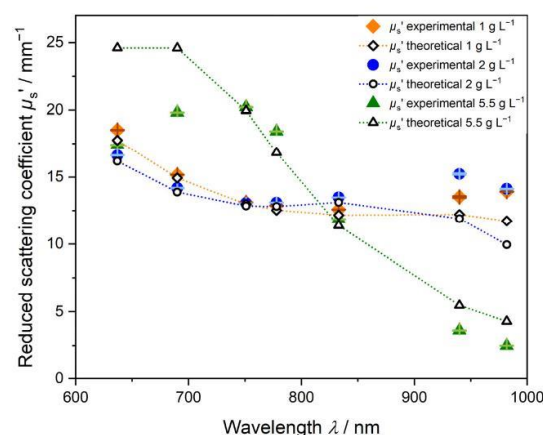


**Figure 6.** Theoretical  $\mu_s'$  values (open symbols) fitted to experimental  $\mu_s'$  values (closed symbols) from a Mie-theory- and global-analysis-based PDW spectroscopy measurement without assumption of water swelling. Three different PVAc-PVA dispersions with increasing content of PVA in the iC are shown. The orange curve shows  $\mu_s'$  for 1 g L<sup>-1</sup> PVA in the iC, blue 2 g L<sup>-1</sup>, and green 5.5 g L<sup>-1</sup>. Error bars are indicated in brown, light blue and light green respectively.

Figures 7 and 8 show the results of the iterative approach explained earlier in the section “2.3 PDW Spectroscopy Dispersion Analysis” to determine the water swelling of the particles by a PDW spectroscopy fit analysis of theoretically calculated  $\mu_s'$  to experimentally determined values. For the dispersion PVAc-PVA 2 g L<sup>-1</sup> shown in Figure 7,  $\mu_s'$  shows a minimum at approx. 750 nm and increases again to a maximum at 940 nm. The fit of the non-swollen curve (black line) cannot match the experimental results (red squares) and gives a very high value of  $X^2 = 5486$ . Assumed percentages of water swelling leads to a better fit and, correspondingly, smaller  $X^2$  values (Figure 8). The smallest  $X^2 = 1352$  for this sample was calculated at 17.01% water swelling and a mean size of  $391 \pm 43$  nm, improving the fit quality by factor four.

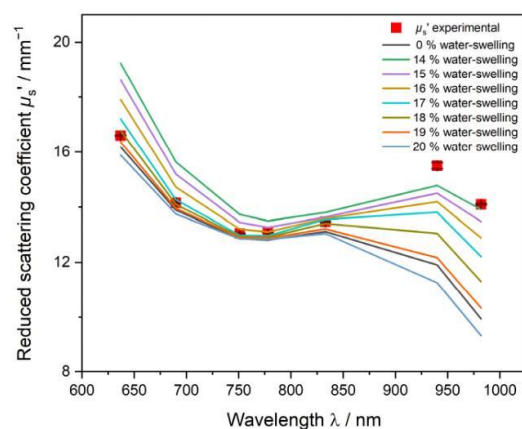


**Figure 7.** Iterative approach of PDW spectroscopy fit of the reduced scattering coefficient  $\mu_s'$  to minimize  $X^2$  by increasing the water-swelling factor of the PVAc-PVA particle. Sample with 2 g L<sup>-1</sup> PVA in the iC. Black line shows the  $\mu_s'$  fit without any water swelling assumed.

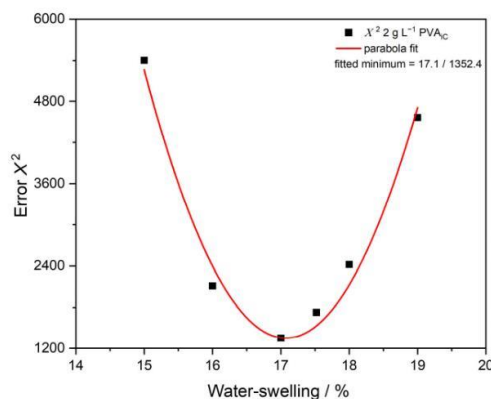


**Figure 8.** Assumed water swelling, with corresponding  $X^2$  values fitted with a parabola fit to find the lowest  $X^2$  value and, therefore, assumed best PDW spectroscopy fit. Parabola fit used gives  $R^2 = 0.96$ .

Figure 8 shows the  $X^2$  values of assumed iterative water swelling between 15% and 19%. The minimum is calculated with a parabola fit to be at 17.1% water swelling.

Table 4 gives the data of assumed water-swelling and  $X^2$  values on the other PVAc-PVA syntheses and clearly shows that, for all PVAc-PVA samples, assumed water-swelling leads to a significant increase in the fit quality and reduction in  $X^2$ . Improvement leads from  $X^2$  reduction by a factor of three to an improvement of over ten times for two samples. The results show that, for all these syntheses, a certain degree of water swelling needs to be considered and it is very likely that the particles are swollen in the dispersion.

**Table 4.** Degree of water swelling determined by PDW spectroscopy iterative fitting to lowest  $X^2$  and corresponding improvement factor to non-swollen fit.

Sample	Degree of Swelling $\theta_{\text{swollen}}/\%$	$X^2$	$X^2$ Improvement Factor
PVAc-PVA 0 g L <sup>-1</sup>	19.29	87	13.7
PVAc-PVA 1 g L <sup>-1</sup>	22.00	250	7.2
PVAc-PVA 2 g L <sup>-1</sup>	17.07	1352	4.06
PVAc-PVA 5.5 g L <sup>-1</sup>	12.38	2,5944	3.38
PVAc-PVA 11 g L <sup>-1</sup>	38.41	4084	12.1

### 3.2.3. Method Comparison DLS, SLS, EM, and PDW Spectroscopy

Mean particle diameter for all dispersions was also determined by DLS, SLS, and PDW spectroscopy. The determined mean particle diameters for each sample with the determined swelling factor by iterative approach described before to minimize  $X^2$  are given in Table 5. Deviations between methods again range from 5% to 27% whereas DLS always gives an approx. 5 to 15% bigger mean  $d_p$  value due to measuring the hydrodynamic radius rather than the hard-sphere particle diameter.

The dispersion was analyzed additionally by EM, using the Hough Circle transformation method with a circularity cut off at  $c \leq 0.8$ . A total of 70 particles were analyzed by determining a histogram and normalized Gaussian distribution. Mean  $d_p$  of  $352 \pm 27$  nm was determined. Figure 9 shows that all the methods are in good agreement. EM analysis delivers the smallest mean  $d_p$  as the sample is measured in a dried state and the water-swollen particle might collapse during sample preparation and measurement under vacuum conditions. After assumption of the swelling factor of 17.01%, PDW spectroscopy is able to deliver a result for the mean  $d_p = 392$  nm, with a narrow PSD. If one assumes that EM measures only the particle core and the swollen particle is collapsed completely, the mean  $d_p$  values between EM and PDW spectroscopy reflect the calculated swelling factor within the range of error. According to PDW spectroscopy, 17.01% of the volume of



the 392 nm polymer are caused by water swelling, leading to a mean  $d_p$  of the collapsed particle of 325 nm which lies just within the range of errors of the calculated mean  $d_p$  from electron microscopy of  $352 \pm 27$  nm.

**Table 5.** Mean  $d_p$  values of PVAc-PVA particles in dispersion given from volume frequency distribution of PDW spectroscopy, SLS, and DLS measurements.

Sample ID	Mean $d_p$ PDW	Mean $d_p$ SLS	Mean $d_p$ DLS	PDW/SLS	PDW/DLS
PVAc-PVA 0 g L <sup>-1</sup>	507.91	438.51	579.78	1.16	0.88
PVAc-PVA 1 g L <sup>-1</sup> _1 *	412.34	401.17	483.30	1.03	0.85
PVAc-PVA 1 g L <sup>-1</sup> _2 *	409.86	403.54	493.21	1.02	0.83
PVAc-PVA 2 g L <sup>-1</sup>	391.57	385.50	470.77	1.02	0.83
PVAc-PVA 5.5 g L <sup>-1</sup> *	306.82	324.11	359.60	0.95	0.85
PVAc-PVA 11 g L <sup>-1</sup>	271.37	213.27	284.80	1.27	0.95

\* syntheses compared in Figure 5.

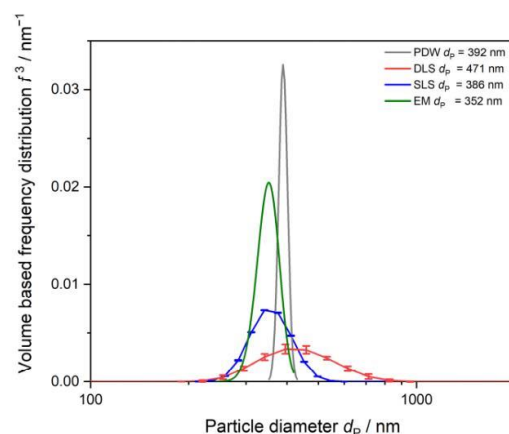


**Figure 9.** PSD of PVAc-PVA 2 g L<sup>-1</sup> dispersion. Comparison between SLS, DLS, EM, and PDW spectroscopy. PDW spectroscopy distribution is determined with the calculated water-swelling factor of 17.01%. DLS and SLS values are shown as mean out of three measurements with calculated mean value and standard deviation as error bars.

#### 4. Conclusions

The presented PDW spectroscopy technique offers a wide range of applications, even for material with extreme scattering properties and high solid contents. This study shows that, for both polymer particles analyzed, size determination is possible at industrially relevant reaction conditions without dilution or necessary changes to the sample.

For basic systems like polystyrene dispersions with an SDS stabilizer, which do not incorporate water, the fitting of the experimental data with PDW spectroscopy leads to very good results with low error values of  $X^2$ . In polyvinyl acetate dispersions, however, the theoretical fit to the experimental data is lacking accuracy and the fitted values deviate from the experimental data points, if no water swelling is assumed. Comparing the two polymer systems reveals that analysis of the PS-SDS system compared to the PVAc-PVA system is less challenging and analysis of PS-SDS shows better agreement to offline-based techniques without further adjustment. In this study, we showed that PDW spectroscopy is a solid technique to determine the swelling of the polymer by iterative assumption of the swelling factor and consecutive adaptation of physical parameters.

#### 5. Outlook

For the PVAc-PVA system, the applied model for the  $\mu_s'$  fit needs to be modified, because of the incorporation of water in the PVAc-PVA particle. The incorporated water

causes inconsistencies and deviations from the model assumptions for the physical particle properties like solid content and volume fraction, respectively, density, and refractive index, which are necessary for PSD analysis by PDW spectroscopy. The amount of free water and bound water is difficult to determine separately; differential scanning calorimetry (DSC) and further thermogravimetric analysis methods combined are necessary to investigate the amount of water in PVAc-PVA particles. Literature suggests a combination of thermal analysis methods like DSC, TGA, and IR analysis in order to determine the content of bound water in the particle structure.

In future work, the proposed iterative swelling approach and simultaneous adaptation of PDW spectroscopy input parameters needs to be incorporated in the particle size analysis of water-swollen polymers in the automated PDW spectroscopy size calculation algorithm.

**Author Contributions:** The manuscript was written through contributions of all authors. All authors have given approval to the final version of the manuscript. Conceptualization, S.S. and L.B.; methodology, S.S. and L.B.; software, M.M. and L.B.; validation, S.S., L.B., M.M. and O.R.; formal analysis, S.S.; investigation, S.S.; writing—original draft preparation, S.S.; writing—review and editing, S.S., L.B., M.M. and O.R.; visualization, S.S.; project administration, L.B., M.M. and O.R.; funding acquisition, M.M., L.B. and O.R. All authors have read and agreed to the published version of the manuscript.

**Funding:** This study was financed by the financial support of the German Federal Ministry of Education and Research (grants 03Z22AN12, 03IHS048A and 03Z22AB1B) and the University of Potsdam. Funded by the Deutsche Forschungsgemeinschaft (DFG, German Research Foundation)—Project-number 491466077.

**Institutional Review Board Statement:** Not applicable.

**Data Availability Statement:** The data that support the findings of this study are available on request from the corresponding author.

**Acknowledgments:** The authors would like to acknowledge funding by the German Federal Ministry of Education and Research (grants 03Z22AN12 and 03Z22AB1B) and the Deutsche Forschungsgemeinschaft (DFG, German Research Foundation)—Project-number 491466077 and the University of Potsdam.

**Conflicts of Interest:** The authors declare no conflict of interest.

## Appendix A

**Table A1.** Mean particle diameters  $d_p$  determined by particle-sizing techniques for different PS-SDS dispersions produced.

Sample ID	Mean $d_p$ PDW	Mean $d_p$ SLS	Mean $d_p$ DLS	PDW/SLS	PDW/DLS
PS_001 *	49.00	80.85	58.50	0.61	0.84
PS_003	271.96	287.79	319.57	0.94	0.85
PS_004	296.42	318.80	356.29	0.93	0.83
PS_007 **	100.02	72.23	114.77	1.38	0.87
PS_009_1	99.14	71.83	115.27	1.38	0.86
PS_009_2	101.17	72.10	131.54	1.40	0.77
PS_011 *	75.87	82.99	78.06	0.91	0.97
PS_012 **	97.32	71.07	109.13	1.37	0.89
PS_013 **	99.00	71.65	116.47	1.38	0.85
PS_014	251.77	250.56	254.23	1.00	0.99
PS_015 **	96.46	72.09	113.04	1.34	0.85
PS_016	274.34	321.80	283.50	0.85	0.97
PS_018	259.82	288.54	278.27	0.90	0.93
PS_019	259.48	315.30	271.33	0.82	0.96
PS_020 *	56.96	69.27	80.46	0.82	0.71

\* seed synthesis after Table 1. \*\* syntheses compared in Figure 2.



## References

- Koltzenburg, S.; Maskos, M.; Nuyken, O. *Polymere: Synthese, Eigenschaften und Anwendungen*; Springer: Berlin/Heidelberg, Germany, 2014; ISBN 978-3-642-34772-6/978-3-642-34773-3.
- Asua, J.M. On-line control of emulsion polymerization reactors: A perspective. *Can. J. Chem. Eng.* **2023**, 1–7. [\[CrossRef\]](#)
- Lerche, D.; Miller, R.; Schaeffler, M. *Dispersionseigenschaften 2D-Rheologie, 3D-Rheologie, Stabilität*, 1st ed.; Eigenverlag: Berlin-Potsdam, Germany, 2015.
- Aguirre, M.; Ballard, N.; Gonzalez, E.; Hamzehlou, S.; Sardon, H.; Calderon, M.; Paulis, M.; Tomovska, R.; Dupin, D.; Bean, R.H.; et al. Polymer Colloids: Current Challenges, Emerging Applications, and New Developments. *Macromolecules* **2023**, 56, 2579–2607. [\[CrossRef\]](#)
- Ober, C.K.; Lok, K.P.; Hair, M.L. Monodispersed, micron-sized polystyrene particles by dispersion polymerization. *J. Polym. Sci. Polym. Lett. Ed.* **1985**, 23, 103–108. [\[CrossRef\]](#)
- Chicoma, D.L.; Sayer, C.; Giudici, R. In-Line Monitoring of Particle Size during Emulsion Polymerization under Different Operational Conditions using NIR Spectroscopy: In-Line Monitoring of Particle Size during Emulsion Polymerization. *Macromol. React. Eng.* **2011**, 5, 150–162. [\[CrossRef\]](#)
- Frauendorfer, E.; Wolf, A.; Hergeth, W.-D. Polymerization Online Monitoring. *Chem. Eng. Technol.* **2010**, 33, 1767–1778. [\[CrossRef\]](#)
- Ito, K.; Kato, T.; Ona, T. Non-destructive method for the quantification of the average particle diameter of latex as water-based emulsions by near-infrared Fourier transform Raman spectroscopy. *J. Raman Spectrosc.* **2002**, 33, 466–470. [\[CrossRef\]](#)
- Besseling, R.; Damen, M.; Wijgengangs, J.; Hermes, M.; Wynia, G.; Gerich, A. New unique PAT method and instrument for real-time inline size characterization of concentrated, flowing nanosuspensions. *Eur. J. Pharm. Sci.* **2019**, 133, 205–213. [\[CrossRef\]](#)
- Hergeth, W.-D.; Frauendorfer, E. Online-Reaktionsverfolgung bei der Polymerisation. *Chem. Ing. Tech.* **2010**, 82, 503–507. [\[CrossRef\]](#)
- de Kanter, M.; Meyer-Kirschner, J.; Viell, J.; Mitsos, A.; Kather, M.; Pich, A.; Janzen, C. Enabling the measurement of particle sizes in stirred colloidal suspensions by embedding dynamic light scattering into an automated probe head. *Measurement* **2016**, 80, 92–98. [\[CrossRef\]](#)
- Calzolari, L.; Gilliland, D.; Rossi, F. Measuring nanoparticles size distribution in food and consumer products: A review. *Food Addit. Contam. Part A Chem. Anal. Control Expo. Risk Assess.* **2012**, 29, 1183–1193. [\[CrossRef\]](#)
- Heiligt, F.J.; Niederberger, M. The fascinating world of nanoparticle research. *Mater. Today* **2013**, 16, 262–271. [\[CrossRef\]](#)
- Modena, M.M.; Rühle, B.; Burg, T.P.; Wuttke, S. Nanoparticle Characterization: What to Measure? *Adv. Mater.* **2019**, 31, e1901556. [\[CrossRef\]](#) [\[PubMed\]](#)
- Caputo, F.; Vogel, R.; Savage, J.; Vella, G.; Law, A.; Della Camera, G.; Hannon, G.; Peacock, B.; Mehn, D.; Ponti, J.; et al. Measuring particle size distribution and mass concentration of nanoplastics and microplastics: Addressing some analytical challenges in the sub-micron size range. *J. Colloid. Interface Sci.* **2021**, 588, 401–417. [\[CrossRef\]](#)
- Schärtl, W. *Light Scattering from Polymer Solutions and Nanoparticle Dispersions*; Springer: Berlin/Heidelberg, Germany, 2007; ISBN 978-3-540-71950-2.
- Pecora, R. Dynamic Light Scattering Measurement of Nanometer Particles in Liquids. *J. Nanoparticle Res.* **2020**, 2, 9. [\[CrossRef\]](#)
- Takahashi, K.; Kato, H.; Saito, T.; Matsuyama, S.; Kinugasa, S. Precise Measurement of the Size of Nanoparticles by Dynamic Light Scattering with Uncertainty Analysis. *Part Part. Syst. Charact.* **2008**, 25, 31–38. [\[CrossRef\]](#)
- Jia, Z.; Li, J.; Gao, L.; Yang, D.; Kanaev, A. Dynamic Light Scattering: A Powerful Tool for In Situ Nanoparticle Sizing. *Colloids Interfaces* **2023**, 7, 15. [\[CrossRef\]](#)
- Schlappa, S.; Brenker, L.J.; Bressel, L.; Hass, R.; Münzberg, M. Process Characterization of Polyvinyl Acetate Emulsions Applying Inline Photon Density Wave Spectroscopy at High Solid Contents. *Polymers* **2021**, 13, 669. [\[CrossRef\]](#) [\[PubMed\]](#)
- Jacob, L.I.; Pauer, W. In-line monitoring of latex-particle size during emulsion polymerizations with a high polymer content of more than 60. *RSC Adv.* **2020**, 10, 26528–26534. [\[CrossRef\]](#)
- Bressel, L.; Hass, R.; Reich, O. Particle sizing in highly turbid dispersions by Photon Density Wave spectroscopy. *J. Quant. Spectrosc. Radiat. Transf.* **2013**, 126, 122–129. [\[CrossRef\]](#)
- Schiewe, T.; Gutschmann, B.; Santolin, L.; Waldburger, S.; Neubauer, P.; Hass, R.; Riedel, S.L. Real-time monitoring of biomass during *Escherichia coli* high-cell-density cultivations by in-line photon density wave spectroscopy. *Biotechnol. Bioeng.* **2023**, 1–10. [\[CrossRef\]](#)
- Li, W.; Xue, F.; Cheng, R. States of water in partially swollen poly(vinyl alcohol) hydrogels. *Polymer* **2005**, 46, 12026–12031. [\[CrossRef\]](#)
- Hodge, R.M.; Edward, G.H.; Simon, G.P. Water absorption and states of water in semicrystalline poly(vinyl alcohol) films. *Polymer* **1996**, 37, 1371–1376. [\[CrossRef\]](#)
- Higuchi, A.; Iijima, T. DSC investigation of the states of water in poly(vinyl alcohol) membranes. *Polymer* **1985**, 26, 1207–1211. [\[CrossRef\]](#)
- Ochigbo, S.; Suleiman, M. Comparisons between Polyvinyl Alcohol (PVOH) and Sodium Dodecyl Sulphate (SDS) as Surfactants in Natural Rubber (NR)/Polyvinyl Acetate (PVAc) Latex Blends. *IRJPAC* **2015**, 5, 99–105. [\[CrossRef\]](#)
- Guan, L.; Xu, H.; Huang, D. The investigation on states of water in different hydrophilic polymers by DSC and FTIR. *J. Polym. Res.* **2011**, 18, 681–689. [\[CrossRef\]](#)

29. Hatakeyama, T.; Nakamura, K.; Hatakeyama, H. Determination of bound water content in polymers by DTA, DSC and TG. *Thermochim. Acta* **1988**, *123*, 153–161. [CrossRef]
30. Wang, R.; Wang, Q.; Li, L. Evaporation behaviour of water and its plasticizing effect in modified poly(vinyl alcohol) systems: Evaporation of water and plasticizing effect in modified PVA. *Polym. Int.* **2003**, *52*, 1820–1826. [CrossRef]
31. Bajpai, A.K.; Saini, R. Preparation and characterization of novel biocompatible cryogels of poly (vinyl alcohol) and egg-albumin and their water sorption study. *J. Mater. Sci. Mater. Med.* **2006**, *17*, 49–61. [CrossRef] [PubMed]
32. Hodge, R.M.; Bastow, T.J.; Edward, G.H.; Simon, G.P.; Hill, A.J. Free Volume and the Mechanism of Plasticization in Water-Swollen Poly(vinyl alcohol). *Macromolecules* **1996**, *29*, 8137–8143. [CrossRef]
33. Miyagi, Z.; Tanaka, K. Sorption of water vapor by poly(vinyl acetate). *Colloid. Polym. Sci.* **1979**, *257*, 259–265. [CrossRef]
34. Jain, N.; Singh, V.K.; Chauhan, S. A review on mechanical and water absorption properties of polyvinyl alcohol based composites/films. *J. Mech. Behav. Mater.* **2017**, *26*, 213–222. [CrossRef]
35. Gonzalez, G.S.M.; Dimonie, V.L.; Sudol, E.D.; Yue, H.J.; Klein, A.; El-Aasser, M.S. Characterization of poly(vinyl alcohol) during the emulsion polymerization of vinyl acetate using poly(vinyl alcohol) as emulsifier. *J. Polym. Sci. Part. A Polym. Chem.* **1996**, *34*, 849–862. [CrossRef]
36. Shaheen, S.M.; Yamaura, K. Preparation of theophylline hydrogels of atactic poly(vinyl alcohol)/NaCl/H<sub>2</sub>O system for drug delivery system. *J. Control. Release* **2002**, *81*, 367–377. [CrossRef]
37. Lepizzera, S.M.; Hamielec, A.E. Nucleation of particles in seeded emulsion polymerization of vinyl acetate with poly(vinyl alcohol) as emulsifier. *Macromol. Chem. Phys.* **1994**, *195*, 3103–3115. [CrossRef]
38. Capek, I.; Lin, S.-Y.; Hsu, T.-J.; Chern, C.-S. Effect of temperature on styrene emulsion polymerization in the presence of sodium dodecyl sulfate. II. *J. Polym. Sci. Part A Polym. Chem.* **2000**, *38*, 1477–1486. [CrossRef]
39. Mariz, I.d.F.; de La Cal, J.C.; Leiza, J.R. Control of particle size distribution for the synthesis of small particle size high solids content latexes. *Polymer* **2010**, *51*, 4044–4052. [CrossRef]
40. Liu, B.; Zhang, M.; Liu, Y.; Tan, Z.; Zhou, C.; Zhang, H. Particle Nucleation and Growth in the Emulsion Polymerization of Styrene: Effect of Monomer/Water Ratio and Electrolyte Concentration. *J. Macromol. Sci. Part A* **2015**, *52*, 147–154. [CrossRef]
41. Jacob, L.I.; Pauer, W.; Schröter, B. Influence of redox initiator component ratios on the emulsion copolymerisation of vinyl acetate and neodecanoic acid vinyl ester. *RSC Adv.* **2022**, *12*, 14197–14208. [CrossRef]
42. Zecha, H.; Weitzel, H.-P. Method for Producing Vinyl Ester Polymers Having Specifically Settable Dispersity and Low Polydispersity. U.S. Patent US 9,650,507, 2 April 2013.
43. Hass, R.; Münzberg, M.; Bressel, L.; Reich, O. Industrial applications of photon density wave spectroscopy for in-line particle sizing Invited. *Appl. Opt.* **2013**, *52*, 1423–1431. [CrossRef] [PubMed]
44. Hass, R.; Münzke, D.; Ruiz, S.V.; Tippmann, J.; Reich, O. Optical monitoring of chemical processes in turbid biogenic liquid dispersions by Photon Density Wave spectroscopy. *Anal. Bioanal. Chem.* **2015**, *407*, 2791–2802. [CrossRef] [PubMed]
45. Bressel, K.; Müller, W.; Leser, M.E.; Reich, O.; Hass, R.; Wooster, T.J. Depletion-Induced Flocculation of Concentrated Emulsions Probed by Photon Density Wave Spectroscopy. *Langmuir* **2020**, *36*, 3504–3513. [CrossRef]
46. Münzberg, M.; Hass, R.; Reich, O. In-line characterization of phase inversion temperature emulsification by photon density wave spectroscopy. *SOFW J.* **2013**, *4*, 38–46.
47. Häne, J.; Brühwiler, D.; Ecker, A.; Hass, R. Real-time inline monitoring of zeolite synthesis by Photon Density Wave spectroscopy. *Microporous Mesoporous Mater.* **2019**, *288*, 109580. [CrossRef]
48. Jacob, L.I.; Pauer, W. Scale-up of Emulsion Polymerisation up to 100 L and with a Polymer Content of up to 67 wt%, Monitored by Photon Density Wave Spectroscopy. *Polymers* **2022**, *14*, 1574. [CrossRef] [PubMed]
49. Bressel, L. Bedeutung Der Abhängigen Streuung Für Die Optischen Eigenschaften Hochkonzentrierter Dispersionen. Ph.D. Thesis, University of Potsdam, Potsdam, Germany, 2016.
50. Reich, O. Photonendichtewellenspektroskopie Mit Intensitätsmodulierten Diodenlasern. Ph.D. Thesis, University of Potsdam, Potsdam, Germany, 2005.
51. Hass, R. Angewandte Photonendichtewellen Spektroskopie. Ph.D. Thesis, University of Potsdam, Potsdam, Germany, 2011.
52. What Is the Z-Average Size Determined by DLS. Available online: [https://www.horiba.com/en\\_en/dynamic-light-scattering-dls-z-average/](https://www.horiba.com/en_en/dynamic-light-scattering-dls-z-average/) (accessed on 28 December 2021).
53. Thomas, J.C. The determination of log normal particle size distributions by dynamic light scattering. *J. Colloid. Interface Sci.* **1987**, *117*, 187–192. [CrossRef]
54. Stetefeld, J.; McKenna, S.A.; Patel, T.R. Dynamic light scattering: A practical guide and applications in biomedical sciences. *Biophys. Rev.* **2016**, *8*, 409–427. [CrossRef] [PubMed]
55. Kou, L.; Labrie, D.; Chylek, P. Refractive indices of water and ice in the 0.65- to 2.5- $\mu$ m spectral range. *Appl. Opt.* **1993**, *32*, 3531–3540. [CrossRef]
56. Pope, R.M.; Fry, E.S. Absorption spectrum (380–700 nm) of pure water. II. Integrating cavity measurements. *Appl. Opt.* **1997**, *36*, 8710–8723. [CrossRef]

**Disclaimer/Publisher's Note:** The statements, opinions and data contained in all publications are solely those of the individual author(s) and contributor(s) and not of MDPI and/or the editor(s). MDPI and/or the editor(s) disclaim responsibility for any injury to people or property resulting from any ideas, methods, instructions or products referred to in the content.



## Synopsis

### Polyvinyl acetate with SDS (*not published*)

As it was shown by means of  $\chi^2$  analysis by PDW spectroscopy, PS/SDS particles are not prone to incorporate water. PDW spectroscopy analysis regarding the theoretical calculated  $\mu_s'$  fits well to the experimental  $\mu_s'$  data without any assumption of water-swelling. Further syntheses were carried out to approximate a comparability of the two systems. To show that the water swelling of the PVAc/PVA system is specific to that system, synthesis of PVAc particles stabilized with SDS was analyzed, too.

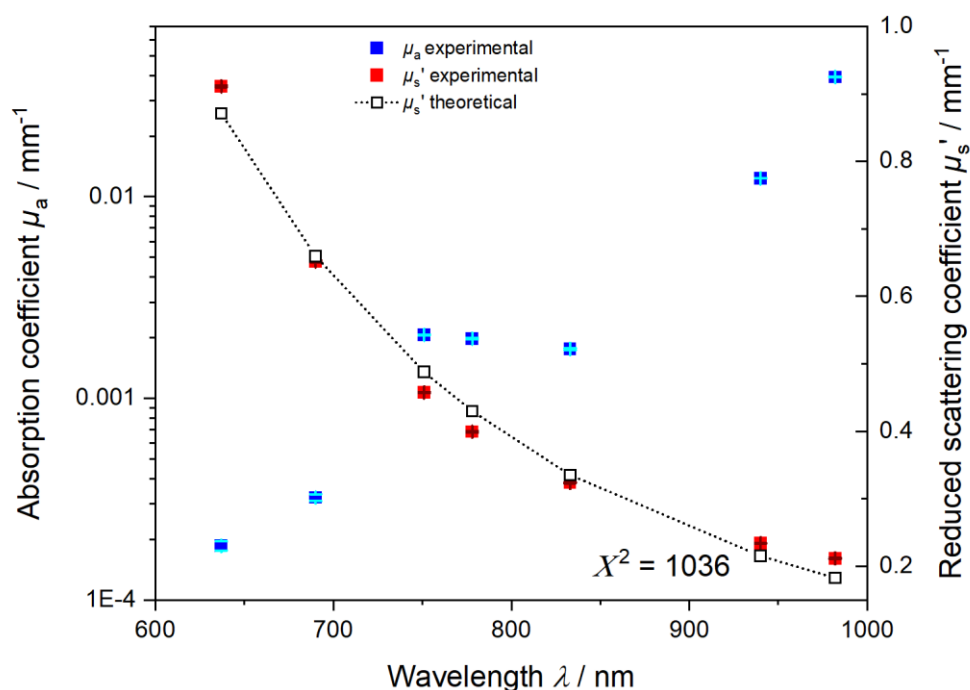


Figure 14 PVAc-SDS PDW spectroscopy analysis of final dispersion  $\phi = 31\%$

The synthesis of PVAc stabilized with SDS instead of PVA in Figure 14 shows that for PVAc/SDS experimental and theoretical  $\mu_s'$  show a good fit. Experimental set up is described in Table 3 in the appendix. Based on the results published it is shown that PVAc/SDS particles do not incorporate water. The PDW spectroscopy fit of unmodified theoretical  $\mu_s'$  to experimentally determined  $\mu_s'$  show good agreement with a  $\chi^2 = 1036$ . The dispersion was analyzed with a volume fraction of  $\phi_{\text{tot}} = 31\%$  (w/w),  $\rho_{\text{PVAc-SDS}} = 1.20 \text{ g cm}^{-3}$  and  $n_{\text{PVAc-SDS}} = 1.455$ .

### 5.3 Harnessing Photon Density Wave Spectroscopy for the inline monitoring of up to 100 L vinyl acetate-Versa<sup>®</sup> 10 polymerization: Insights into dispersion dynamics and mixing

This paper has been published in *Polymers* 2025

ISSN: 2073-4360

Digital object identifier (DOI): 10.3390/polym17050629

Online available at: <https://www.mdpi.com/2073-4360/17/5/629>

© 2025 The Authors. *Polymers* published by MDPI AG

Reproduced with permission of MDPI (Basel, Switzerland) under the terms and conditions of an Open Access license, creative commons licensing by mentioning who the research is by when its used (CC BY license).

Impact factor: 4.7

#### 5.3.1 Aim of this research

The aim of this research was to apply PDW spectroscopy to a proposed scale-up procedure of the emulsion polymerization of a PVAc:Versa<sup>®</sup> 10 co-monomer mixture. The scale-up was proposed to reach continuous dispersion qualities and particle properties of the final product. With PDW spectroscopy early scale-up inconsistencies and polymerization issues are detectable by means of intensity measurements of the early stages of emulsion polymerization. This research shows that with PDW spectroscopy scale-up procedures can be monitored and optimized by means of congruent measurement of the reduced scattering coefficient  $\mu_s'$  across reaction volumes of 1 L to 100 L. It aims at strengthening the PAT technique for polymerization monitoring and powerful tool for process optimization.

## Article

# Harnessing Photon Density Wave Spectroscopy for the Inline Monitoring of up to 100 L Vinyl Acetate—Versa<sup>®</sup> 10 Polymerization: Insights into Dispersion Dynamics and Mixing

Stephanie Schlappa<sup>1,2,\*</sup>, Werner Pauer<sup>1</sup>, Oliver Reich<sup>3</sup> and Marvin Münzberg<sup>2,3</sup>

<sup>1</sup> Institute for Technical and Macromolecular Chemistry, University of Hamburg, Bundesstraße 45, 20146 Hamburg, Germany

<sup>2</sup> Department of Physical Chemistry—InnoFSPEC, University of Potsdam, Am Mühlenberg 3, 14476 Potsdam, Germany

<sup>3</sup> Professorship of Knowledge and Technology Transfer, Faculty of Science, University of Potsdam, Am Mühlenberg 3, 14476 Potsdam, Germany

\* Correspondence: stephanie.schlappa@studium.uni-hamburg.de

**Abstract:** Photon Density Wave (PDW) spectroscopy is used as process analytical technology (PAT) in three batch sizes, 1 L, 10 L and 100 L, of polyvinyl acetate—neodecanoic acid vinyl ester (Versa<sup>®</sup> 10) copolymerization. The effects on particle formation and growth are comparably analyzed. The data show comparability across scales up to a polymer volume fraction of around 0.15. Deviations beyond this suggest differences in particle growth dynamics. A detailed analysis of the dispersion dynamics and mixing properties provides an enhanced understanding compared to previous studies. Furthermore, the PDW spectroscopy data suggest inhomogeneity due to insufficient mixing at the beginning of the syntheses, despite very low feed-rates of the monomer mixture. PDW spectroscopy is thus capable of monitoring deviations in syntheses at different reaction volumes in real-time. These findings underline the potential of PDW spectroscopy not only for monitoring synthesis but also for enabling inhomogeneity analysis as a new application area. The integration of offline conversion and particle size measurements emphasizes the critical role of mixing efficiency in achieving optimal polymer dispersion properties and final product quality.

**Keywords:** photon density wave spectroscopy; emulsion polymerization; multiple light scattering; polyvinyl acetate; scale-up; inline monitoring



Academic Editor: Bernhard V. K. J. Schmidt

Received: 22 January 2025

Revised: 19 February 2025

Accepted: 23 February 2025

Published: 26 February 2025

**Citation:** Schlappa, S.; Pauer, W.; Reich, O.; Münzberg, M. Harnessing Photon Density Wave Spectroscopy for the Inline Monitoring of up to 100 L Vinyl Acetate—Versa<sup>®</sup> 10

Polymerization: Insights into Dispersion Dynamics and Mixing. *Polymers* **2025**, *17*, 629. <https://doi.org/10.3390/polym17050629>

**Copyright:** © 2025 by the authors. Licensee MDPI, Basel, Switzerland. This article is an open access article distributed under the terms and conditions of the Creative Commons Attribution (CC BY) license (<https://creativecommons.org/licenses/by/4.0/>).

## 1. Introduction

Inline monitoring of industrially relevant manufacturing procedures, synthesis and automated processes has gained increasing relevance in recent years. The ongoing automation and implementation of smart sensor systems offers advantages for the producing industry. In polymerization synthesis, automated systems are widely used for automated dosing, stirring and other process control parameters. Smart solutions for inline monitoring, however, are rare and not generally used despite their potential economic impact [1–3]. The available inline control methods for polymer synthesis are not yet well optimized.

Vinyl acetate (VAc) and its polymers have been widely developed, used and intensively analyzed since the early days of polymerization theory [4,5]. But very little on inline analysis in liquid dispersions is published. Most analysis is conducted post-synthesis on dried films. Polyvinyl acetate (PVAc) blend films are formed and analyzed regarding swelling and mechanical characteristics [6–9]. For inline dispersion monitoring, a few

methods, like in situ ATR-IR and inline Raman spectroscopy of the modification of the OH end groups by decrease of specific chemical vibrational bands and simultaneous conversion calculations, are possible [10–12]. The methods, however, can only be applied at low polymer concentrations and seem complicated and time consuming. Modeling of polymerization reactions is on a good path; however, it needs further optimization [13–15].

The inline monitoring of industrially relevant dispersions depends on process analytical technology (PAT). Problems with high-solid-content dispersions arise from the significant increase in emulsion viscosity with increasing solid content. The high amount of solids in the dispersion changes the macroscopic properties of the emulsion. Classical DLVO Theory is no longer applicable. The probability of coagulation is highly increased, leading to waste batches, increasing costs and safety issues [16–19]. To prevent coagulation and ensure a safe process, PAT tools, like Photon Density Wave (PDW) spectroscopy, can be implemented. Successful inline monitoring of high solid content (up to 63 wt % PVAc dispersions) by PDW spectroscopy of small reaction volumes up to 1 L has already been shown and reported [20–22].

In this research, PDW spectroscopy is further established as a powerful PAT tool that determines the absorption coefficient  $\mu_a$  and reduced scattering coefficient  $\mu_s'$  independently of each other without dilution or sampling. Jacob and Pauer reported on the scale-up process of the PVAc-Versa<sup>®</sup> 10 synthesis [23]. The authors showed that inline particle size determination by PDW spectroscopy was successful. The authors also showed that inline measurements of the particle size agree very well with the theoretically calculated mean particle diameter. In contrast, measurements of particle sizes with dynamic light scattering (DLS) and disc centrifuge (DC) show huge deviations at solid contents over 30% polymer fraction [23].

Different approaches to synthesis scale-up are available but involve complicated steps to ensure a safe process [14]. The choice of polymerization technique has significant effects on the properties of the polymer product [24,25]. The upscaling of emulsion polymerization processes to large volumes might face many challenges. The nonlinear scalability of components often leads to safety issues, imperfect mixing and accumulation of reactive monomer [26–29]. Additional issues are reduced heat transfer [30], coagulation and reactor fouling by polymer precipitates and many more. The colloidal stability of the particles is affected in larger reaction volumes by dilution, reactor geometry and interactions between particles [31–34]. A proper scale-up procedure is important to maintain colloidal stability, prevent coagulum and ensure consistent material properties [35–37]. To guarantee safety and continuous product quality, PAT applications are highly valuable. However, only basic process analysis like flow rate control, pH control, temperature control and offline sample analysis are used in a standardized manner [34,38,39].

The main finding of this study is the ability to use PDW spectroscopy as a very early detection measure by means of the presented  $I_{\text{raw}}$  and  $\mu_s'$  values in the initial reaction minutes. From these data, early deviations from an ideal process are detectable. These inconsistencies are proven by well-established methods like gravimetric conversion control and particle sizing by DLS. The inconsistencies detected by PDW spectroscopy in  $I_{\text{raw}}$  are very useful to check if a polymerization process is progressing as desired. These findings are suitable to be transferred from the PVAc-copolymer analyzed here to various types of other polymer reactions and polymer systems.

The results and safety measures shown here for risk minimization of the given process are specific for the analyzed PVAc/Versa<sup>®</sup> 10 copolymer synthesis. It is possible to adapt the results to other polymer reactions; safety measures, however, need to be revised and applied for each process individually.



## 2. Materials and Methods

The chemicals used for the starved-feed emulsion polymerization processes at different volume scales are described in Jacob and Pauer [23]. Table 1 shows the components used and their masses at the three different reaction volumes  $V_R$ . Semi-continuous batch syntheses at a reaction temperature of  $T_R = 60\text{ }^\circ\text{C}$  were conducted, as these showed better integration of Versa<sup>®</sup> 10 into the copolymer and fewer safety issues with the generation of heat during the polymerization process [40,41]. To start a reaction, the amount of water was put into the reactor. The stirrer was placed at the height according to Table S1 in the Supplementary Materials. Stirring and  $\text{N}_2$  purging were started (cf. Table S2 in the Supplementary Materials). The reactors were equipped with automated temperature control by external thermostats (Julabo Cryo Compact F30-C thermostat, Huber Unistat Tango thermostat, Huber Unistat 405wl thermostat, regulated to constant jacket temperature by Huber, Offenburg, Germany). The reactor was heated to  $60\text{ }^\circ\text{C}$ . After a temperature equilibrium of about 10 min, polyvinyl alcohol Mowiol 4-88<sup>®</sup> was added. The polyvinyl alcohol needed to be dissolved completely before starting the redox and monomer feed. This took several minutes, depending on the reactor size. The initial charge consisted consecutively of a 4.8% by mass polyvinyl alcohol aqueous solution.

**Table 1.** Experimental set up of semi continuous emulsion polymerization reactions. Initial masses of water and polyvinyl alcohol Mowiol 4-88<sup>®</sup> in the initial charge (iC) in the respective reactor as well as total mass of monomer mixture VAc—neodecanoic acid Versa<sup>®</sup> 10 dosed during the reaction with the given feed-rate.

Reaction Volume $V_R$	Water <sub>iC</sub> /g	Stabilizing Agent Mowiol 4-88 <sup>®</sup> <sub>iC</sub> /g	Monomer Mixture 9:1 VAc:Versa <sup>®</sup> 10 Total /g	Feed-Rate Monomer Mixture /g min <sup>-1</sup>	Initiator Redox Pair Ascorbic Acid (3.4% aq) TBHP (3.4% aq) /g	Feed-Rate Redox Initiators /mL h <sup>-1</sup>
1 L	385	19.7	819	1.2	31.9	10
10 L	2442	123	4543.4	12	374.2	25
100 L	27,503	1383.4	60,017	120	4013.4	530.4

The PVAc/Versa<sup>®</sup> 10 copolymerization mechanism is explained in detail by Agirre et al. [40]. The chemical structures of the used monomers are shown in Figure 1. Versa<sup>®</sup> 10 is less soluble in water than VAc; it diffuses faster into the active polymer particles and converts to polymer faster. As both monomers are water soluble to a certain extent, the diffusion into the active particles is fast [42]. The rate of polymerization can be assumed to be nearly equal to the feed-rate of the monomer. As polymerizations are run at a constant reaction temperature, it can be assumed that the rate of chain transfer to propagation stays constant throughout the experiment. Due to an excess of initiator radicals in the dispersion, termination reactions are suppressed to keep the polymerization alive and running [43].

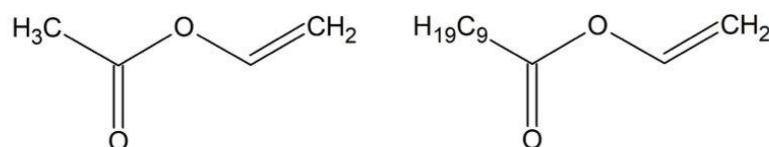


**Figure 1.** Representative chemical structures of monomers vinyl acetate (left) and neodecanoic acid vinyl ester (right).

PDW spectroscopy data analysis and evaluation were performed using LabView-based PDW spectroscopy software (v. 2025 Q1) developed, optimized and maintained

by the University of Potsdam–innoFSPEC, Potsdam, Germany. The experimental data were checked for consistency. Data with a significant deviation were not used for further data treatment. At least three runs were conducted for each reaction volume to check the reproducibility of the experiments.

Input parameters like refractive index  $n$ , density  $\rho$  and particle volume fraction  $\phi$  of the dispersion components were used equally, as in Jacob and Pauer, in order to keep the data comparable [23]. The refractive index of the pure polymer was determined by a customized refractometer DSR- $\lambda$  by Schmidt and Haensch (Berlin, Germany); details can be found in our previous work [20]. The experimentally determined values are shown in Table 2. The formula used to determine the particle density is given below.

$$\rho_{Disp} = \frac{\rho_D \rho_P}{\omega[\rho_D - \rho_P] + \rho_P} \leftrightarrow \frac{1}{\rho_{Disp}} = \omega \left[ \frac{1}{\rho_P} - \frac{1}{\rho_D} \right] + \frac{1}{\rho_D}$$

**Table 2.** Experimentally determined refractive index  $n$  and density  $\rho$  data used in this research.

Component	Density $\rho$ at $T = 20^\circ\text{C}/\text{gcm}^{-3}$	Refractive Index $n$ at $\lambda = 638\text{ nm}$ at $T = 20^\circ\text{C}$	Refractive Index $n$ at $\lambda = 855\text{ nm}$ at $T = 20^\circ\text{C}$
Dispersion Medium	0.997	1.3315	1.3272
PVAc/Versa <sup>®</sup> 10 copolymer particle	1.214	1.4849	1.4769

$\rho_{Disp}$ ,  $\rho_D$  and  $\rho_P$  are the densities of the dispersion, the dispersant and the polymer.  $\omega$  is the solid content of the dispersion. For the density of zero polymer content, the density of pure water was considered. These data are necessary for the experimental determination of the reduced scattering coefficient and absorption coefficient.

### 2.1. Photon Density Wave Spectroscopy

PDW spectroscopy has been optimized as a technique and established as a promising PAT tool. Detailed description of the technique, set-up [44,45] and application can be found in various publications [46–50]. As a PAT tool for the inline monitoring of polymerizations, PDW spectroscopy has been applied to small-scale reaction volumes in emulsion polymerization and other processes. It delivered reproducible results on the inline synthesis analysis, undiluted dispersion analysis and particle size analysis of high-solid-content, highly turbid liquid dispersions [20,22,46,51].

An advantage of inline PDW spectroscopy is its wide range of application. Using a simple optical fiber probe, it can be either implemented directly into the bulk reactor via an inlet port or it can be used in a bypass of the reactor where other PAT sensors are also implemented. Consequently, the volume, reactor set-up and probe positioning are key aspects. Measurements far away from the stirrer might not represent the conditions in the overall reactor. Sufficient mixing at the point of data acquisition is therefore crucial to produce a reliable PAT result.

A PDW spectroscopy measurement for one wavelength consists of a scan of 15 fiber distances  $d_f$  over a modulation frequency  $f$ , ranging from 10 to 510 MHz. Each distance  $d_f$  creates an intensity signal  $I_{\text{raw}}$  over the set frequency range. In a well-mixed dispersion, smaller distances result in higher intensity data, e.g., small  $d_f$  lead to higher  $I_{\text{raw}}$ . Detected photons travelled a shorter measurement path length through the sample and have been scattered less often than at larger distances. For longer pathways, i.e., larger  $d_f$ , lower intensities are expected as more scattering events and stronger absorption occur on the random walk of the photons through the sample from emission to the detection fiber.

A detailed description of the measurement principle can be found in Bressel et al. [52]. Formula 27 in that paper describes the derivation of the optical coefficients  $\mu_a$  and  $\mu_s'$  from the distance-dependent measurements by PDW spectroscopy based on the theory of radiative transport [47,49].

As data are acquired based on manually set boundaries for the measurement distances  $d_f$  and used modulation frequencies, data curation after the measurement might be necessary. This is performed manually after the experiment has been completed. The initially set number of distances  $d_f$  and modulation frequencies  $f$  can be cut if the signal to noise ratio is too high. Too high noise might be interpreted as valuable data. This leads to errors in the analysis, as the used noise does not describe the particulate system. For each experiment, the data thereof are analyzed, and the used  $d_f$  and modulation frequencies are cut manually so that a proper fit of intensity and phase [52] can be applied by the algorithm in the used LabView analysis software (v. 2025 Q1).

## 2.2. Microwave Analyser

For offline conversion analysis, samples were dried with a Smart System 5 device from CEM (Kamp-Lintfort, Germany). A small sample of approx. 3 g was dried at 120 °C until mass consistency. Determination of the total solid content  $\omega$  was performed by gravimetric mass comparison between the wet and dried sample. This determined total mass (i.e., dried mass of polymer and stabilizing agent) was used for calculation of the respective volume fraction  $\varphi$ . The volume fractions have been calculated accordingly with the densities of the medium and polymer described in Table 2. The formula is shown below.

$$\varphi = \frac{\frac{\omega}{\rho_P}}{\frac{\omega}{\rho_P} + \left(\frac{1-\omega}{\rho_D}\right)}$$

with solid content  $\omega$ ; density of the polymer and the dispersant  $\rho_P$  and  $\rho_D$ .

## 2.3. Dynamic Light Scattering

DLS measurements were performed on a Zetasizer Nano ZS from Malvern Instruments (Malvern Panalytical GmbH, Malvern, UK), using single-use polyethylene UV cuvettes with a diameter of 10 mm. The laser position and attenuator settings were determined automatically by the device itself. A scattering angle of 173° was used. The data analysis was based on the general-purpose model. For the sample preparation, one drop of dispersion sample was diluted in 5 mL demineralized water. The sizes shown here are shown as mean of three consecutive measurements, each individually consists of 18 measurements at 25 °C. The error bars indicate the deviation of the mean diameter between three measurements.

## 3. Results and Discussion

The results presented here are ordered in the way that the data would be temporally available during or after a synthesis performed in real-time in the laboratory. Therefore, inline-determined PDW spectroscopy data are shown for one synthesis first by means of the  $I_{\text{raw}}$  trends (Section 3.1), which are readily available in real-time while the synthesis proceeds.  $I_{\text{raw}}$  data are observed at the control unit of the PDW spectrometer. Further, inline  $\mu_a$  and  $\mu_s'$  data are simultaneously plotted and can be analyzed onsite. The data are analyzed for three reaction volumes (Section 3.2 and following). Next, offline data analysis of conversion by means of the solid content analysis and offline-determined particle size is additionally taken into account. Conversion measurements using a microwave analyzer are only available minutes after the time point of sampling due to sample withdrawal, preparation and sample analysis by drying at elevated temperatures. Data on the mean



particle diameter by DLS are only available at a later point in time due to sampling, sample preparation by dilution, DLS analysis and subsequent evaluation.

In the end, in Section 3.5, the inline monitoring by PDW spectroscopy of the 100 L synthesis is shown to explore its suitability in high volume reactors and specify the effect of mixing on the dispersion properties.

### 3.1. Inline Process Analysis of PDW Spectroscopy Intensity Data

For rapid and high conversion and particle formation, a well-mixed and homogeneous reaction dispersion is crucial. Indications for an inhomogeneous dispersion can be observed in the PDW spectroscopy raw intensity data  $I_{\text{raw}}$ . If a particle or droplet system, like an emulsion or dispersion, is homogeneously mixed and entities are evenly distributed, the  $I_{\text{raw}}$  signal shows a decrease from lowest to highest  $d_f$ . An example is shown in Figure 2.

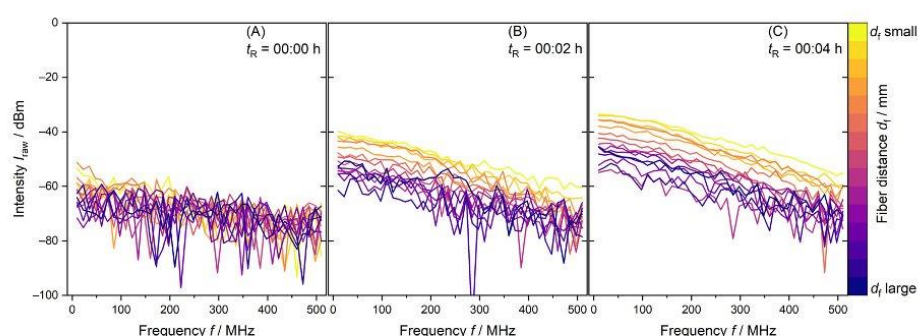


**Figure 2.** PDW spectroscopy  $I_{\text{raw}}$  data measurements at  $\lambda = 638$  nm of the first minutes of a synthesis with 1 L reaction volume. (A) shows  $I_{\text{raw}}$  just before addition of monomer mixture, (B) after two minutes and (C) after four minutes of monomer dosing.

Figure 2 shows PDW spectroscopy  $I_{\text{raw}}$  data for a 1 L synthesis.  $t_R = 00:00$  h shows a measurement of 15 fiber distances of the reaction mixture containing only water and redox initiator. Due to the absence of strongly scattering droplets and particles, measurement of this initial charge only leads to noise in the  $I_{\text{raw}}$  data in Figure 2A.  $t_R = 00:01$  h indicates the addition of VAc/Versa<sup>®</sup> 10 monomer mixture to the reaction vessel. Within two minutes and one PDW spectroscopy measurement, the  $I_{\text{raw}}$  values increase. An ordered decrease in  $I_{\text{raw}}$  from small to larger fiber distances  $d_f$  is established in Figure 2B. A further two minutes of reactant dosing causes  $I_{\text{raw}}$  to increase overall. A higher order of the fiber distances is visible in Figure 2C. These data are expected for a well-mixed, homogenous reaction mixture.

Figure 3 shows PDW spectroscopy data  $I_{\text{raw}}$  over the modulation frequency  $f$  of all measured distances taken from a 10 L synthesis. From Figure 3A–F, the synthesis proceeds from  $t_R = 00:02$  h to  $t_R = 01:00$  h reaction time. The intensity  $I_{\text{raw}}$  values for the smallest  $df$  (yellow line) and smallest modulation frequency  $f$  (10 MHz) increase with increasing reaction time from  $-30$  to  $-18$  dBm. The intensity of the measurement with highest  $d_f$  (purple line) and smallest modulation frequency increases from approx.  $-60$  dBm with high noise to above  $-40$  dBm. In a homogeneous dispersion, the measured intensity  $I_{\text{raw}}$  would decrease from  $d_f$  small to  $d_f$  large (from yellow to purple). With the proceeding polymerization, the reaction mixture becomes more turbid. More and larger particles contribute to absorption and scattering in the measurement path length. The detected inconsistencies by PDW spectroscopy in  $I_{\text{raw}}$  by means of a deviated order from the smallest

to biggest measurement distances  $d_f$  are very useful to check if a polymerization process is progressing as desired.

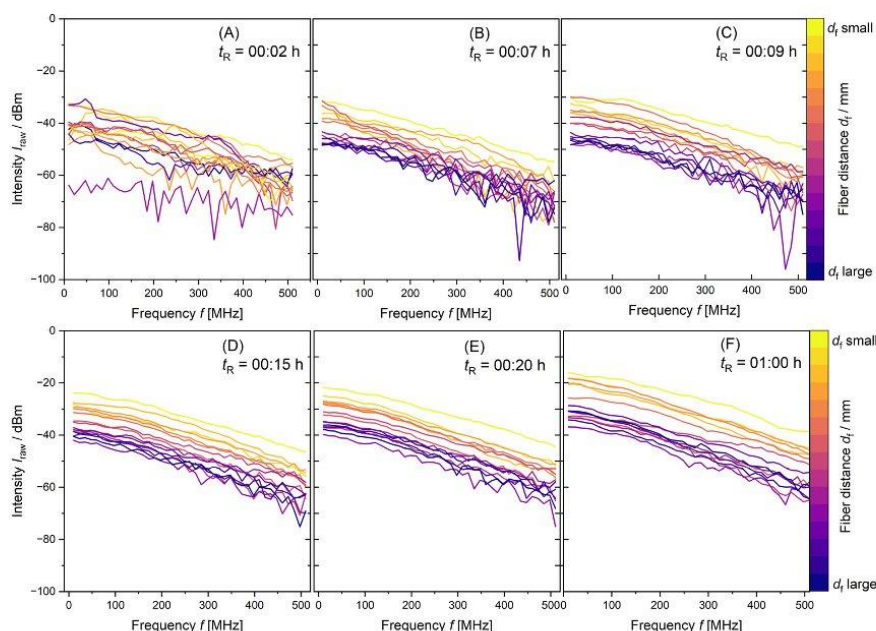


**Figure 3.** PDW spectroscopy  $I_{\text{raw}}$  data measurements at  $\lambda = 638$  nm of a synthesis with 10 L reaction volume from  $t_R = 00:02$  h to  $t_R = 01:00$  h. With monomer mixture dosing time  $t_R$  increasing from (A–F) as shown and increasing order of  $d_f$ .

With increasing reaction time  $t_R$ , the order of the distance-dependent measurements from  $d_{f, \text{small}}$  to  $d_{f, \text{large}}$  of  $I_{\text{raw}}$  data changes. The irregularity of the measurements in Figure 3 for the 10 L synthesis proposes that inhomogeneity of the reaction mixture is present for reaction times up to at least  $t_R = 00:20$  h. This might be caused by insufficient mixing. All dispersions analyzed in this paper have been produced with low feed-rates of the components. The monomer mixture is dosed into the dispersion at  $r_{\text{Mon}1\text{L}} = 1.2 \text{ mL min}^{-1}$ ,  $r_{\text{Mon}10\text{L}} = 12 \text{ mL min}^{-1}$  and  $r_{\text{Mon}100\text{L}} = 120 \text{ mL min}^{-1}$ , respectively. The stabilizer was completely added to the initial charge. With insufficient mixing, the high conversions needed for a starved feed polymerization are not guaranteed. The resulting particle properties will deviate from the desired product properties, leading to inconsistencies in product quality. As data acquisition is fast and the reaction mixture is not homogeneous, the measurements deviate strongly from each other. With increasing reaction time, particle formation and particle growth, the mixture becomes more homogeneous (see Figure 3D–F). PDW spectroscopy intensity measurements  $I_{\text{raw}}$  arrange to the measurement distance from smallest  $d_f$  to biggest  $d_f$ , as anticipated.

The  $I_{\text{raw}}$  measurements for the 100 L synthesis also indicates incomplete mixing. The data can be found in Supplementary Material Figure S1.

### 3.2. Inline Analysis of Optical Coefficients—Initial Particle Nucleation and Growth

Additionally to the  $I_{\text{raw}}$  data, data on the reduced scattering coefficient  $\mu_s'$  are measured inline by PDW spectroscopy and are readily available during the synthesis. Figure 4

shows the reduced scattering coefficient  $\mu_s'$  measured inline in dependency of the particle volume fraction  $\phi$  for batch sizes of 1 L, 10 L and 100 L.  $\phi$  was calculated as the dosed mass of monomer and colloidal stabilizer at an assumed 100% conversion to polymer. The reaction temperature was kept constant at  $T_R = 60^\circ\text{C}$ . Until  $\phi = 0.15$ , the scattering properties are comparable across all scales. The measured  $\mu_s'$  indicates that up to  $\phi = 0.15$  particle nucleation and growth happens at a comparable rate of polymerization. Exceeding  $\phi > 0.15$ , the measured  $\mu_s'$  trends start to deviate from each other significantly.

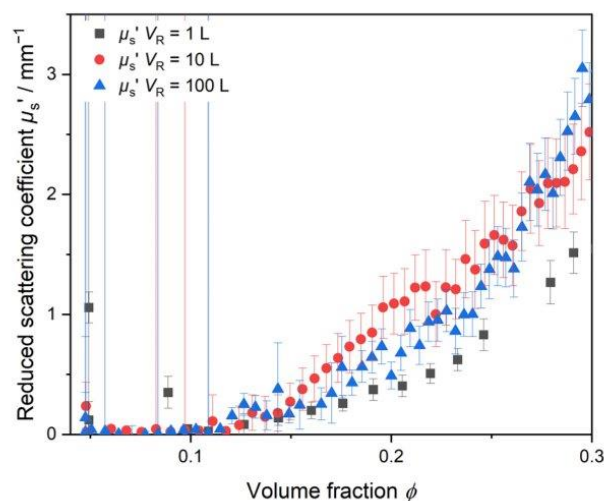


**Figure 4.** Initial polymerization phase monitored inline by PDW spectroscopy by means of the reduced scattering coefficient  $\mu_s'$  inline trend at  $\lambda = 638\text{ nm}$ . Measurement of  $\mu_s'$  at three different reaction volumes derived from a scale-up procedure from reaction volume of 1 L to 10 L and 100 L.

Here, reliable PDW spectroscopy inline data can only be derived for volume fractions greater than  $\phi > 0.1$ . Before, the scattering was too small to comply with the assumption of significant multiple scattering during the data analysis procedure. Due to the partial solubility of the monomer and small oligomers in water, larger, phase-separated polymer particles with a high refractive index in a significant amount, and thus strong scattering, are only formed later. The reduced scattering coefficient  $\mu_s'$  shows a significant increase at all three reaction scales, starting around  $\phi \approx 0.11$ . The deviation of the  $\mu_s'$  trends and different particle growth might be explained by the initial inhomogeneity of the respective reaction mixture.

From the  $I_{\text{raw}}$  data and the  $\mu_s'$  trends, it can already be observed that the syntheses do not proceed in the same way, as anticipated. Deviations in the  $\mu_s'$  trend clearly show that the dispersion properties are different after reaching a volume fraction of  $\phi \approx 0.15$ . PDW spectroscopy analysis is based on Mie theory. The  $\mu_s'$  dependency on particle size according to Mie shows that smaller particles at low volume fractions lead to lower values for  $\mu_s'$ . As mixing of the 1 L sample is sufficient to create a homogeneous reaction mixture, many small active radical reaction centers are formed where the polymerization proceeds. Therefore,  $\mu_s'$  is smallest for the 1 L sample up to  $\phi < 0.3$ . The bigger reaction volumes show homogeneity issues, leading to less active reaction centers for polymerization to be formed and therefore larger  $\mu_s'$  values.



### 3.3. Offline Dispersion Analysis

Further analysis of the synthesis was performed by offline conversion analysis by means of drying samples and determining the solid content and respective conversion.

Figure 5 shows the experimental and theoretical solid content of each synthesis over the reaction time. The experimentally determined solid content  $\omega_{\text{exp}}$  deviates from the theoretical amount of solids at 100% monomer conversion. This deviation is relatively small for a total reaction volume of 1 L. Due to sufficient mixing, the conversion of monomer to polymer is high, and little deviation between theoretical and experimental solid content  $\omega$  is detected. The difference between  $\omega_{\text{theo}}$  and  $\omega_{\text{exp}}$  is the largest for the 10 L synthesis. The further each synthesis proceeds, the more divergence between theoretical solid content  $\omega_{\text{theo}}$  and measured values  $\omega_{\text{exp}}$  is observed. The redox initiator and monomer mixture are dosed into the dispersion at very low feed-rates. In the beginning of the synthesis, the small amount of monomer added to the dispersion is still quickly converted to a high extent. The further the synthesis proceeds, the deviation increases, and the non-converted monomer stays unreacted within the dispersion.

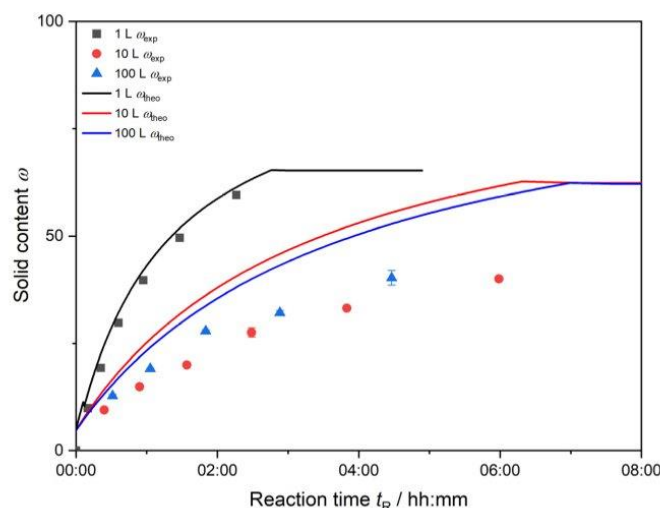


**Figure 5.** Calculation of theoretical solid content from 100% monomer conversion  $\omega_{\text{theo}}$  (lines) and experimentally determined solid content  $\omega_{\text{exp}}$  (symbols are color coded, respectively) of each reaction volume.

Note: For the 100 L synthesis, further measurements of the solid content and respective conversion calculation after  $t_R = 04:20$  h were not possible due to heavy aggregation.

Figure 6 shows offline-determined mean particle sizes by DLS for each reaction volume up to a volume fraction of  $\phi = 0.3$ . The final products from the reactions should have the same properties like particle size and particle size distribution and therefore the same reduced scattering coefficient  $\mu_s'$ . From these offline measurements, it is evident that the growth of particles between the reaction volumes differs already at early reaction stages. Already at low volume fractions less than  $\phi < 0.2$ , a difference in the determined mean particle size is detectable. The smallest reaction scale of 1 L reaction volume (black squares) produces the smallest particles. Exceeding  $\phi > 0.2$ , the 100 L synthesis (blue triangles) contains particle aggregates in the micrometer size regime, with high deviations between the measurements indicated by the very big error bar. As the reduced scattering coefficient  $\mu_s'$  strongly depends on the particle size within the dispersion, the deviations of the trends

between the reaction scales are far earlier detected by PDW spectroscopy in real-time in Figures 3 and 4. From the DLS data in Figure 6, it can be derived that the final particle sizes in the dispersions differ from each other. To achieve a successful scale-up procedure leading to equal properties across reaction scales, PDW spectroscopy can determine deviations already at low volume fractions in real-time much faster than common offline analysis.

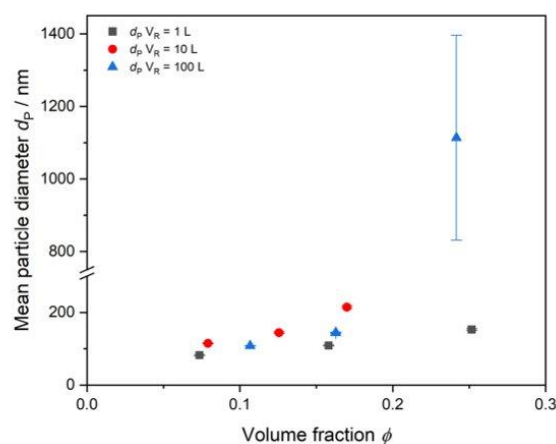


**Figure 6.** Volume-based mean particle diameter determined by DLS up to a volume fraction of  $\phi = 0.3$ . Volume fractions have been calculated based on experimentally determined conversion data (cf. Figure 5). Depicted error values are standard deviations of three DLS replicate measurements.

### 3.4. Comparative Analysis Across Reaction Scales

Figure 7 shows the reduced scattering coefficient  $\mu_s'$  of three syntheses monitored over the complete reaction course in dependence of the volume fraction  $\phi$ .  $\phi > 0.57$  is reached for all reaction volumes. Figure 7 shows PDW spectroscopy measurements at two different wavelengths,  $\lambda_1 = 638$  nm (Figure 7A) and  $\lambda_2 = 855$  nm (Figure 7B), respectively. An initial increase phase, a plateau phase and a decrease in scattering can be observed. A deviation of the  $\mu_s'$  trends between different scales occurs around  $\phi = 0.15$  at  $\lambda = 638$  nm and  $\phi = 0.25$  at  $\lambda = 855$  nm. For all three reaction volumes, a plateau phase of  $\mu_s'$  is found. In this plateau, the  $\mu_s'$  value decreases with increasing reaction volume from  $\mu_{s'1L} = 18 \text{ mm}^{-1}$  to  $\mu_{s'10L} = 12 \text{ mm}^{-1}$  and  $\mu_{s'100L} = 7 \text{ mm}^{-1}$ . The difference in the plateaued  $\mu_s'$  value indicates that the used scale-up procedure by Jacob et al. might not maintain particle properties in the final dispersion throughout reaction scales. It indicates that the particle growth phase between the reactions deviate from one another. To underline this, a second PDW spectroscopy measurement at  $\lambda_2 = 855$  nm is simultaneously analyzed. Figure 7B also shows a deviation in the final  $\mu_s'$  values. Compared to Figure 7A, the discrepancy between the final  $\mu_s'$  values in Figure 7B decreases. The final values are  $\mu_{s'1L} \approx 12 \text{ mm}^{-1}$  to  $\mu_{s'10L} \approx 8 \text{ mm}^{-1}$  and  $\mu_{s'100L} \approx 5 \text{ mm}^{-1}$ . Taking all the inline data produced by PDW spectroscopy into account, it is determined in real-time that the final particle properties will deviate from each other.

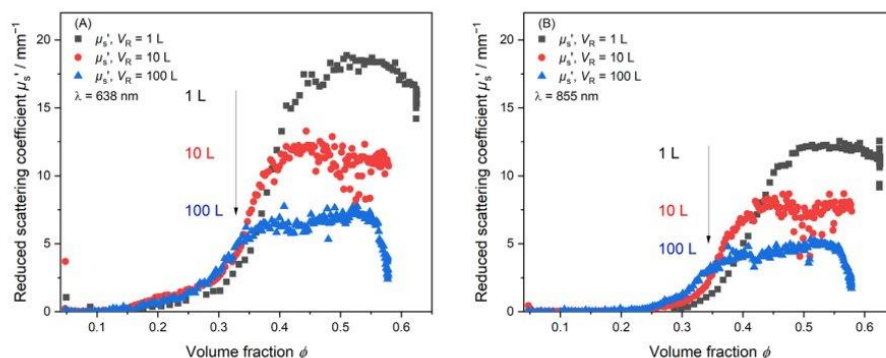


**Figure 7.** Inline monitoring of the synthesis process by PDW spectroscopy at  $T_R = 60$  °C by means of  $\mu_s'$ . Measurement of  $\mu_s'$  at three different reaction volumes. 1 L (black), 10 L (red) and 100 L (blue) at two different wavelengths. (A)  $\lambda_1 = 638$  nm and (B)  $\lambda_2 = 855$  nm measured simultaneously.

### 3.5. 100 L Synthesis Inline Analysis by PDW Spectroscopy—Effect of Mixing

In this section, the complete reaction of a 100 L synthesis is monitored by PDW spectroscopy. The reaction period of over  $t_R = 07:00$  h is completely monitored. The PDW spectroscopy data shown are collected in real-time without any dilution of the dispersion. The PDW spectroscopy probe is directly inserted into the dispersion at all times of the synthesis.

Figure 8 displays the inline trends of the reduced scattering coefficient  $\mu_s'$  and the absorption coefficient  $\mu_a$  as well as the total volume fraction  $\phi$  over time and the total conversion  $\chi$  for a 100 L synthesis.

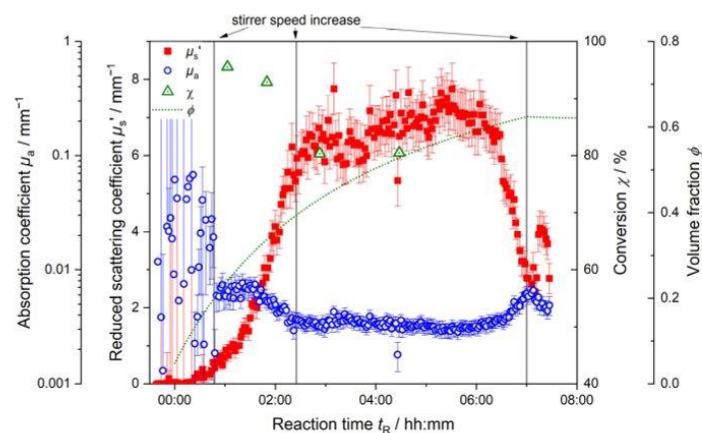


**Figure 8.** Inline monitoring of 100 L synthesis by PDW spectroscopy at  $\lambda = 638$  nm with reduced scattering coefficient  $\mu_s'$  (red) and absorption coefficient  $\mu_a$  (blue). Offline-determined total conversion  $\chi$  (green) and total volume fraction  $\phi$  (green dotted line) are shown along the reaction progress. Vertical lines indicate manual increases of the stirrer speed.

In the beginning of the reaction up until  $t_R = 00:50$  h, the absorption coefficient  $\mu_a$  (blue circles) does not yield consistent data points. Collected  $\mu_a$  data are very noisy; error bars are high, and no trend is derivable. An increase in the stirrer speed at  $t_R = 00:50$  h results in steady  $\mu_a$  measurements. With the manual increase in stirrer speed,  $\mu_a$  stays



constant for approx. 00:30 h and decreases afterwards. This decrease in the total dispersion absorption is explained by the changes within the reaction dispersion. In the beginning up until the increase in stirrer speed, the system shown signs of inhomogeneity. The inhomogeneity itself is not at all increased. Due to this insufficient mixing, the assumed conditions for PDW spectroscopy measurements are not met, and PDW spectroscopy cannot deliver conclusive measurements for  $\mu_a$ . (PDW spectroscopy  $I_{\text{raw}}$  inline data are shown in Figure S1.) Further, with proceeding synthesis and increasing homogeneity due to the increased stirring speed after  $t_R = 00:50$  h, the absorption decreases. This decrease is caused by the combined changes happening in the dispersion. As absorption is a sum parameter, it is influenced by all the entities available in the dispersion. In the beginning of the synthesis, the absorption of the dispersion is mostly influenced by the high absorption of the aqueous medium and a high number of active radicals. It was found before that created radicals from the initiator and monomers show a high absorption [53]. Due to insufficient mixing, possible monomer droplets in the dispersion also contribute to the higher  $\mu_a$  values. With proceeding synthesis, the radical number and residual monomer in the dispersion decreases. Simultaneously, polymer particles start to form and grow. As the absorption of polymer particles is lower than that of the radicals and the aqueous medium, the overall absorption of the dispersion decreases. After a second manual stirrer increase at  $t_R = 02:30$  h, it levels off at values around  $0.003 \text{ mm}^{-1}$ .

Only after approx. 06:00 h of reaction time, the absorption starts to increase again without any applied extrinsic changes. This increase is caused by the aggregation of polymer particles in the dispersion. The total number of particles decreases as individual particles coagulate and form aggregates. A further stirrer speed increase was applied at  $t_R = 07:00$  h in order to counteract coagulation of the dispersion. However, coagulation could not be averted. The final product achieved was a paste rather than a liquid dispersion.

In Figure 8, the trend of the reduced scattering coefficient  $\mu_s'$  (red squares) starts to increase slowly in the beginning at  $t_R = 00:15$  h. The formation of particles starts to influence the scattering properties of the dispersion. The slope of  $\mu_s'$  increases continuously as polymer particles are formed and continue growing. The manual increase in stirrer speed at  $t_R = 00:50$  h does not show such a significant effect on  $\mu_s'$  as it has on  $\mu_a$ .  $\mu_s'$  continues to grow; its slope becoming steeper as more polymer particles as scattering entities are formed and increase in size, contributing to the overall scattering. At the second manual increase in stirring speed at  $t_R = 02:30$  h,  $\mu_s'$  still increases for a while, but the acquired datapoints become noisier, and a slight overall increase is observed up until approx.  $t_R = 06:00$  h. During the course of the reaction, the changes in scattering become less pronounced; initially,  $\mu_s'$  increases strongly with a steep slope. With the continuous addition of monomer to the dispersion (green dotted line), the particles continue to grow. However, the changes in their volume, the overall volume fraction and particle number are less pronounced, creating a decreasing slope of  $\mu_s'$ . After  $t_R = 06:00$  h,  $\mu_s'$  suddenly decreases significantly. Both optical coefficients  $\mu_a$  and  $\mu_s'$  change. As discussed before here and in Schlappa et al., this can be a sign of particle aggregation in the dispersion [20].

In Figure 8, for the 100 L synthesis, the conversion  $\chi$  (green triangles) decreases from over 95% to approx. 80%. Due to the initial inhomogeneity (cf. Figures 4, 5 and 7), a conversion of only 96% is achieved in the beginning. Although very low feed-rates of monomer are used, it is not fully converted. The conversion decreases over the whole course of the reaction. Despite manual increases in stirring speed, the initial lack of full conversion cannot be retrieved. As the monomer is continuously fed into the dispersion, it is not completely converted. The running reaction cannot recover the effects the insufficient mixing had on the conversion. The presumed starved-feed process is not reached. Conversion measurements after  $t_R = 04:20$  h were not possible here. The high solid contents

of the samples drawn from the reactor lead to inconclusive microwave analyzer results. The inline monitoring of the synthesis shows that the initial inhomogeneities detected in the PDW spectroscopy  $I_{\text{raw}}$  measurements are also detectable in the noisy inline data acquisition of  $\mu_a$  and the low conversion of the reaction.

#### 4. Conclusions

For the first time, the suitability of monitoring 10 L and 100 L reaction volumes with inline PDW spectroscopy for high-solid-content emulsion polymerization synthesis has been described in detail. It is shown that the technique delivers inline data on the optical coefficients without dilution of the dispersion. The feasibility of PDW spectroscopy for the 100 L reaction scale with industrially relevant dispersion properties was successfully demonstrated. The PVAc copolymerization was successfully monitored in real-time. It was shown here that PDW spectroscopy data provide much physical and chemical information about polymerization processes. These findings can be adapted for various other emulsion polymerization systems. On top of the optical coefficients of a polymer dispersion, insights into its dynamics can be drawn. For the scale-up process adapted here with reaction volumes from 1 L to 10 L and 100 L, the reduced scattering coefficient  $\mu_s'$  increases comparably only for up to  $\phi = 0.15$ , indicating similar initial particle nucleation and growth rates throughout the different reaction volumes. However, as the reactions proceed, deviations in both measured inline trends of  $\mu_a$  and  $\mu_s'$  suggest differences in the final dispersion properties. It is shown by DLS particle size analysis that the particle size indeed starts to grow deviant to that in the Model 1 L system. These data are particularly valuable and relatable to various polymerization processes as they capture real-time changes in optical properties, which reflect critical aspects of the reaction's progression in particle growth. Initial deviations between the syntheses can already be seen inline via PDW spectroscopy  $I_{\text{raw}}$  data in real-time in the first synthesis minutes.

Instead of relying on experience, data-driven knowledge can be used to ensure safe operation of large-scale syntheses and consistent product quality. PDW spectroscopy inline data reveal these early reaction inconsistencies. Insufficient mixing and resulting inhomogeneity, especially in the larger volumes, hint that starved-feed conditions are not achieved. It is detected that the scale-up procedure is not feasible to deliver identical dispersion properties. This was only found after advanced analysis of PDW spectroscopy data in combination with offline conversion data. Earlier studies based on basic data evaluation could not deliver these progressive results. The inline data highlight the importance of sufficient mixing at early reaction stages to achieve high conversion values. Further, the implemented PDW spectroscopy as PAT was able to indicate coagulation incidents during synthesis. Both inline trends  $\mu_a$  and  $\mu_s'$  significantly change during coagulation, and countermeasures could be introduced to the dispersion to prevent it.

**Supplementary Materials:** The following supporting information can be downloaded at: <https://www.mdpi.com/article/10.3390/polym17050629/s1>, Figure S1: PDW spectroscopy  $I_{\text{raw}}$  data measurements at  $\lambda = 638$  nm of a synthesis with 100 L reaction volume from  $t_R = 00:02$  h to  $t_R = 00:38$  h. Initial measurements up to at least  $t_R = 00:22$  h show irregularities in the order of  $I_{\text{raw}}$  and  $df$ . This might be caused by an inhomogeneous dispersion due to insufficient mixing; Figure S2: Inline monitoring of 10 L synthesis by PDW spectroscopy at  $\lambda = 638$  nm with reduced scattering coefficient  $\mu_s'$  (red) and absorption coefficient  $\mu_a$  (blue). Offline determined total conversion  $X$  (green) and total volume fraction  $\phi$  (green dotted line) are shown along the reaction progress. Vertical lines indicate manual increases of the stirrer speed; Table S1: Overview of the measurements of the experimental set-up of all three reactor sizes at different polymerization reaction volumes  $V_R$ , with  $H$  as height of the reactor,  $D$  as diameter of the reactor,  $d$  as diameter of the used anchor stirrer,  $H_1$  as height of



initial Charge before starting the reaction and  $h$  as height from the bottom of the reactor to the anchor stirrer; Table S2: Initial stirring rates for the different reaction volumes  $V_R$ .

**Author Contributions:** Conceptualization, W.P., S.S., M.M. and O.R.; methodology, S.S. and M.M.; software, M.M.; validation, S.S.; formal analysis, S.S.; data curation, S.S., M.M. and O.R.; writing—original draft preparation, S.S.; writing—review and editing, S.S., O.R. and M.M.; visualization, S.S.; supervision, M.M. and O.R.; project administration, W.P.; funding acquisition, M.M. and W.P. All authors have read and agreed to the published version of the manuscript.

**Funding:** This study was financed by the financial support of the German Federal Ministry of Education and Research (grants 03Z22AN12 and 03Z22AB1B) and the University of Potsdam. It was funded by the Deutsche Forschungsgemeinschaft (DFG, German Research Foundation)—Project-number 491466077. We further acknowledge financial support from the Open Access Publication Fund of the University of Hamburg.

**Institutional Review Board Statement:** Not applicable.

**Data Availability Statement:** The original contributions presented in the study are included in the article/supplementary material, further inquiries can be directed to the corresponding author.

**Acknowledgments:** The authors would like to acknowledge the cooperation between the University of Potsdam and University of Hamburg, Roland Hass for establishing the cooperation and Laurence Jacob for conducting the experiments, beneficial discussions and an overall cordial joint work.

**Conflicts of Interest:** The authors declare no conflicts of interest.

## References

1. Brodhagen, A.; Grünwald, M.; Kleiner, M.; Lier, S. Erhöhung der Wirtschaftlichkeit durch beschleunigte Produkt- und Prozessentwicklung mit Hilfe modularer und skalierbarer Apparate. *Chem. Ing. Tech.* **2012**, *84*, 624–632. [\[CrossRef\]](#)
2. Kammona, O.; Chatzi, E.G.; Kiparissides, C. Recent Developments in Hardware Sensors For the On-Line Monitoring of Polymerization Reactions. *J. Macromol. Sci. Part C Polym. Rev.* **1999**, *39*, 57–134. [\[CrossRef\]](#)
3. Hamzehlou, S.; Asua, J.M. On-line monitoring and control of emulsion polymerization reactors. In *Advances in Polymer Reaction Engineering*; Elsevier: Cambridge, MA, USA, 2020; pp. 31–57. ISBN 9780128206454.
4. Flory, P.J. The mechanism of vinyl polymerizations I. *J. Am. Chem. Soc.* **1937**, *59*, 241–253. [\[CrossRef\]](#)
5. Mardare, D.; Matyjaszewski, K. “Living” radical polymerization of vinyl acetate. *Macromolecules* **1994**, *27*, 645–649. [\[CrossRef\]](#)
6. Samide, A.; Tutunaru, B.; Merişanu, C.; Cioateră, N. Thermal analysis: An effective characterization method of polyvinyl acetate films applied in corrosion inhibition field. *J. Therm. Anal. Calorim.* **2020**, *142*, 1825–1834. [\[CrossRef\]](#)
7. Berber, H.; Tamer, Y.; Yildirim, H. The effects of feeding ratio on final properties of vinyl acetate-based latexes via semi-continuous emulsion copolymerization. *Colloid. Polym. Sci.* **2018**, *296*, 211–221. [\[CrossRef\]](#)
8. Horkay, F.; Burchard, W.; Hecht, A.M.; Geissler, E. Scattering properties of poly (vinyl acetate) gels in different solvents. *Macromolecules* **1993**, *26*, 4203–4207. [\[CrossRef\]](#)
9. Abad, C.; De La Cal, J.C.; Asua, J.M. Emulsion copolymerization of vinyl esters in continuous reactors: Comparison between loop and continuous stirred tank reactors. *J. Appl. Polym. Sci.* **1995**, *56*, 419–424. [\[CrossRef\]](#)
10. Fischer, D.; Sahre, K.; Abdelrhim, M.; Voit, B.; Sadhu, V.B.; Pionteck, J.; Komber, H.; Hutschenreuter, J. Process monitoring of polymers by in-line ATR-IR, NIR and Raman spectroscopy and ultrasonic measurements. *C. R. Chim.* **2006**, *9*, 1419–1424. [\[CrossRef\]](#)
11. Haven, J.J.; Junkers, T. Online Monitoring of Polymerizations: Current Status. *Eur. J. Org. Chem.* **2017**, *2017*, 6474–6482. [\[CrossRef\]](#)
12. Pasquale, A.J.; Long, T.E. Real-Time Monitoring of the Stable Free Radical Polymerization of Styrene via in-Situ Mid-Infrared Spectroscopy. *Macromolecules* **1999**, *32*, 7954–7957. [\[CrossRef\]](#)
13. Araújo, P.H.H.; De La Cal, J.C.; Asua, J.M.; Pinto, J.C. Modeling Particle Size Distribution (PSD) in Emulsion Copolymerization Reactions in a Continuous Loop Reactor. *Macromol. Theory Simul.* **2001**, *10*, 769–779. [\[CrossRef\]](#)
14. Monsalve-Bravo, G.M.; Moscoso-Vasquez, H.M.; Alvarez, H. Scaleup of Batch Reactors Using Phenomenological-Based Models. *Ind. Eng. Chem. Res.* **2014**, *53*, 9439–9453. [\[CrossRef\]](#)
15. Fortuny, M.; Graillat, C.; McKenna, T.F.; Araújo, P.H.H.; Pinto, J.C. Modeling the nucleation stage during batch emulsion polymerization. *AIChE J.* **2005**, *51*, 2521–2533. [\[CrossRef\]](#)
16. Kemmere, M.F.; Meuldijk, J.; Drinkenburg, A.A.H.; German, A.L. Colloidal stability of high-solids polystyrene and polyvinyl acetate latices. *J. Appl. Polym. Sci.* **1999**, *74*, 1780–1791. [\[CrossRef\]](#)



17. Verwey, E.J.W. Theory of the stability of lyophobic colloids. *J. Phys. Chem.* **1947**, *51*, 631–636. [\[CrossRef\]](#)
18. Melis, S.; Kemmere, M.; Meuldijk, J.; Storti, G.; Morbidelli, M. A model for the coagulation of polyvinyl acetate particles in emulsion. *Chem. Eng. Sci.* **2000**, *55*, 3101–3111. [\[CrossRef\]](#)
19. Baade, W.; Moritz, H.U.; Reichert, K.H. Kinetics of high conversion polymerization of vinyl acetate. Effects of mixing and reactor type on polymer properties. *J. Appl. Polym. Sci.* **1982**, *27*, 2249–2267. [\[CrossRef\]](#)
20. Schlappa, S.; Brenker, L.J.; Bressel, L.; Hass, R.; Münzberg, M. Process Characterization of Polyvinyl Acetate Emulsions Applying Inline Photon Density Wave Spectroscopy at High Solid Contents. *Polymers* **2021**, *13*, 669. [\[CrossRef\]](#)
21. Aspiazu, U.O.; Gómez, S.; Paulis, M.; Leiza, J.R. Real-Time Monitoring of Particle Size in Emulsion Polymerization: Simultaneous Turbidity and Photon Density Wave Spectroscopy. *Macromol. Rapid Commun.* **2024**, *45*, e2400374. [\[CrossRef\]](#)
22. Jacob, L.L.; Pauer, W. In-line monitoring of latex-particle size during emulsion polymerizations with a high polymer content of more than 60. *RSC Adv.* **2020**, *10*, 26528–26534. [\[CrossRef\]](#) [\[PubMed\]](#)
23. Jacob, L.L.; Pauer, W. Scale-up of Emulsion Polymerisation up to 100 L and with a Polymer Content of up to 67 wt%, Monitored by Photon Density Wave Spectroscopy. *Polymers* **2022**, *14*, 1574. [\[CrossRef\]](#) [\[PubMed\]](#)
24. Ishibe, T.; Kaneko, T.; Uematsu, Y.; Sato-Akaba, H.; Komura, M.; Iyoda, T.; Nakamura, Y. Tunable Thermal Switch via Order-Order Transition in Liquid Crystalline Block Copolymer. *Nano Lett.* **2022**, *22*, 6105–6111. [\[CrossRef\]](#) [\[PubMed\]](#)
25. Song, H.; Cai, K.; Wang, J.; Shen, S. Influence of polymerization method on the thermoelectric properties of multi-walled carbon nanotubes/polypyrrole composites. *Synth. Met.* **2016**, *211*, 58–65. [\[CrossRef\]](#)
26. Pohn, J.; Heniche, M.; Fradette, L.; Cunningham, M.; McKenna, T. Computational Analysis of Mixing and Scale-Up in Emulsion Polymerization Reactors. *Macromol. Symp.* **2011**, *302*, 133–141. [\[CrossRef\]](#)
27. Gustin, J.-L.; Laganier, F. Understanding Vinyl Acetate Polymerization Accidents. *Org. Process Res. Dev.* **2005**, *9*, 962–975. [\[CrossRef\]](#)
28. Azpeitia, M.; Leiza, J.R.; Asua, J.M. Safety in Emulsion Polymerization Reactors: An Experimental Study. *Macromol. Mater. Eng.* **2005**, *290*, 242–249. [\[CrossRef\]](#)
29. Meyer, T. Scale-Up of Polymerization Process: A Practical Example. *Org. Process Res. Dev.* **2003**, *7*, 297–302. [\[CrossRef\]](#)
30. Wang, Y.-W.; Mei, Y. Thermal runaway evaluation on batch polyvinyl acetate emulsion polymerization from calorimetric measurement. *J. Therm. Anal. Calorim.* **2023**, *148*, 4801–4810. [\[CrossRef\]](#)
31. Chern, C.S.; Kuo, Y.N. Shear-induced coagulation kinetics of semibatch seeded emulsion polymerization. *Chem. Eng. Sci.* **1996**, *51*, 1079–1087. [\[CrossRef\]](#)
32. Copelli, S.; Derudi, M.; Sempere, J.; Serra, E.; Lunghi, A.; Pastureni, C.; Rota, R. Emulsion polymerization of vinyl acetate: Safe optimization of a hazardous complex process. *J. Hazard. Mater.* **2011**, *192*, 8–17. [\[CrossRef\]](#)
33. Elgebrandt, R.C.; Romagnoli, J.A.; Fletcher, D.F.; Gomes, V.G.; Gilbert, R.G. Analysis of shear-induced coagulation in an emulsion polymerisation reactor using computational fluid dynamics. *Chem. Eng. Sci.* **2005**, *60*, 2005–2015. [\[CrossRef\]](#)
34. Asua, J.M. On-line control of emulsion polymerization reactors: A perspective. *Can. J. Chem. Eng.* **2023**, *101*, 4907–4913. [\[CrossRef\]](#)
35. Cheng, D.; Ariafar, S.; Sheibat-Othman, N.; Pohn, J.; McKenna, T.F.L. Particle Coagulation of Emulsion Polymers: A Review of Experimental and Modelling Studies. *Polym. Rev.* **2018**, *58*, 717–759. [\[CrossRef\]](#)
36. Chern, C.S. Emulsion polymerization mechanisms and kinetics. *Prog. Polym. Sci.* **2006**, *31*, 443–486. [\[CrossRef\]](#)
37. Aguirre, M.; Ballard, N.; Gonzalez, E.; Hamzehlou, S.; Sardon, H.; Calderon, M.; Paulis, M.; Tomovska, R.; Dupin, D.; Bean, R.H.; et al. Polymer Colloids: Current Challenges, Emerging Applications, and New Developments. *Macromolecules* **2023**, *56*, 2579–2607. [\[CrossRef\]](#)
38. Abeykoon, C. Sensing technologies for process monitoring in polymer extrusion: A comprehensive review on past, present and future aspects. *Meas. Sens.* **2022**, *22*, 100381. [\[CrossRef\]](#)
39. Chen, Y.; Jahanzad, F.; Sajjadi, S. Semicontinuous monomer-starved emulsion polymerization as a means to produce nanolatexes: Analysis of nucleation stage. *Langmuir* **2013**, *29*, 5650–5658. [\[CrossRef\]](#)
40. Agirre, A.; Calvo, I.; Weitzel, H.-P.; Hergeth, W.-D.; Asua, J.M. Semicontinuous Emulsion Co-polymerization of Vinyl Acetate and VeoVa10. *Ind. Eng. Chem. Res.* **2014**, *53*, 9282–9295. [\[CrossRef\]](#)
41. Agirre, A.; Weitzel, H.-P.; Hergeth, W.-D.; Asua, J.M. Process intensification of VAc–VeoVa10 latex production. *Chem. Eng. J.* **2015**, *266*, 34–47. [\[CrossRef\]](#)
42. Chai, X.-S.; Schork, F.J.; DeCinque, A.; Wilson, K. Measurement of the Solubilities of Vinylic Monomers in Water. *Ind. Eng. Chem. Res.* **2005**, *44*, 5256–5258. [\[CrossRef\]](#)
43. Britton, D.; Heatley, F.; Lovell, P.A. Effect of Monomer Feed Rate on Chain Transfer to Polymer in Semibatch Emulsion Polymerization of Vinyl Acetate Studied by NMR Spectroscopy. *Macromolecules* **2000**, *33*, 5048–5052. [\[CrossRef\]](#)
44. Bressel, L. Bedeutung der abhaengigen Streuung für die optischen Eigenschaften hochkonzentrierter Dispersionen. Ph.D. Thesis, University of Potsdam, Potsdam, Germany, 2016.
45. Reich, O. Photonendichtewellenspektroskopie mit intensitätsmodulierten Diodenlasern (Photon Density Wave Spectroscopy with Intensity-Modulated Diode Lasers). Ph.D. Thesis, University of Potsdam, Potsdam, Germany, 2005.

46. Schlappa, S.; Bressel, L.; Reich, O.; Münzberg, M. Advanced Particle Size Analysis in High-Solid-Content Polymer Dispersions Using Photon Density Wave Spectroscopy. *Polymers* **2023**, *15*, 3181. [[CrossRef](#)] [[PubMed](#)]
47. Hass, R.; Reich, O. Photon density wave spectroscopy for dilution-free sizing of highly concentrated nanoparticles during starved-feed polymerization. *Chemphyschem* **2011**, *12*, 2572–2575. [[CrossRef](#)]
48. Bressel, K.; Müller, W.; Leser, M.E.; Reich, O.; Hass, R.; Wooster, T.J. Depletion-Induced Flocculation of Concentrated Emulsions Probed by Photon Density Wave Spectroscopy. *Langmuir* **2020**, *36*, 3504–3513. [[CrossRef](#)]
49. Hass, R.; Münzberg, M.; Bressel, L.; Reich, O. Industrial applications of photon density wave spectroscopy for in-line particle sizing Invited. *Appl. Opt.* **2013**, *52*, 1423–1431. [[CrossRef](#)]
50. Zimmermann, S.; Reich, O.; Bressel, L. Exploitation of inline photon density wave spectroscopy for titania particle syntheses. *J. Am. Ceram. Soc.* **2023**, *106*, 671–680. [[CrossRef](#)]
51. Aspiazú, U.O.; Paulis, M.; Leiza, J.R. Photon Density Wave spectroscopy to monitor the particle size in seeded semibatch emulsion copolymerization reactions. *Chem. Eng. J.* **2024**, *483*, 149292. [[CrossRef](#)]
52. Bressel, L.; Hass, R.; Reich, O. Particle sizing in highly turbid dispersions by Photon Density Wave spectroscopy. *J. Quant. Spectrosc. Radiat. Transf.* **2013**, *126*, 122–129. [[CrossRef](#)]
53. Johnston, L.J.; Schepp, N.P. Reactivities of radical cations: Characterization of styrene radical cations and measurements of their reactivity toward nucleophiles. *J. Am. Chem. Soc.* **1993**, *115*, 6564–6571. [[CrossRef](#)]

**Disclaimer/Publisher's Note:** The statements, opinions and data contained in all publications are solely those of the individual author(s) and contributor(s) and not of MDPI and/or the editor(s). MDPI and/or the editor(s) disclaim responsibility for any injury to people or property resulting from any ideas, methods, instructions or products referred to in the content.

## 6 Discussion

The first two research papers are based on the same type of emulsion polymerization experiments, involving changes to the system by either an increase in the amount of monomer VA added, or an increase in the amount of stabilizer PVA added to the reaction system. Simple design of experiment by varying one parameter accounts for access to effect correlations. Both papers show the utility of PDW spectroscopy for the specific analysis of high solid content VA dispersions at a laboratory reaction scale of up to 1 L reaction volume. The first research presents applied PDW spectroscopy in different semi-continuous starved-feed syntheses with varying amount of monomer added to the system and correspondingly increasing the feed rates of the other components. A spectrum of mean particle sizes and PSD is produced. In the follow up research an increase in the initial amount of PVA delivers an increase in the final particle size and creates particles within the same size range of approx. 100-600 nm in  $d_p$ .

PDW spectroscopy is applied to monitor and optimize the processes, whereas first a focus on inline monitoring of the optical coefficients during the synthesis is developed. The increase in monomer content significantly affects the particle size and scattering behavior of the system. Publication 1 describes samples with a wide solid content range between 41 % (w/w) and 57 % (w/w), whereas in the second set of experiments the solid content for the PVAc system is not significantly altered. This progresses into the detailed analysis of particle size and PSD in the dispersions. Initially the syntheses are monitored with continuous change of the volume fraction during the polymer synthesis. High error values for inline  $\mu_s'$  are detected. The model assumptions have not yet been adapted to the physical parameters of the sample analyzed. An increase in data accuracy and quality was achieved by focusing the following research onto a small range of possible solid content dispersions between only 40.8 (w/w) and 41.6 (w/w) % to better understand the influence of PVA. Especially its water binding abilities and the effects on the PDW spectroscopy model assumptions and resulting particle size have been analyzed deeply.

The second study continues on the findings of the first paper. The reduced scattering coefficient and mean particle size analysis is upgraded into analysis of the PSD. The detailed analysis of the particle system enhances the primary study of the reduced scattering coefficient trend into a more comprehensive analysis of PSD. To specify the findings of the water binding PVAc/PVA system, another model system was added to the research in order to eliminate erroneous assumptions. To show that individual adaptations of the refractive index, density and volume fraction for PDW spectroscopy analysis to determine the PSD are necessary, the second publication uses PS/SDS particles as example and best practice system. The PS/SDS system was chosen as it is known to not incorporate water into its macromolecular structure. Without the proposed in-depth and iterative approach to recalculate the density and refractive

index no precise determination of the real particle size during the syntheses are possible for PVAc/PVA particles. It still is a big challenge, as the changes caused during the synthesis are continuously affecting the particle characteristics and therefore its physical values. These are not continuously adaptable during inline analysis with PDW spectroscopy to date. Further research is needed to incorporate real-time changes, water binding and simultaneous alteration of the polymer particles properties for a reliable, continuous particle size determination during emulsion polymerization synthesis of PVAc/PVA.

The analysis of the final PVAc/PVA dispersions lead to the assumption that up to 20 % volume of the PVAc/PVA particle volume is swollen with bound water. To determine these factors, downstream analysis from PDW spectroscopy measurements lead to a shift in focus from inline analysis of the synthesis to analysis of the final PVAc/PVA water dispersion product. The actual measurable scattering coefficient in the dispersion is a true and concise value. The physical particle may only consist of PVAc polymer blocks, PVA stabilizer and incorporated water. These might lead to swelling, impurities and decrease in density, refractive index and the volume fraction of particles. These are crucial factors to determine the correct particle size from PDW spectroscopy based on theory of radiative transport and Mie Theory. The determined error  $\chi^2$  from the PDW spectroscopy algorithm gave immense high error values indicating, that the used parameters do not fit well to the actual properties of the analyzed particles.

Starting from the assumption, that no water is incorporated into the system and no swelling is occurring the refractive index and density of the particle was calculated and taken as reference parameters for PDW spectroscopy size analysis (typical values are stated in publication 1 in Table 3).

Systematic evaluation of the water-polymer ratio caused the error in  $\chi^2$  to decrease. The  $\chi^2$  regression displays a minimum, in which the lowest possible error can be determined by the first derivative at  $\bar{\chi}^2 = 0$  (cf. Fig 8, Paper 2). The analyzed system is best described in the exact minimum of the curve. With this iterative approach all five dispersions with different amount of stabilizer in the system have been analyzed. It was found that there is no significant trend derivable within the experimental set-up limitations. However, the range of total colloidal stabilizer PVA used in the dispersions is very low. Future research should focus on a wider range of PVA addition to samples and whether a trend in the amount of PVA in the system and correlation to the water swelling factor is derivable. A significant improvement of the error values was obtained by taking the water swelling into account. The problem of the particle size determination of PVAc/PVA systems with a constant volume fraction has been solved. To take it a step further the PSD of the analyzed dispersions were compared to offline derived distributions by commonly used light scattering techniques DLS and SLS and electron

microscopy. The undiluted measurement of the particle size from PDW spectroscopy with the incorporation of water swelling gives comparable results to the ones shown by light scattering techniques. It is to consider, that both SLS and DLS are dilution-based techniques. Based on the findings that PVAc/PVA particles are keen to absorb a lot of water these techniques might deliver false results for this system.

For ongoing and further research additionally the analyzed reaction scale has been increased from laboratory scale of 1 L to meta and production scales of 10 L and 100 L reaction volume respectively. A linear scale-up procedure has been proposed by JACOB et al. to produce PVAc:Versa® 10/PVA dispersions with the same properties and particles with the same particle diameter and distribution. As discussed the water binding properties of PVAc/PVA were found to be very critical for PDW spectroscopy analysis. Therefore the monomer system has been changed from PVAc homopolymer to a 9:1 PVAc:Versa® 10 co-monomer mixture. The water binding was negligible for this system. It was left out of the inline analysis context as it makes the analysis too complicated for the bigger reaction volumes. The inline monitoring of the reduced scattering coefficient reveals early deviations between reaction stages. Based on this it can be drawn to attention that a linear proposed scale-up procedure does not lead to consistent dispersion and particle properties.

To gain understanding of the whole polymerization process the focus of inline PDW spectroscopy analysis shifts back from the particle size analysis of the final product to the inline analysis of the optical dispersion properties of the critical early reaction stages. The initial nucleation and particle growth phases are analyzed in depth by intensity measurements of  $I_{raw}$  against the applied modulation frequency  $f$ . With the introduced measurements of  $I_{raw}$  inhomogeneity of the reaction mixture can be explicitly detected. These inhomogeneities cause sustainable effects on the whole polymerization process, especially on the conversion, final particle diameter and scale-up procedure.

Significant advantage of inline monitoring by PDW spectroscopy is drawn from the first publication 1 Fig. 7 and publication 3 in Figures 7 and 8. In both cases deviations from the regular emulsion polymerization process are detected by the first derivative of the inline PDW spectroscopy trends in  $\mu_s'$  and  $\mu_a$ . In the first publication gelation of the polymer dispersion can be detected inline as a sudden change in  $\mu_s'$  and  $\mu_a$  derivative. Gelation of the dispersion due to high solid content and increased viscosity is averted by stopping further monomer addition and respective dilution of the sample with water. Further in the third publication inhomogeneity and aggregation events in the dispersion are detectable in the same matter. As synthesis proceeds aggregation cannot be averted by an increase in the stirring speed (cf. Publication 3, Figure 8). It is questionable if addition of water to dilute the dispersion would have stabilized



the system during the synthesis here as well. JACOB at al. reported that the formed paste was easily re-dispersible by addition of water after the process was completed.<sup>39</sup>

For emulsion polymerizations, good mixing of the reaction mass with minimal shear is required to obtain the lowest possible energy input and to prevent aggregation of the particles. For homogenization a critical stirrer speed required individually for each reaction scale to achieve the intrinsic polymerization rate. For experiments with insufficient mixing and inhomogeneities in the early reaction stages, the rate of mass transfer from the monomer phase to the growing polymer particles is low.<sup>84,85</sup> Mixing is very important to quickly compensate for temperature gradients and to avoid local hotspots where the temperature cannot be controlled and other, usually undesirable, properties of the particles are preserved.<sup>52</sup> Mixing is also crucial for mass transfer, especially in very fast emulsion polymerizations, which are popular due to the short reaction times and smaller particle diameters. Excessive shear forces and thus high energy dissipation can lead to aggregation of the particles or monomer droplets if the energy introduced is sufficient to overcome the emulsifier shell between the particle or droplet surfaces.

To sum up, PDW spectroscopy can be used to draw remarkable insights of a polymerization process. It can be used in the beginning of a synthesis to detect for example early inhomogeneities, during the synthesis to prevent unwanted gelation, deviations from the synthesis protocol and even aggregation of polymer particles in the final product. It is a powerful tool for the analysis of the final dispersion characteristics.\*gAI

---

\*gAI This whole paragraph 6. Discussion has been drafted and written by the author. Proofreading and optimization has been done using generative AI via ChatGPT at openai.com

## 7 Conclusion

During this research the inline measurements of the reduced scattering coefficient  $\mu_s'$  and the application of PDW spectroscopy for the emulsion polymerization of PVAc homopolymerization and PVAc/Versa® 10 copolymerization has been increased in its TRL from 5 to early TRL 7. It has been proven to be useful as reliable and reproducible PAT tool for the inline monitoring of this specific emulsion polymerization process. The process can be monitored in an industrially relevant environment, at large reaction scale and commercially distributed dispersion properties. The PDW spectroscopy implementation as PAT tool was successfully demonstrated on several experiments and optimized to an operative application for industry environment.

In this work it was further evaluated and validated that different types of polymer systems need different adjusted ways of analysis, when monitored and analyzed by PDW spectroscopy. This work showed that differentiations clearly need to be made regarding the particle systems, its contents, characteristics and physical parameters. To show that in principle PDW spectroscopy is applicable for polymer analysis, in-depth analysis of polystyrene particles showed that with significant and specific system characterization the polymerization monitoring and particle size determination by PDW spectroscopy is low in error and high in precision and accuracy. For the PVAc homopolymer system studied, it was found here, that several adjustments are necessary regarding the particle properties. The iterative determination of particle swelling by water based on PDW spectroscopy analysis yielded comparable results of the particle size and PSD in comparison with standard particle sizing techniques. The results enhanced the capabilities of PDW spectroscopy for the analysis of polymer particles and the downstream determination of their physical composition. Dispersion end products are readily characterizable, as polymer characteristics are determined in detail by offline analysis in their undiluted state at elevated volume fractions.

It has been shown that PDW spectroscopy is applicable also for very early stages of the polymerization as it effectively describes inhomogeneities in the system by fluctuations in the intensity data  $I_{raw}$ . During the synthesis data administration gets less noisy as the growing particles and homogeneity of the system can be described better by theories and model assumptions used for PDW spectroscopy calculations. This research showed clearly that for the analyzed PVAc/PVA system preventive actions can be taken before synthesis failure occurs. The inline monitoring allows to detect early inhomogeneities. Adjustments of the stirrer speed can be applied to enhance conversion and generate a homogeneous reaction mixture. These early measures help to prevent low conversions and deviations in the final product properties.

During the further course of the reaction other safety risks and process failures are also detectable by a sudden change in the optical dispersion properties. Too high solid contents and following gelation of the dispersion is detectable by a sudden change in the optical parameters and simultaneous increase in reaction temperature. To prevent a run-away process, counteractions to the system can be taken in real time.

## 8 Outlook

It is commonly known that in starved feed polymerization reactions small particles are neglected by growth compared to the larger particles in solution. This phenomenon is called stochastic broadening and leads to a positively skewed PSD in the final product. Using PDW spectroscopy with the correct particle properties during the synthesis with respect to density, volume fraction and refractive index the PSD can be deduced at different stages during the reaction. The inline PSD could be analyzed regarding statistic broadening and its general evolution during the course of the reaction. Further the applicability onto other polymer systems is already checked in further research at our lab and in cooperation with POLYMAT Institute, San Sebastián, Spain.

The implementation as a plug-and-play system of PDW spectroscopy still needs optimization and especially adaptation to each polymer or other particulate system analyzed. Further real-life applications in the producing industry, biochemistry and further application ranges.

On a technical note, the built spectrometer needs to be better protected against temperature fluctuations in the respective production area. This problem will be addressed in the future with an updated control unit. Further real-time application of inline dosing will be implemented in the software to reduce post-process analysis steps and mirror the process in real-time even better.

For even bigger reaction volumes than analyzed in this work, higher spatial resolution of PDW spectroscopy needs to be implemented. Using for example a multi probe system to compare homogeneities inside the reactor will deliver more reliable data.

## 9 References

- (1) Fact.MR. *Vinyl Acetate Market. Vinyl Acetate Market Analysis by Polyvinyl Acetate, Polyvinyl Alcohol, and Ethylene Vinyl Acetate for Solar, Automotive, Building & construction, Packaging, and Textiles from 2023 to 2033*. <https://www.factmr.com/report/vinyl-acetate-market> (accessed 2024-09-26).
- (2) Asua, J. M. Emulsion polymerization: From fundamental mechanisms to process developments. *J. Polym. Sci. A Polym. Chem.* **2004**, *42* (5), 1025–1041. DOI: 10.1002/pola.11096.
- (3) Sosa, N.; Peralta, R. D.; López, R. G.; Ramos, L. F.; Katime, I.; Cesteros, C.; Mendizábal, E.; Puig, J. E. A comparison of the characteristics of poly(vinyl acetate) latex with high solid content made by emulsion and semi-continuous microemulsion polymerization. *Polymer* **2001**, *42* (16), 6923–6928. DOI: 10.1016/S0032-3861(01)00157-4.
- (4) Castellanos, S. G.; Fernández-Escamilla, V. V. A.; Corona-Rivera, M. Á.; González-Iñiguez, K. J.; Barrera, A.; Moscoso-Sánchez, F. J.; Figueroa-Ochoa, E. B.; Ceja, I.; Rabelero, M.; Aguilar, J. Coagulative Nucleation in the Copolymerization of Methyl Methacrylate-Butyl Acrylate under Monomer-Starved Conditions. *Polymers* **2023**, *15* (7). DOI: 10.3390/polym15071628. Published Online: Mar. 24, 2023.
- (5) Carro, S.; Herrera-Ordóñez, J.; Castillo-Tejas, J. On the mechanism of particle formation above the CMC in emulsion polymerization. *Polym. Bull.* **2018**, *75* (3), 1027–1035. DOI: 10.1007/s00289-017-2075-2.
- (6) Abad, C.; La Cal, J. C. de; Asua, J. M. Emulsion copolymerization of vinyl esters in continuous reactors: Comparison between loop and continuous stirred tank reactors. *J. Appl. Polym. Sci.* **1995**, *56* (4), 419–424. DOI: 10.1002/app.1995.070560402.
- (7) Peter A. Lovell, Mohamed S. El-Aasser, Ed. *Emulsion polymerization and emulsion polymers*, Reprinted.; Wiley, 1997.
- (8) Thickett, S. C.; Gilbert, R. G. Emulsion polymerization: State of the art in kinetics and mechanisms. *Polymer* **2007**, *48* (24), 6965–6991. DOI: 10.1016/j.polymer.2007.09.031.
- (9) Münzberg, M.; Hass, R.; Dinh Duc Khanh, N.; Reich, O. Limitations of turbidity process probes and formazine as their calibration standard. *Analytical and bioanalytical chemistry* **2017**, *409* (3), 719–728. DOI: 10.1007/s00216-016-9893-1. Published Online: Oct. 1, 2016.
- (10) van Herk, A. M. *Chemistry and Technology of Emulsion Polymerisation*, 2. ed.; Wiley, 2013.
- (11) Sheibat-Othman, N.; Vale, H. M.; Pohn, J. M.; McKenna, T. F. L. Is Modeling the PSD in Emulsion Polymerization a Finished Problem? An Overview. *Macro Reaction Engineering* **2017**, *11* (5). DOI: 10.1002/mren.201600059.



- (12) Elizalde, O.; Azpeitia, M.; Reis, M. M.; Asua, J. M.; Leiza, J. R. Monitoring Emulsion Polymerization Reactors: Calorimetry Versus Raman Spectroscopy. *Ind. Eng. Chem. Res.* **2005**, *44* (18), 7200–7207. DOI: 10.1021/ie050451y.
- (13) Brunier, B. Modeling of Pickering Emulsion Polymerization, 2015.
- (14) Baldur Lorenz Schroeter. Kinetik von Redoxinitiatoren für die Emulsionspolymerisation. Dissertation, Universität Hamburg, Hamburg, 2018.
- (15) Nagaraja, G. K.; Demappa, T.; Mahadevaiah. Polymerization kinetics of acrylonitrile by oxidation: Reduction system using potassium persulfate/ascorbic acid in an aqueous medium. *J. Appl. Polym. Sci.* **2011**, *121* (3), 1299–1303. DOI: 10.1002/app.33365.
- (16) Agirre, A.; Calvo, I.; Weitzel, H.-P.; Hergeth, W.-D.; Asua, J. M. Semicontinuous Emulsion Co-polymerization of Vinyl Acetate and VeoVa10. *Ind. Eng. Chem. Res.* **2014**, *53* (22), 9282–9295. DOI: 10.1021/ie4032499.
- (17) Da Cunha, L.; Ilundain, P.; Salazar, R.; Alvarez, D.; Barandiaran, M.; Asua, J. VOC formation during monomer removal by post-polymerization. *Polymer* **2001**, *42* (2), 391–395. DOI: 10.1016/S0032-3861(00)00377-3.
- (18) Ilundain, P.; Da Cunha, L.; Salazar, R.; Alvarez, D.; Barandiaran, M. J.; Asua, J. M. Postpolymerization of vinyl acetate-containing latexes. *J. Appl. Polym. Sci.* **2002**, *83* (4), 923–928. DOI: 10.1002/app.10151.
- (19) Hansen, F. K.; Ugelstad, J. Particle nucleation in emulsion polymerization. I. A theory for homogeneous nucleation. *J. Polym. Sci. Polym. Chem. Ed.* **1978**, *16* (8), 1953–1979. DOI: 10.1002/pol.1978.170160814.
- (20) Wessling, Ritchie, A. Kinetics of Continuous Addition Emulsion Polymerization. *Journal of Applied Polymer Science* **1968** (12), 309–319. Published Online: Mar. 9, 2023.
- (21) Chen, Y.; Jahanzad, F.; Sajjadi, S. Semicontinuous monomer-starved emulsion polymerization as a means to produce nanolatexes: analysis of nucleation stage. *Langmuir : the ACS journal of surfaces and colloids* **2013**, *29* (19), 5650–5658. DOI: 10.1021/la4000654. Published Online: May. 3, 2013.
- (22) Sajjadi, S. Particle formation under monomer-starved conditions in the semibatch emulsion polymerization of styrene. I. Experimental. *J. Polym. Sci. A Polym. Chem.* **2001**, *39* (22), 3940–3952. DOI: 10.1002/pola.10031.
- (23) Aguirre, M.; Ballard, N.; Gonzalez, E.; Hamzehlou, S.; Sardon, H.; Calderon, M.; Paulis, M.; Tomovska, R.; Dupin, D.; Bean, R. H.; Long, T. E.; Leiza, J. R.; Asua, J. M. Polymer Colloids: Current Challenges, Emerging Applications, and New Developments. *Macromolecules* **2023**, *56* (7), 2579–2607. DOI: 10.1021/acs.macromol.3c00108. Published Online: Mar. 23, 2023.

- (24) Sajjadi, S.; Brooks, B. W. Semibatch emulsion polymerization of butyl acrylate. I. Effect of monomer distribution. *J. Appl. Polym. Sci.* **1999**, *74* (13), 3094–3110. DOI: 10.1002/(SICI)1097-4628(19991220)74:13<3094:AID-APP12>3.0.CO;2-Z.
- (25) Sajjadi, S.; Brooks, B. W. Unseeded semibatch emulsion polymerization of butyl acrylate: Bimodal particle size distribution. *J. Polym. Sci. A Polym. Chem.* **2000**, *38* (3), 528–545. DOI: 10.1002/(SICI)1099-0518(20000201)38:3<528:AID-POLA19>3.0.CO;2-H.
- (26) Sajjadi, S.; Brooks, B. W. Semibatch emulsion polymerization of butyl acrylate. II. Effects of emulsifier distribution. *J. Appl. Polym. Sci.* **2001**, *79* (4), 582–597. DOI: 10.1002/1097-4628(20010124)79:4<582:AID-APP20>3.0.CO;2-T.
- (27) Sajjadi, S.; Brooks, B. Semibatch emulsion polymerisation reactors: polybutyl acrylate case study. *Chemical Engineering Science* **2000**, *55* (20), 4757–4781. DOI: 10.1016/S0009-2509(00)00112-3.
- (28) Flory, P. J. The mechanism of vinyl polymerizations. *Journal of the American Chemical Society* **1937**, *59* (2), 241–253.
- (29) Mardare, D.; Matyjaszewski, K. Living" radical polymerization of vinyl acetate. *Macromolecules* **1994**, *27* (3), 645–649.
- (30) Chem Analyst. *Vinyl Acetate Monomer (VAM) Market Analysis: Industry Market Size, Plant Capacity, Production, Operating Efficiency, Demand & Supply, End-Use, Foreign Trade, Sales Channel, Regional Demand, Company Share, 2015-2032: Decode the Future of Vinyl Acetate Monomer*. <https://www.chemanalyst.com/industry-report/vinyl-acetate-monomer-market-605> (accessed 2023-08-16).
- (31) Erbil, Y. H. *Vinyl Acetate Emulsion Polymerization and Copolymerization with Acrylic Monomers*; CRC Press, 2000. DOI: 10.1201/9781420038804.
- (32) Sakurada, I. *Polyvinyl alcohol fibers*; International Fiber Science and technology Series, Vol. 6; Dekker, 1985.
- (33) Zecha, H.; Weitzel, H.-P. Method for producing Vinyl ester polymers having specifically settable dispersity and low polydispersity. 14/390,120.
- (34) Inkson, B. J. Scanning electron microscopy (SEM) and transmission electron microscopy (TEM) for materials characterization. In *Materials Characterization Using Nondestructive Evaluation (NDE) Methods*; Elsevier, 2016; pp 17–43. DOI: 10.1016/B978-0-08-100040-3.00002-X.
- (35) Hawkes, P. W.; Lotsch, H. K. V.; Reimer, L. *Scanning Electron Microscopy*, Vol. 45; Springer Berlin Heidelberg, 1998. DOI: 10.1007/978-3-540-38967-5.
- (36) Hough, P. C. V. Method and means for recognizing complex patterns. 17715.
- (37) Unzu, M. J.; Urretabizkaia, A.; Asua, J. M. Maximizing production rate and scrub resistance of vinyl acetate-VeoVa 10 latexes. *J. Appl. Polym. Sci.* **2000**, *78* (3), 475–485. DOI: 10.1002/1097-4628(20001017)78:3<475:AID-APP10>3.0.CO;2-U.

- (38) Bohórquez, S. J.; Asua, J. M. Particle nucleation in high solids batch miniemulsion polymerization stabilized with a polymeric surfactant. *J. Polym. Sci. A Polym. Chem.* **2008**, *46* (19), 6407–6415. DOI: 10.1002/pola.22948.
- (39) Jacob, L. I.; Pauer, W. Scale-up of Emulsion Polymerisation up to 100 L and with a Polymer Content of up to 67 wt%, Monitored by Photon Density Wave Spectroscopy. *Polymers* **2022**, *14* (8). DOI: 10.3390/polym14081574. Published Online: Apr. 12, 2022.
- (40) Aleid, G. M.; Alshammari, A. S.; Tripathy, D. B.; Gupta, A.; Ahmad, S. Polymeric Surfactants: Recent Advancement in Their Synthesis, Properties, and Industrial Applications. *Macro Chemistry & Physics* **2023**, *224* (17). DOI: 10.1002/macp.202300107.
- (41) Raffa, P.; Wever, D. A. Z.; Picchioni, F.; Broekhuis, A. A. Polymeric Surfactants: Synthesis, Properties, and Links to Applications. *Chemical reviews* **2015**, *115* (16), 8504–8563. DOI: 10.1021/cr500129h. Published Online: Jul. 16, 2015.
- (42) Hodge, R. M.; Bastow, T. J.; Edward, G. H.; Simon, G. P.; Hill, A. J. Free Volume and the Mechanism of Plasticization in Water-Swollen Poly(vinyl alcohol). *Macromolecules* **1996**, *29* (25), 8137–8143. DOI: 10.1021/ma951073j.
- (43) Jain, N.; Singh, V. K.; Chauhan, S. A review on mechanical and water absorption properties of polyvinyl alcohol based composites/films. *Journal of the Mechanical Behavior of Materials* **2017**, *26* (5-6), 213–222. DOI: 10.1515/jmbm-2017-0027.
- (44) Hodge, R. M.; Edward, G. H.; Simon, G. P. Water absorption and states of water in semicrystalline poly(vinyl alcohol) films. *Polymer* **1996**, *37* (8), 1371–1376. DOI: 10.1016/0032-3861(96)81134-7.
- (45) Bajpai, A. K.; Saini, R. Preparation and characterization of novel biocompatible cryogels of poly (vinyl alcohol) and egg-albumin and their water sorption study. *Journal of materials science. Materials in medicine* **2006**, *17* (1), 49–61. DOI: 10.1007/s10856-006-6329-z.
- (46) Shaheen, S. M.; Yamaura, K. Preparation of theophylline hydrogels of atactic poly(vinyl alcohol)/NaCl/H<sub>2</sub>O system for drug delivery system. *Journal of controlled release : official journal of the Controlled Release Society* **2002**, *81* (3), 367–377. DOI: 10.1016/s0168-3659(02)00085-8.
- (47) U.S. Department of Health and Human Services Food and Drug Administration. *Guidance for Industry PAT — A Framework for Innovative Pharmaceutical Development, Manufacturing, and Quality Assurance*. <https://www.fda.gov/regulatory-information/search-fda-guidance-documents/pat-framework-innovative-pharmaceutical-development-manufacturing-and-quality-assurance> (accessed 2024-08-29).
- (48) Carol E. Cleland. Historical science, experimental science, and the scientific method. *Geology* **20001**, *29* (11), 987–990.
- (49) Friedrich Steinle. Entering New Fields: Exploratory Uses of Experimentation. *Philosophy of Science* **1997**, *64*, 65–74.

- (50) Ian Willis. *Trial and Error*. [https://www.academia.edu/25601615/Trial\\_and\\_error](https://www.academia.edu/25601615/Trial_and_error).
- (51) Steinle, F. Experiments in History and Philosophy of Science. *Perspectives on Science* **2002**, 10 (4), 408–432. DOI: 10.1162/106361402322288048.
- (52) Simon, L. L.; Pataki, H.; Marosi, G.; Meemken, F.; Hungerbühler, K.; Baiker, A.; Tummala, S.; Glennon, B.; Kuentz, M.; Steele, G.; Kramer, H. J. M.; Rydzak, J. W.; Chen, Z.; Morris, J.; Kjell, F.; Singh, R.; Gani, R.; Gernaey, K. V.; Louhi-Kultanen, M.; O'Reilly, J.; Sandler, N.; Antikainen, O.; Yliruusi, J.; Frohberg, P.; Ulrich, J.; Braatz, R. D.; Leyssens, T.; Stosch, M. von; Oliveira, R.; Tan, R. B. H.; Wu, H.; Khan, M.; Des O'Grady; Pandey, A.; Westra, R.; Delle-Case, E.; Pape, D.; Angelosante, D.; Maret, Y.; Steiger, O.; Lenner, M.; Abbou-Oucherif, K.; Nagy, Z. K.; Litster, J. D.; Kamaraju, V. K.; Chiu, M.-S. Assessment of Recent Process Analytical Technology (PAT) Trends: A Multiauthor Review. *Org. Process Res. Dev.* **2015**, 19 (1), 3–62. DOI: 10.1021/op500261y.
- (53) Sistare, F.; St. Pierre Berry, L.; Mojica, C. A. Process Analytical Technology: An Investment in Process Knowledge. *Org. Process Res. Dev.* **2005**, 9 (3), 332–336. DOI: 10.1021/op0402127.
- (54) Bakeev, K. A., Ed. *Process Analytical Technology: Spectroscopic tools and implementation strategies for the chemical and pharmaceutical industries*, 2. ed.; Wiley, 2010.
- (55) Kamble, R.; Sharma, S.; Varghese, V.; Mahadik, K. Process Analytical Technology (PAT) in Pharmaceutical Development and its Application: Review Article. *International Journal of Pharmaceutical Sciences Review and Research* **2013**, 23 (2), 212–223.
- (56) Reid, G. L.; Ward, H. W.; Palm, A. S.; Muteki, K. Process Analytical Technology (PAT) in Pharmaceutical Development. *American Pharmaceutical Review* **2012**, 15 (49).
- (57) Hergeth, W.-D.; Frauendorfer, E. Online-Reaktionsverfolgung bei der Polymerisation. *Chemie Ingenieur Technik* **2010**, 82 (4), 503–507. DOI: 10.1002/cite.200900132.
- (58) Rouse, P. E. A Theory of the Linear Viscoelastic Properties of Dilute Solutions of Coiling Polymers. *The Journal of Chemical Physics* **1953**, 21 (7), 1272–1280. DOI: 10.1063/1.1699180.
- (59) Del Giudice, F.; Haward, S. J.; Shen, A. Q. Relaxation time of dilute polymer solutions: A microfluidic approach. *J. Rheol.* **2017**, 61 (2), 327–337. DOI: 10.1122/1.4975933.
- (60) Rubinstein, M.; Colby, R. H. *Polymer Physics*; Oxford University Press Oxford, 2003. DOI: 10.1093/oso/9780198520597.001.0001.
- (61) Strobl, G. R. *The physics of polymers: Concepts for understanding their structures and behavior*, 2., corr. ed.; Springer, 1997.
- (62) Hank de Bruyn. The Emulsion Polymerization of Vinyl Acetate. Dissertation, University of Sydney, Sydney, 1999.

- (63) Azpeitia, M.; Leiza, J. R.; Asua, J. M. Safety in Emulsion Polymerization Reactors: An Experimental Study. *Macro Materials & Eng* **2005**, 290 (4), 242–249. DOI: 10.1002/mame.200400311.
- (64) Lee Josephine Brenker. Inline monitoring of the growth of nano-scaled polyvinyl acetate particles during emulsion polymerization using Photon Density Wave spectroscopy: Influence of monomer content. Bachelorthesis, University of Potsdam, Potsdam, 2020 (accessed 2024-08-29).
- (65) Mettler Toledo. *OptiMax 1001 Thermostat:Prozessentwicklung im Literbereich*. [https://www.mt.com/ch/de/home/products/L1\\_AutochemProducts/chemical-synthesis-reactor-systems/optimax.html](https://www.mt.com/ch/de/home/products/L1_AutochemProducts/chemical-synthesis-reactor-systems/optimax.html) (accessed 2024-08-31).
- (66) Schmälzlin, E. *innoFSPEC innovative faseroptische Spektroskopie und Sensorik:From molecules to galaxies*. <https://innofspec.de/en/> (accessed 2024-10-02).
- (67) Reich, O. Photonendichtewellenspektroskopie mit intensitätsmodulierten Diodenlasern (Photon density wave spectroscopy with intensity-modulated diode lasers). PhD Thesis, University of Potsdam, Potsdam, 2005.
- (68) Hass, R. Angewandte Photonendichtewellen Spektroskopie. PhD Thesis, University of Potsdam, Potsdam, 2011.
- (69) Bressel, L. Bedeutung der abhaengigen Streuung für die optischen Eigenschaften hochkonzentrierter Dispersionen. PhD Thesis, University of Potsdam, Potsdam, 2016.
- (70) Zimmermann, S.; Scouten, J.; Reich, O.; Münzberg, M. Expression of the anisotropy factor of fractal aggregates to enable their characterization using photon density wave spectroscopy. *Journal of Quantitative Spectroscopy and Radiative Transfer* **2024**, 325, 109106. DOI: 10.1016/j.jqsrt.2024.109106.
- (71) Zimmermann, S.; Reich, O.; Bressel, L. Exploitation of inline photon density wave spectroscopy for titania particle syntheses. *J Am Ceram Soc.* **2023**, 106 (1), 671–680. DOI: 10.1111/jace.18744.
- (72) Gutschmann, B.; Schiewe, T.; Weiske, M. T. H.; Neubauer, P.; Hass, R.; Riedel, S. L. In-Line Monitoring of Polyhydroxyalkanoate (PHA) Production during High-Cell-Density Plant Oil Cultivations Using Photon Density Wave Spectroscopy. *Bioengineering (Basel, Switzerland)* **2019**, 6 (3). DOI: 10.3390/bioengineering6030085. Published Online: Sep. 19, 2019.
- (73) Aspiazu, U. O.; Paulis, M.; Leiza, J. R. Photon Density Wave spectroscopy to monitor the particle size in seeded semibatch emulsion copolymerization reactions. *Chemical Engineering Journal* **2024**, 483, 149292. DOI: 10.1016/j.cej.2024.149292.
- (74) Aspiazu, U. O.; Zimmermann, S.; Münzberg, M.; Leiza, J. R.; Paulis, M. Sensitivity of the particle size determined inline by Photon Density Wave Spectroscopy with respect to sample properties and measurement settings during emulsion copolymerization reactions. *Polymer Testing* **2025**, 142, 108668. DOI: 10.1016/j.polymertesting.2024.108668.



- (75) Hass, R.; Munzke, D.; Ruiz, S. V.; Tippmann, J.; Reich, O. Optical monitoring of chemical processes in turbid biogenic liquid dispersions by Photon Density Wave spectroscopy. *Analytical and bioanalytical chemistry* **2015**, *407* (10), 2791–2802. DOI: 10.1007/s00216-015-8513-9. Published Online: Mar. 1, 2015.
- (76) Jacob, L. I.; Pauer, W. In-line monitoring of latex-particle size during emulsion polymerizations with a high polymer content of more than 60. *RSC advances* **2020**, *10* (44), 26528–26534. DOI: 10.1039/d0ra02523b. Published Online: Jul. 15, 2020.
- (77) Brar, S. K.; Verma, M. Measurement of nanoparticles by light-scattering techniques. *TrAC Trends in Analytical Chemistry* **2011**, *30* (1), 4–17. DOI: 10.1016/j.trac.2010.08.008.
- (78) Modena, M. M.; Rühle, B.; Burg, T. P.; Wuttke, S. Nanoparticle Characterization: What to Measure? *Advanced materials (Deerfield Beach, Fla.)* **2019**, *31* (32), e1901556. DOI: 10.1002/adma.201901556. Published Online: May. 30, 2019.
- (79) Thomas, J. C. The determination of log normal particle size distributions by dynamic light scattering. *Journal of Colloid and Interface Science* **1987**, *117* (1), 187–192. DOI: 10.1016/0021-9797(87)90182-2.
- (80) Dörfler, H.-D. *Grenzflächen und kolloid-disperse Systeme: Physik und Chemie ; mit 579, zum Teil farbigen Abb. und 88 Tabellen*; Springer, 2002.
- (81) Brian Dunbar Maria Werries. *Technology Readiness Levels Demystified*. [https://www.nasa.gov/topics/aeronautics/features/trl\\_demystified.html](https://www.nasa.gov/topics/aeronautics/features/trl_demystified.html) (accessed 2023-06-08).
- (82) Buchner, G. A.; Stepputat, K. J.; Zimmermann, A. W.; Schomäcker, R. Specifying Technology Readiness Levels for the Chemical Industry. *Ind. Eng. Chem. Res.* **2019**, *58* (17), 6957–6969. DOI: 10.1021/acs.iecr.8b05693.
- (83) European Union. *HORIZON 2020 – WORK PROGRAMME 2014-2015: Technology readiness levels (TRL)*. [https://ec.europa.eu/research/participants/data/ref/h2020/wp/2014\\_2015/annexes/h2020-wp1415-annex-g-trl\\_en.pdf](https://ec.europa.eu/research/participants/data/ref/h2020/wp/2014_2015/annexes/h2020-wp1415-annex-g-trl_en.pdf) (accessed 2023-06-08).
- (84) Genwen Zhou; Suzanne M. Kresta. Impact of tank geometry on the maximum turbulence energy dissipation rate for impellers. *Aiche Journal* **1996**, *42*, 2476–2490.
- (85) Kemmere, M. F.; Meuldijk, J.; Drinkenburg, A. A. H.; German, A. L. Colloidal stability of high-solids polystyrene and polyvinyl acetate latices. *J. Appl. Polym. Sci.* **1999**, *74* (7), 1780–1791. DOI: 10.1002/(SICI)1097-4628(19991114)74:7<1780:AID-APP21>3.0.CO;2-U.

## 10 Appendix

Table 3 Recipe for PVAc/SDS synthesis shown in Figure 14.

Component	Mass / g	Feedrate / g min <sup>-1</sup>
Water	300.1	-
FAS	0.01987	-
SDS	0.436	-
3.5 % (AA) <sub>aq</sub>	27.3	0.33
4.5 % (NaPS) <sub>aq</sub>	27.3	0.33
0.3 % (SDS) <sub>aq</sub>	190	2.46
VAc monomer	295	4.52

Experimental conditions:

First fill of reactor with 300 g distilled water and 0.436 g of SDS, stirring speed of 100 rpm, heating of iC to 50 °C. After 10 min of temperature equilibrium, dosing of 3.5 % AA solution and 4.5 % NaPS solution was started. 10 minutes later 0.3 % SDS solution and VAc monomer dosing was started. Ramping of stirrer speed to 300 rpm within 60 min. After dosing of SDS and VAc is completed, AA and NaPS were continued for 10 minutes. After that the temperature was decreased to  $T_R = 20^\circ \text{C}$  in 30 min. At  $T_R = 20^\circ \text{C}$  the reaction was terminated and the sample stored in an airtight container for further analysis.

Table 4 experiments list of PVAc homopolymerization with PVA as stabilizing agent. Experimental set up of five experiments with increasing amount of PVA in the initial charge (iC).

Experiment Name	Nr.	iC PVA / g	total amount water iC / g	iC PVA / g L <sup>-1</sup>
SMS_WiC0g/L_PVA	1	0	302	0
SMS_WiC1g/L_PVA	2	0.333	302	0.991
SMS_WiC2g/L_PVA	3	0.667	302	1.984
SMS_WiC5g/L_PVA	4	1.667	302	5.500
SMS_WiC10g/L_PVA	5	3.333	302	10.960

Table 5 experimentally determined dispersion properties of synthesized PVAc dispersions.

Experiment Name	solid content / %	Mass content monomer / %	Density / g cm <sup>-3</sup>
SMS_WiC0g/L_PVA	41.07	38.623	1.216
SMS_WiC1g/L_PVA	41.61	38.628	1.214
SMS_WiC2g/L_PVA	40.92	38.621	1.216
SMS_WiC5g/L_PVA	41.57	38.594	1.212

SMS\_WiC10g/L\_PVA | 40.77 | 38.592 | 1.214

Table 6 experimentally determined particle size by DLS of PVAc homopolymer by DLS and SLS with  $n$  as number of samples analyzed and  $\sigma$  as width of the distribution.

Experiment Name	$n$	average particle size DLS	$\sigma$ (DLS)
SMS_WiC0g/L_PVA	9	579.78 $\pm$ 19.13	148.04 $\pm$ 9.27
SMS_WiC1g/L_PVA	9	483.3 $\pm$ 81.47	122.73 $\pm$ 50.39
SMS_WiC2g/L_PVA	9	470.77 $\pm$ 17.76	117.99 $\pm$ 18.13
SMS_WiC5g/L_PVA	9	359.6 $\pm$ 14.93	97.19 $\pm$ 14.74
SMS_WiC10g/L_PVA	9	284.8 $\pm$ 13.59	79.09 $\pm$ 13.96

Table 7 experimentally determined particle size by SLS of PVAc homopolymer by DLS and SLS with  $n$  as number of samples analyzed and  $\sigma$  as width of the distribution.

Experiment Name	$n$	average particle size SLS	$\sigma$ (SLS)
SMS_WiC0g/L_PVA	9	438.51 $\pm$ 1.21	62.0316 $\pm$ 0.09
SMS_WiC1g/L_PVA	9	401.17 $\pm$ 2.03	57.49 $\pm$ 1.33
SMS_WiC2g/L_PVA	9	385.5 $\pm$ 0.37	55.31 $\pm$ 0.40
SMS_WiC5g/L_PVA	9	324.11 $\pm$ 0.69	52.86 $\pm$ 0.26
SMS_WiC10g/L_PVA	9	213.27 $\pm$ 0.09	41.59 $\pm$ 0.09

Table 8 Styrene seed synthesis general recipe.

Component	Mass / g
Water	530
Styrene	135
17.1 % SDS <sub>aq</sub>	36.2
Na-Tetra Borate <sub>aq</sub> *	0.125
5 % KPS <sub>aq</sub>	30





\* used as purchased

First fill of reactor with 500 g of Milli-Q® water in the 1 L batch reactor, stirring speed of 100 rpm and N<sub>2</sub> purging, heating of iC to 100 °C for 60 min to degas by setting the reactor-jacket temperature  $T_J = 130$  °C. The reaction temperature  $T_R$  was reduced to 55 °C over 45 min. At 55 °C temperature equilibrium, 135 g styrene, 6.2 g SDS in 30 g water, and 0.125 g of Na-Tetra Borate were added. After a short waiting period for the emulsion to form, 30 mL of a 5% KPS solution were added automatically via a computer-controlled dosing unit at 6 mL min<sup>-1</sup>. Simultaneously, stirrer speed was increased to 200 rpm. The emulsion polymerized at 55 °C for 24 h. A post-polymerization at 83 °C for 3 h followed. The system was finally cooled to 20 °C over 30 min.

Table 9 Styrene seed synthesis recipes.




Experiment Name	Reaction temperature $T_R / ^\circ\text{C}$	total amount water iC / g	total amount Styrene monomer dosed (i Control) / mL	Concentration SDS solution / $\text{g mL}^{-1}$	total amount SDS solution / mL	total amount SDS / g	total amount KPS / g	water from KPS / g	mass Catalyst Na-tetraborat / g
PS_001	55	530.312	135.1	0.012	29.97	6.203	2.21	52.471	0.124
PS_011	55	530	135.03	0.012	30	6.201	2.214	52.505	0.127
PS_020	55	500.08	135.55	0.012	36.66	6.203	5	95	0.147






Table 10 GHS danger symbols and H/P statements of the used chemical compounds. \* gAI




Chemical compound	Hazardous symbols	Hazard Statements	Precautionary Statements
Vinyl acetate monomer	  	<p>H225: Highly flammable liquid and vapor</p> <p>H332: Harmful if inhaled</p> <p>H335: May cause respiratory irritation</p> <p>H351: Suspected of causing cancer</p> <p>H412: Harmful to aquatic life with long lasting effects</p>	<p>P202: Do not handle until all safety precautions have been read and understood</p> <p>P210: Keep away from heat, hot surfaces, sparks, open flames and other ignition sources. No smoking</p> <p>P233: Keep container tightly closed</p> <p>P273: Avoid release to the environment</p> <p>P304+P340: IF INHALED: Remove person to fresh air and keep comfortable for breathing</p>
Neodecanoic acid vinyl ester (Versa <sup>®</sup> 10)		<p>H410: Very toxic to aquatic life with long lasting effects</p>	<p>P273: Avoid release to the environment</p> <p>P391: Collect spillage</p> <p>P501: Dispose of contents/container to an appropriate treatment and disposal facility in accordance with</p>





\*gAI This table has been compiled by perplexity.AI. the author listed the chemical compounds for the search of the H and P statements and gAI via perplexity listed the given H and P statements. The author checked the table for consistency with the safety data sheets available.






			applicable laws and regulations, and product characteristics at time of disposal
Potassium persulfate (KPS)	  	<p>H272: May intensify fire; oxidizer</p> <p>H302: Harmful if swallowed</p> <p>H315: Causes skin irritation</p> <p>H317: May cause an allergic skin reaction</p> <p>H319: Causes serious eye irritation</p> <p>H334: May cause allergy or asthma symptoms or breathing difficulties if inhaled</p> <p>H335: May cause respiratory irritation</p>	<p>P210: Keep away from heat, hot surfaces, sparks, open flames and other ignition sources. No smoking</p> <p>P220: Keep/Store away from clothing/combustible materials</p> <p>P261: Avoid breathing dust/fume/gas/mist/vapors/spray</p> <p>P280: Wear protective gloves/protective clothing/eye protection/face protection</p> <p>P302+P352: IF ON SKIN: Wash with plenty of water</p> <p>P304+P340: IF INHALED: Remove person to fresh air and keep comfortable for breathing</p> <p>P305+P351+P338: IF IN EYES: Rinse cautiously with water for several minutes. Remove contact lenses, if present and easy to do. Continue rinsing</p>




			P342+P311: If experiencing respiratory symptoms: Call a POISON CENTER or doctor/physician
tert-butyl hydroperoxide (tBHP)	    	<p>H226: Flammable liquid and vapor</p> <p>H242: Heating may cause a fire</p> <p>H302: Harmful if swallowed</p> <p>H311: Toxic in contact with skin</p> <p>H314: Causes severe skin burns and eye damage</p> <p>H317: May cause an allergic skin reaction</p> <p>H330: Fatal if inhaled</p> <p>H335: May cause respiratory irritation</p> <p>H341: Suspected of causing genetic defects</p> <p>H351: Suspected of causing cancer</p>	<p>P201: Obtain special instructions before use</p> <p>P202: Do not handle until all safety precautions have been read and understood</p> <p>P210: Keep away from heat, hot surfaces, sparks, open flames and other ignition sources. No smoking</p> <p>P220: Keep/Store away from clothing/combustible materials</p> <p>P233: Keep container tightly closed</p> <p>P234: Keep only in original container</p> <p>P261: Avoid breathing dust/fume/gas/mist/vapors/spray</p> <p>P280: Wear protective gloves/protective clothing/eye protection/face protection</p>


		<p>H411: Toxic to aquatic life with long lasting effects</p>	<p>P303+P361+P353: IF ON SKIN (or hair): Take off immediately all contaminated clothing. Rinse skin with water</p> <p>P304+P340: IF INHALED: Remove person to fresh air and keep comfortable for breathing</p> <p>P305+P351+P338: IF IN EYES: Rinse cautiously with water for several minutes. Remove contact lenses, if present and easy to do. Continue rinsing</p>
Sodium Persulfate (NaPS)	  	<p>H272: May intensify fire; oxidizer</p> <p>H302: Harmful if swallowed</p> <p>H315: Causes skin irritation</p> <p>H317: May cause an allergic skin reaction</p> <p>H319: Causes serious eye irritation</p> <p>H334: May cause allergy or asthma symptoms or breathing difficulties if inhaled</p>	<p>P210: Keep away from heat, hot surfaces, sparks, open flames and other ignition sources. No smoking</p> <p>P220: Keep/store away from clothing/combustible materials</p> <p>P260: Do not breathe dust</p> <p>P280: Wear protective gloves/protective clothing/eye protection/face protection</p> <p>P302+P352: IF ON SKIN: Wash with plenty of water</p>


		<p>H335: May cause respiratory irritation</p>	<p>P304+P340: IF INHALED: Remove person to fresh air and keep comfortable for breathing</p> <p>P305+P351+P338: IF IN EYES: Rinse cautiously with water for several minutes. Remove contact lenses, if present and easy to do. Continue rinsing</p> <p>P312: Call a POISON CENTER/doctor if you feel unwell</p>
Hydroquinone	   	<p>H302: Harmful if swallowed</p> <p>H317: May cause an allergic skin reaction</p> <p>H318: Causes serious eye damage</p> <p>H341: Suspected of causing genetic defects</p> <p>H351: Suspected of causing cancer</p> <p>H400: Very toxic to aquatic life</p> <p>H410: Very toxic to aquatic life with long lasting effects</p>	<p>P273: Avoid release to the environment</p> <p>P280: Wear protective gloves/protective clothing/eye protection/face protection</p> <p>P301+P312: IF SWALLOWED: Call a POISON CENTER or doctor if you feel unwell</p> <p>P305+P351+P338: IF IN EYES: Rinse cautiously with water for several minutes. Remove contact lenses, if present and easy to do. Continue rinsing</p>



Styrene monomer	  	<p>H226: Flammable liquid and vapor</p> <p>H304: May be fatal if swallowed and enters airways</p> <p>H315: Causes skin irritation</p> <p>H319: Causes serious eye irritation</p> <p>H332: Harmful if inhaled</p> <p>H335: May cause respiratory irritation</p> <p>H351: Suspected of causing cancer</p> <p>H361d: Suspected of damaging the unborn child</p> <p>H372: Causes damage to organs (hearing organs) through prolonged or repeated exposure</p> <p>H401: Toxic to aquatic life</p>	<p>P201: Obtain special instructions before use</p> <p>P210: Keep away from heat, hot surfaces, sparks, open flames and other ignition sources. No smoking</p> <p>P243: Take precautionary measures against static discharge</p> <p>P260: Do not breathe vapor/spray</p> <p>P280: Wear protective gloves/protective clothing/eye protection/face protection</p> <p>P303+P361+P353: IF ON SKIN (or hair): Take off immediately all contaminated clothing. Rinse skin with water/shower</p> <p>P305+P351+P338: IF IN EYES: Rinse cautiously with water for several minutes. Remove contact lenses, if present and easy to do. Continue rinsing</p> <p>P308+P311: IF exposed or concerned: Call a POISON CENTER or doctor</p>
-----------------	---	--	--



		<p>H412: Harmful to aquatic life with long lasting effects</p>	<p>P403+P233: Store in a well-ventilated place. Keep container tightly closed</p> <p>P501: Dispose of contents/container in accordance with national regulations</p>
Sodium dodecyl sulfate (SDS)	  	<p>H228: Flammable solid</p> <p>H302: Harmful if swallowed</p> <p>H311: Toxic in contact with skin</p> <p>H315: Causes skin irritation</p> <p>H318: Causes serious eye damage</p> <p>H335: May cause respiratory irritation</p> <p>H412: Harmful to aquatic life with long lasting effects</p>	<p>P210: Keep away from heat, hot surfaces, sparks, open flames and other ignition sources. No smoking</p> <p>P261: Avoid breathing dust/fume/gas/mist/vapors/spray</p> <p>P264: Wash hands thoroughly after handling</p> <p>P273: Avoid release to the environment</p> <p>P280: Wear protective gloves/protective clothing/eye protection/face protection</p> <p>P301+P312: IF SWALLOWED: Call a POISON CENTER or doctor if you feel unwell</p> <p>P302+P352: IF ON SKIN: Wash with plenty of water</p>

			<p>P305+P351+P338: IF IN EYES: Rinse cautiously with water for several minutes. Remove contact lenses, if present and easy to do. Continue rinsing</p> <p>P310: Immediately call a POISON CENTER or doctor</p> <p>P370+P378: In case of fire: Use appropriate media to extinguish</p>
Ferric ammonium sulfate (FAS)		<p>H290: May be corrosive to metals</p> <p>H302: Harmful if swallowed</p> <p>H318: Causes serious eye damage</p> <p>H319: Causes serious eye irritation</p> <p>H335: May cause respiratory irritation</p>	<p>P261: Avoid breathing dust/fume/gas/mist/vapors/spray</p> <p>P264: Wash hands thoroughly after handling</p> <p>P270: Do not eat, drink or smoke when using this product</p> <p>P271: Use only outdoors or in a well-ventilated area</p> <p>P280: Wear protective gloves/protective clothing/eye protection/face protection</p> <p>P301+P312: IF SWALLOWED: Call a POISON CENTER or doctor if you feel unwell</p>

			<p>P302+P352: IF ON SKIN: Wash with plenty of water</p> <p>P304+P340: IF INHALED: Remove person to fresh air and keep comfortable for breathing</p> <p>P305+P351+P338: IF IN EYES: Rinse cautiously with water for several minutes. Remove contact lenses, if present and easy to do. Continue rinsing</p> <p>P312: Call a POISON CENTER or doctor if you feel unwell</p> <p>P390: Absorb spillage to prevent material damage</p> <p>P403+P233: Store in a well-ventilated place. Keep container tightly closed</p>
N <sub>2</sub> gas for purging		H280: Contains gas under pressure; may explode if heated	P403: Store in a well-ventilated place

Sodium Tetraborate		<p>H319: Causes serious eye irritation</p> <p>H360FD: May damage fertility. May damage the unborn child</p>	<p>P201: Obtain special instructions before use</p> <p>P264: Wash thoroughly after handling</p> <p>P280: Wear protective gloves/protective clothing/eye protection/face protection</p> <p>P308+P313: IF exposed or concerned: Get medical advice/attention</p> <p>P403: Store in a well-ventilated place</p>
Sodium hydroxide		<p>H290: May be corrosive to metals</p> <p>H314: Causes severe skin burns and eye damage</p> <p>H402: Harmful to aquatic life</p>	<p>P260: Do not breathe dust/fume/gas/mist/vapors/spray</p> <p>P280: Wear protective gloves/protective clothing/eye protection/face protection</p> <p>P301+P330+P331: IF SWALLOWED: Rinse mouth. Do NOT induce vomiting</p> <p>P303+P361+P353: IF ON SKIN (or hair): Take off immediately all contaminated clothing. Rinse skin with water [or shower]</p>

			<p>P304+P340: IF INHALED: Remove person to fresh air and keep comfortable for breathing</p> <p>P305+P351+P338: IF IN EYES: Rinse cautiously with water for several minutes. Remove contact lenses, if present and easy to do. Continue rinsing</p> <p>P310: Immediately call a POISON CENTER/doctor</p>
--	--	--	---



## 10.1 Supplementary Materials

### Supplementary Material to section 5.1:

The following are available online at <https://www.mdpi.com/2073-4360/13/4/669/s1>, Figure S1: Schematic description of the reactor Set-Up. 1 L automated Lab reactor equipped with automated temperature control, stirring control, dosing control, overhead reflux condenser, and N<sub>2</sub> purging. The PDW inline probe is directly inserted into the reactor via an inlet port., Figure S2: Electron microscopy picture of produced particles from emulsion polymerization synthesis VAc\_1.5 with 525 mL VAc., Figure S3: Refractive index of the particles from syntheses VAc\_1, VAc\_1.5, VAc\_1.6, and VAc\_1.8 extrapolated from values of a concentration series of the dispersions measured with a refractometer at seven discrete wavelengths and inter- and extrapolated to wavelengths between 500 nm and 1000 nm, shown with +95% and –95% confidence interval as dashed lines., Figure S4: Density measurements of dilutions of dispersions Vac\_1 to Vac\_1.8 in dilutions up to 30% and extrapolated density values (i.e., 100% Polymer) measured with a densitometer.

### Supplementary Material to section 5.3:

The following supporting information can be downloaded at: <https://www.mdpi.com/article/10.3390/polym17050629/s1>, Figure S1: PDW spectroscopy  $I_{raw}$  data measurements at  $\lambda = 638$  nm of a synthesis with 100 L reaction volume from  $t_R = 00:02$  h to  $t_R = 00:38$  h. Initial measurements up to at least  $t_R = 00:22$  h show irregularities in the order of  $I_{raw}$  and  $d_t$ . This might be caused by an inhomogeneous dispersion due to insufficient mixing; Figure S2: Inline monitoring of 10 L synthesis by PDW spectroscopy at  $\lambda = 638$  nm with reduced scattering coefficient  $\mu_s'$  (red) and absorption coefficient  $\mu_a$  (blue). Offline determined total conversion  $\chi$  (green) and total volume fraction  $\phi$  (green dotted line) are shown along the reaction progress. Vertical lines indicate manual increases of the stirrer speed; Table S1: Overview of the measurements of the experimental set-up of all three reactor sizes at different polymerization reaction volumes  $V_R$ . with H as height of the reactor, D as diameter of the reactor, d as diameter of the used anchor stirrer, H1 as height of initial Charge before starting the reaction and h as height from the bottom of the reactor to the anchor stirrer; Table S2: Initial stirring rates for the different reaction volumes  $V_R$ .

## 11.Acknowledgements

I would like to thank my supervisors Werner Pauer and Gerrit Luinstra for the opportunity to finish this research and my PhD with them.

I want to thank University of Potsdam and University of Hamburg for having me and keeping me safely enrolled as a long term student. My students Pascal Riebler, Lee Josephine Brenker, Max Weber and Taron Michael Krzyczmonik for their support with the experiments in the laboratory and research skills. Cevin Braksch for uncountable after work beers and supportive talks. Thank you to POLYMAT Institute in San Sebastián, especially Jose R. Leiza and Miren Aquirre who supervised the work during my research stay at the beginning of my PhD journey.

Everyone at innoFSPEC, for a short or long term shared office space, especially Marvin Münzberg and Oliver Reich for countless feedback loops on publications and this dissertation.

Writing this thesis was a struggle. I would especially like to thank the people that stood beside me and helped me to gain motivation again during the depriving times of my time as a PhD. I would like to thank Julia Becker as fellow PhD candidate who I can always talk to as a friend and Leidensgenossin, who always has time for me. Dr. Nadine Gawlitta who especially in the last phase of my PhD was a great friend to me.

I would like to thank Gina and Nadl who have no idea what I did but made me do it anyway. Franzi, Nadl and Cevin for proofreading of this masterpiece.

My friends Jule and Janine who let me be part of their families and close circles.

Last but not least I am very thankful for my Mam and Robert as well as Papa and Maike who kept my soul on fire. Lukas, you're my little brother and I am extremely proud of you. There's a bright future ahead of us <3

## 12. Declaration on oath

I hereby declare and affirm that this doctoral dissertation is my own work and that I have not used any aids and sources other than those indicated. If electronic resources based on generative artificial intelligence (gAI) were used in the course of writing this dissertation, I confirm that my own work was the main and value-adding contribution and that complete documentation of all resources used is available in accordance with good scientific practice. I am responsible for any erroneous or distorted content, incorrect references, violations of data protection and copyright law or plagiarism that may have been generated by the gAI.

X



---

Stephanie Schlappa  
Autorin